

# EXPLORING TRADE-OFFS IN RESERVOIR OPERATIONS THROUGH MANY OBJECTIVE OPTIMISATION: CASE OF NILE RIVER BASIN

---

Master thesis submitted to Delft University of Technology  
in partial fulfilment of the requirements for the degree of

**MASTER OF SCIENCE**

in **Engineering and Policy Analysis**

Faculty Technology, Policy, and Management

by

Yasin Sari

Student number: 4924851

To be defended in public on August 18<sup>th</sup> 2022

---

## **Graduation committee**

Chairperson	: Prof. Dr. Ir. Jan Kwakkel, Section Policy Analysis
First Supervisor	: Dr. Jazmin Zatarain Salazar, Section Policy Analysis
Second Supervisor	: Dr.ir. Özge Okur, Section Systems Engineering
External Supervisor	: Dr. Seleshi Yalew, UN IHE Delft

---

Code and data files are available at

<https://github.com/ysari97/master-thesis-project>

A photograph of a man in a light-colored blazer and dark trousers standing in front of large, 3D, grey letters that spell out 'TU Delft'. The 'U' is highlighted in a light blue color. The background shows a campus with trees and buildings under a clear sky.

## ACKNOWLEDGEMENTS

This work marks an end to my journey as a master's student in the Engineering and Policy Analysis programme of TU Delft. At this point, I experience a unique combination of feelings. On one hand, there is a great pleasure from making it all the way to the end and having conducted a project that I am proud of. On the other hand, the awareness of how much I will miss the wonderful moments of the master's is already kicking in. Yet, I am very hopeful and excited about the new adventures that life will bring for me.

I owe a debt of gratitude to several people who helped me out along my academic journey. Without the contribution of my thesis committee, this work would be nowhere near its quality. I thank Jazmin Zatarain Salazar for her valuable feedback, especially at the stages when I needed some guidance to move on. Even more importantly, she always expressed her trust in my capabilities to tackle challenging problems. I thank Özge Okur for taking time to think through my plans and providing the out-of-the-box perspective with her suggestions. Our discussions made a major impact on how I shaped my analysis. Jan Kwakkel's research is a great inspiration for the methods I used in this study. His presence in the committee gave me the confidence of having access to the right source of information when I needed. I cannot overstate how much I learned about organising my code only from two e-mails with ten bullet points. Finally, I thank Seleshi Yalew for introducing me to the context of the Nile Basin with his profound knowledge on the case. Our conversations had large impact on how the conceptual model of the Nile system was built. I am genuinely thankful to Gönenç Yücel and Servaas Storm for their sincere support in my pursuit of this degree. The soon-to-be-doctor Javanshir Fouladvand has a special place in my recently started research career. I not only learned a great deal from our collaboration but also truly enjoyed the time we spent together.

For sure, I owe the most to my family. My parents have always stood behind every step I took. My sister and nephew Emir Alp cheered me on our video calls with Emir not getting bored of asking me the names of chess pieces each time. I thank Yaren for making me always feel supported and loved. She has been my shoulder to cry on at the stressful moments and the first person with whom I shared my breakthrough moments. Moreover, I thank all my friends for making life brighter!

Finally, this work is dedicated to my beloved uncle, Mehmet Yılmaz who tragically passed away soon after I came to the Netherlands for my studies. I have no doubt he would have been very interested in discussing about my thesis and bring his original perspective.

An aerial photograph of a wide river basin, likely the Nile, showing a dam structure in the middle ground. The river is surrounded by lush green vegetation and some buildings on the left bank. The background features rolling hills under a clear sky.

## ABSTRACT

Water storage and diversion capacity of reservoirs in the Nile Basin are benefited for various purposes including agricultural irrigation and hydroenergy production. Filling and operation of the recently constructed Grand Ethiopian Renaissance Dam (GERD) have been subject to heated debate for its implications on downstream countries Sudan and Egypt. In this study, we investigated trade-offs between the objectives of the three countries by formulating the problem as many objective optimisation. To this end, we built a simulation model conforming to the evolutionary multi-objective direct policy search (EMODPS) framework. Based on the optimisation results, we discovered two scenarios under which trade-offs exhibit diverging patterns. Our findings suggest that 1) aggressive filling strategies create evident trade-offs between the hydroenergy generation objective of Ethiopia and consumptive uses of Sudan and Egypt, 2) growing demand in the long-term brings the dilemma of maintaining dams operational versus satisfying the demand and 3) increased demand pressure reinforces trade-offs between Egypt's aggregate deficit minimisation and Ethiopia's hydropower maximisation objectives. Our results highlight the potential of compromise policies in managing the objectives of all stakeholders without imposing heavy sacrifices. These policies represent an opportunity for cooperative operation of the dams through which multiple challenges facing the basin can be addressed.

# CONTENT

1	INTRODUCTION	2
1.1	The Nile River Basin	2
1.2	Research Objective	3
1.3	Literature Review	3
1.3.1	Optimal Reservoir Control	4
1.3.2	Dealing with Uncertainty	5
1.3.3	Studies on the Nile	6
1.3.4	Knowledge Gap	6
1.4	Research Question	7
1.4.1	Sub-questions	7
1.5	Organization of the Report	7
2	STUDY AREA	8
2.1	Actor Perspective	9
2.1.1	Ethiopia	9
2.1.2	Egypt	10
2.1.3	Sudan	11
3	METHODS	12
3.1	EMODPS Methodology	12
3.1.1	Modelling the System	14
3.1.2	Policy Function	14
3.2	Simulation Model	16
3.2.1	Model Conceptualisation	16
3.2.2	Model Formulation	19
3.2.3	Data Requirements	23
3.2.4	Key Assumptions	25
3.3	Experimental Setup	26
3.3.1	Baseline Optimisation	26
3.3.2	Uncertainty Analysis	26
4	RESULTS	29
4.1	Baseline Optimisation	29
4.1.1	Objective Trade-offs	29
4.1.2	Physical System Implications	32
4.2	Uncertainty Analysis	36
4.2.1	Global Sensitivity Analysis	36
4.2.2	Robustness of Policies	37
4.2.3	Scenario Discovery	40
4.2.4	Trade-offs under Scenarios	42
5	DISCUSSION	45
5.1	Practical Implications	45
5.1.1	Fillings and Operations of the GERD	45
5.1.2	Challenge of Demand Growth	45
5.1.3	Impacts on Sudan	46
5.1.4	Room for Cooperation	46

5.2	Limitations . . . . .	46
5.2.1	Conceptual Limitations . . . . .	46
5.2.2	Methodological Limitations . . . . .	47
6	CONCLUSION . . . . .	48
6.1	Addressing the Research Question . . . . .	48
6.2	Policy Recommendation . . . . .	49
6.3	Future Research . . . . .	50
A	APPENDICES: METHODS . . . . .	59
A.1	Conceptual Model . . . . .	59
A.1.1	Model Components in Geographical Context . . . . .	59
A.1.2	Component Specification . . . . .	60
A.2	Specific Model Equations . . . . .	61
A.2.1	GERD Inflow . . . . .	61
A.2.2	Roseires Inflow . . . . .	61
A.2.3	Upstream Sennar Received Flow . . . . .	61
A.2.4	Sennar Inflow . . . . .	61
A.2.5	Gezira Received Flow . . . . .	61
A.2.6	Downstream Sennar Received Flow . . . . .	61
A.2.7	Taminiat Received Flow . . . . .	61
A.2.8	Hassanab Received Flow . . . . .	62
A.2.9	HAD Inflow . . . . .	62
A.2.10	Egypt Received Flow . . . . .	62
A.3	Reservoir Data . . . . .	63
A.3.1	Hyro-power Generation Data . . . . .	63
A.3.2	Elevation-Area-Storage Curves . . . . .	64
A.3.3	Evaporation Rates . . . . .	65
A.3.4	Minimum and Maximum Release Constraints . . . . .	66
A.4	District Demand Data . . . . .	67
A.5	Epsilon Values . . . . .	68
B	APPENDICES: RESULTS . . . . .	69
B.1	Convergence Analysis . . . . .	69
B.2	Physical System Implications . . . . .	70
B.3	Dimensional Stacking . . . . .	74
B.4	Scenario Descriptions . . . . .	77

## LIST OF FIGURES

Figure 1.1	Illustration of the XLRM framework . . . . .	5
Figure 2.1	Geographical view of the study area . . . . .	9
Figure 3.1	Visual summary of the EMODPS methodology . . . . .	12
Figure 3.2	Structure of the RBF network . . . . .	15
Figure 3.3	Visual representation of a single Gaussian RBF calculation . . . . .	15
Figure 3.4	Topology of the conceptual model . . . . .	18
Figure 3.5	Flowchart of simulation run time . . . . .	22
Figure 3.6	Average monthly inflow of three main tributaries under baseline conditions . . . . .	24
Figure 4.1	Parallel coordinates plot of Pareto-optimal solutions of baseline optimisation . . . . .	30
Figure 4.2	Overall trade-off patterns within the full Pareto front . . . . .	31
Figure 4.3	Physical system implications of different policies on the GERD . . . . .	33
Figure 4.4	Physical system implications of different policies on Egypt . . . . .	35
Figure 4.5	Gezira received flow versus demand with Best Ethiopia Hydropower policy . . . . .	36
Figure 4.6	Best performers for each objective in the uncertainty space . . . . .	39
Figure 4.7	Dimensional stacking performed for different outcomes of interest . . . . .	41
Figure 4.8	Overall trade-off patterns under the <i>Extreme Stress Scenario</i> . . . . .	43
Figure 4.9	Overall trade-off patterns under the <i>High Blue Nile Scenario</i> . . . . .	44
Figure A.1	Geographical schematic of the scope . . . . .	59
Figure A.2	UML class diagram representation of model objects . . . . .	60
Figure B.1	$\epsilon$ -progress and hypervolume convergence . . . . .	69
Figure B.2	Physical system implications of different policies on the GERD . . . . .	71
Figure B.3	Physical system implications of different policies on Egypt . . . . .	72
Figure B.4	Gezira received flow versus demand with all policies . . . . .	73
Figure B.5	Dimensional stacking for Egypt's irrigation deficits . . . . .	74
Figure B.6	Dimensional stacking for Sudan's irrigation deficits . . . . .	75
Figure B.7	Dimensional stacking for reservoir related objectives . . . . .	76

## LIST OF TABLES

Table 3.1	Overview of optimisation objectives . . . . .	22
Table 3.2	Summary statistics used to generate streamflows of major tributaries . . . . .	24
Table 3.3	Overview of uncertain variables and ranges . . . . .	27
Table 4.1	Feature scores of uncertain parameters on each outcome calculated using extra trees algorithm . . . . .	37
Table 4.2	90th percentile maximum regret scores of policies on each objective	37
Table 4.3	Ranges of objectives achieved by optimized policy set under different scenarios . . . . .	42
Table A.1	Overview of hydropower generation data . . . . .	63
Table A.2	Elevation-Area-Storage curves for reservoirs . . . . .	64
Table A.3	Evaporation rates for reservoirs per month of the year ( <i>cm</i> ) . . . . .	65
Table A.4	Minimum and maximum release for the GERD . . . . .	66
Table A.5	Minimum and maximum release for the Roseires . . . . .	66
Table A.6	Minimum and maximum release for the Sennar . . . . .	66
Table A.7	Minimum and maximum release for the HAD . . . . .	66
Table A.8	District demand data . . . . .	67
Table A.9	Epsilon values used in the optimisation for each objective . . . . .	68
Table B.1	Description of selected scenarios . . . . .	77

## ACRONYMS

**ANN** Artificial Neural Network. 14

**BCM** Billion Cubic Meters. 8

**DMDU** Decision Making Under Deep Uncertainty. 5

**DPS** Direct Policy Search. 4

**EMA** Exploratory Modelling and Analysis. 26

**EMODPS** Evolutionary Multi-Objective Direct Policy Search. 4

**GERD** Grand Ethiopian Renaissance Dam. 3

**HAD** High Aswan Dam. 6

**masl** Meters Above Sea Level. 18

**MORDM** Many-Objective Robust Decision Making. 5

**MW** Megawatt. 8

**NFE** Number of Function Evaluations. 13

**PSO** Parametrization-Simulation-Optimization. 4

**RBF** Radial Basis Function. 14

**RDM** Robust Decision Making. 5

**SDP** Stochastic Dynamic Programming. 4

**SOW** States of the World. 5



# 1

## INTRODUCTION

In response to growing multi-sector demand for water worldwide, river basins are increasingly controlled by the construction of new dams (Zarfl et al., 2014). The positive trend is expected to remain strong in the coming century too (Giuliani et al., 2021; World Bank, 2010). This development is a reflection of the notion that dams are well established means of controlling water availability in river basins. However, construction of a new dam is usually a costly infrastructure investment (Ansar et al., 2014). Moreover, solely having dams is not sufficient to address water related challenges in a river basin. Operating a dam or a system of dams by deciding on how much and when to release water is a pivotal policy problem as the water storage and diversion capacity of reservoirs are benefited for agricultural irrigation, hydroenergy production, flood protection and more (Giuliani et al., 2014; Hakimi-Asiabar et al., 2010).

Challenges of operating reservoir systems are not limited to the multi-sector nature of the demand. In the context of large river basins, it is likely that different administrative zones, be it province, state or country, compete over the right to exploit the resource, particularly for consumptive uses (Keskinen et al., 2016; Liu et al., 2011). Moreover, growing populations and economic activity all over the world lead to increases in the quantity of water demanded to an extent that challenges the renewal rate of the essential resource (Kasprzyk et al., 2009; Liu et al., 2011). Not only the demand side puts pressure on the water balance but also the uncertainty of the supply has grown significantly with the influence of climate change on the occurrence of extreme rainfall and evaporation events (Giuliani et al., 2014; Kasprzyk et al., 2009; Williams, 2009).

### 1.1 THE NILE RIVER BASIN

The Nile, as famously known for giving birth to one of the earliest human civilisations, is a major river located in northeast Africa (Dumont, 2009; NBI, 2022). Its basin is a highly critical resource for the region; it plays a key role in supplying the riparian countries with water to be used for several purposes including hydropower generation, municipal, industrial and agricultural consumption (NBI, 2022). Spreading over 10 countries as a major watershed, the basin is an area where debates over the right to use Nile's water have been taking place for years (Swain, 2002). With more than a dozen of reservoirs scattered in Egypt, Sudan and Ethiopia (NBI, 2022), political tensions have been palpable especially in the eastern part of the Nile Basin (Swain, 2002). Despite being the most downstream country with respect to its riparian position, Egypt has been the country

that exploited the Nile water the most to date (NBI, 2022; Amer, 2015). However, this hegemony has been increasingly challenged by Ethiopia especially with their unilateral action to start the project of Grand Ethiopian Renaissance Dam (GERD) in 2011 (Sharaky et al., 2019; Pemunta et al., 2021).

While Ethiopia communicate that the main ambition behind the GERD project is to unlock hydropower potential of Ethiopian highlands (Soliman et al., 2016), therefore blocking the flow of water will be of no interest to them, downstream countries Sudan and Egypt tend to view it as a threat to their water security and independence (Amer, 2015; Pemunta et al., 2021). One particular concern of the downstream water users is the filling period of the GERD's large reservoir. Negotiations to reach a consensus over a filling scenario remain in a state of deadlock with increased tension between parties (Pemunta et al., 2021).

In addition to the political and technical complexities brought by the GERD to the management of the Nile system, the river is famously known for the adverse effects of water inflow variability (Abu-Zeid and Biswas, 1991). Experience of drought and flood events is commonplace (Taye et al., 2015). Moreover, increasing populations and economic production in the basin signal to a rise of the demand for water (NBI, 2022). Therefore, designing operating policies for reservoirs in the basin is a multi-faceted problem that needs the consideration of physical infrastructure, geopolitics as well as socioeconomic and hydro-climatic uncertainties.

## 1.2 RESEARCH OBJECTIVE

The main objective of this study is to examine alternative policies that govern the release operations of the reservoirs in the Nile Basin. One driver of this ambition is the current political debate over the water use of upstream and downstream countries. High-level impression from the problem situation implies a trade-off between the existence of the GERD and consumptive water needs of Egypt and Sudan. Nonetheless, it is worth questioning whether this stems from a legitimate trade-off or the political will of national authorities for water independence and security. Moreover, if such trade-offs exist, would it be possible to use modelling and optimisation approaches to formulate effective control policies which minimise potential damage to all stakeholders? Finally, given the ambition to improve operational policies, how can the implications of major uncertainties on trade-offs be captured?

## 1.3 LITERATURE REVIEW

We reviewed relevant scientific literature on three branches. Firstly, state-of-the-art theory on optimal reservoir control methods was compiled to support the selection of methods. Moreover, we examined the literature that addresses the integration of uncertainty considerations. Finally, previous reservoir management studies conducted on the Nile Basin were synthesised to diagnose the status of the knowledge base. Several key concepts will be defined throughout this section. Once a key concept is mentioned for the first time, it will be written in italic letters.

### 1.3.1 Optimal Reservoir Control

A pronounced observation from the reservoir control literature is that there is an evolution from traditional exact approaches towards simulation-based heuristic methods. Irrespective of the solution method, model formulations mostly build upon *mass-balance equations* which specify the mathematical relationship between reservoir storage volumes across consecutive time indices (Giuliani et al., 2021). An essential element of that relationship is the release decisions from reservoir(s) which is what the operators seek to optimize. During the last few decades prior to the millennium, the *traditional approach* to make release decisions was using rule curves i.e., rules that indicate the ideal amount of water storage depending on the period of a year (Giuliani et al., 2014). A common approach to find the optimal operation strategy back then was to adopt the linear programming family methods with assumed baseline conditions for future values (Zatarain Salazar et al., 2016).

Approaching 2000s, literature grew into a direction that tackles the inflexibility of rule curves in responding to the dynamics of a system. Oliveira and Loucks (1997) developed a framework by applying a genetic search algorithm to find optimal release decisions, conditioned on more information than mere storage levels. The key to the success of this approach was the idea to specify the input-output relation of a *policy function* in a parametric manner. Scholars have increasingly used exact methods such as *stochastic dynamic programming* (SDP) to optimise those policy function parameters with respect to the particular objectives of a problem (Giuliani et al., 2021). Nonetheless, it was later acknowledged that SDP-based methods have major limitations especially when they are applied on multi-reservoir, multi-objective systems. Attempting to scale up either of the two increases computational burden exorbitantly, hence rendering the approach infeasible quickly (Giuliani et al., 2015). Moreover, multi-objective characteristic of a problem requires *a-priori* specification of the relative importance of different objectives (Zatarain Salazar et al., 2016), which is not only a challenge for the decision-makers (Giuliani et al., 2014) but also a major source of uncertainty on its own (Walker et al., 2013).

To cope with the discussed challenges, researchers came up with alternative problem formulations. Koutsoyiannis and Economou (2003) championed the *parametrization-simulation-optimization* (PSO) approach which differs from the previous methods in the sense that it utilises systematic simulation runs as the engine for optimisation, instead of an exact algorithm. It was shown that the new approach had considerable computational advantages without solution inferiority (Koutsoyiannis and Economou, 2003). Later, the field borrowed the term *direct policy search* (DPS) from the general control theory literature and used it as a replacement for PSO (Zatarain Salazar et al., 2016). Building on top of that, advances in the machine learning theory inspired the water management field to use *evolutionary algorithms*, which brought the advantages associated with the state of the art machine learning knowledge (Maier et al., 2014). Finally, Giuliani et al. (2015) formalized the framework of *evolutionary multi-objective direct policy search* (EMODPS) by coupling the DPS approach with multi-objective evolutionary algorithms. These theoretical foundations paved the way for real-life case study applications with the EMODPS methodology.

### 1.3.2 Dealing with Uncertainty

In the context of policy analysis, a rigorous analysis and classification of different types of uncertainties was made by Walker et al. (2013). This work, building on top of the XLRM framework of Lempert et al. (2003), identified four possible *locations* where the uncertainties exist in any system. Considering the illustration of the XLRM framework given in figure 1.1, Walker et al. (2013) assert that uncertainty can be about external factors (X) and relationships in system (R) which combine and lead to uncertainty in the outcomes of interest (M). Moreover, relative importance placed on different performance metrics by stakeholders of a problem adds to the uncertainty space.

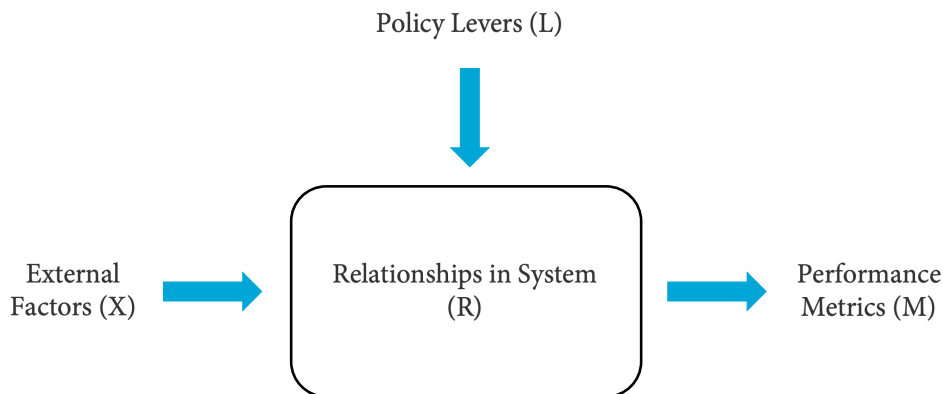


Figure 1.1 Illustration of the XLRM framework. Taken from Kwakkel (2017).

In essence, a core idea of many-objective optimisation approaches is to deal with this last uncertainty type. Irrespective of the exact solution algorithm or heuristic, the output of such a procedure is a set of solutions that constitute a *Pareto-optimal* front with regard to the objectives of the problem. Essentially, it is a set of solution alternatives where the decision maker can improve the system performance with respect to an objective only at the cost of another (Deb et al., 2002). This approach escapes from *a-priori* prioritisation among performance metrics by first incorporating multiple rival framings of stakeholder objectives into the problem formulation (Quinn et al., 2017), and then evaluating potential trade-offs after the optimisation procedure (Reed et al., 2013).

There are several frameworks developed to support decision making under deep uncertainty (DMDU) (Marchau et al., 2019). Robust decision making (RDM), introduced by Lempert et al. (2003), has become a prominent paradigm in the domain of water management. This family of methods is based on the philosophy of stress-testing policy alternatives under plausible divergent future states of the world (SOWs). Taking a step further from solely re-evaluating known policies, Kasprzyk et al. (2013) generated policy alternatives through many-objective evolutionary algorithms and coupled many-objective optimisation with RDM. This methodology which is referred to as many-objective robust decision making (MORDM), has been widely applied in water research since then (Amaranto et al., 2022; Bertoni et al., 2019; Herman et al., 2015).

### 1.3.3 Studies on the Nile

There have been previous studies which applied optimisation for reservoir operations on the Nile Basin. Even the highly cited initial paper that introduced the application of SDP to the domain used the data of High Aswan Dam (HAD) as the test case (Stedinger et al., 1984). There are other studies which also used reservoirs in the Nile Basin as test cases for methodological contributions without much reflection on the implications for the real problem in the region (Sangiorgio and Guariso, 2018; Stamou and Rutschmann, 2018; Guariso and Sangiorgio, 2020). Yet, the number of studies that adopt reservoir modelling with more policy analytic focus started to increase after the initiation of the GERD project in 2011.

Initial filling of the GERD has been a subject that received ample scholarly attention. Researchers emphasised various risks associated with filling (Basheer et al., 2020; Wheeler et al., 2020; Wheeler and Caplan, 2020). Basheer et al. (2020) took the problem from a technical design perspective and reflected on the implications of engineering constraints on release capacity. On the other hand, with the motive of finding cooperative optimal filling strategies, Wheeler et al. (2016) modelled a large part of the basin to include the operations of 9 dams including the GERD. In a later study, Wheeler et al. (2020) applied a similar modelling approach and concluded that with high levels of cooperation, risk of water shortages downstream during the filling is minimal.

There have been more studies that showed the merits of cooperation while operating the reservoirs in the basin. Verhagen et al. (2021) adopted a comprehensive water-energy-food nexus modelling approach to find optimal reservoir control policies under varying levels of cooperation among countries. This study also made a quantification of trade-offs between hydropower and agricultural irrigation within each of the three Eastern Nile countries. Wheeler et al. (2018) had the most similar research endeavour with respect to the objectives of this thesis project. The authors used many-objective optimisation of reservoir release decisions to support stakeholder negotiations for basin-wide cooperative management. Assuming the GERD is already filled, they limited the optimisation on the parameters of pre-defined release rules for the GERD and the HAD.

### 1.3.4 Knowledge Gap

Based on this literature review, we identified a selection of points as currently missing. Firstly, none of the previous studies that considered the GERD in reservoir operations optimisation explored practical implications of the policy alternatives. Therefore, no clear links have been established between objective trade-offs and the dynamics of the physical system variables. Secondly, cooperative management setups for reservoir operations including the GERD were explored previously; nonetheless, none of those studies generated adaptive policies to the best of our knowledge. Finally, despite pressing uncertain factors, the discussion over how management strategies would play out with different future SOWs is underdeveloped. Current literature on the Nile Basin has neither looked into the robustness of policy alternatives nor investigated the stability of trade-offs with respect to different future scenarios.

## 1.4 RESEARCH QUESTION

Considering the initial research objective and the identified gaps in the literature, the main research question of this thesis project was formulated as:

*“How can the trade-offs between different water uses in the Eastern Nile Basin be explored under changing socioeconomic and hydro-climatic uncertainties adopting many-objective optimisation approach?”*

The main goal of this project is to devise a procedure to identify trade-offs yielded by different candidate operational policies after optimising them for the objectives of stakeholders. These candidate policies constitute a set to be experimented under different SOWs.


### 1.4.1 Sub-questions

In addition to the main research question, four sub-questions were formulated as logical subsequent inquiries needed to address the main question:

- **SQ1:** What are the key water related objectives of stakeholders in the Eastern Nile Basin?
- **SQ2:** How can the system of reservoirs be modelled in order to optimise release decisions for problem objectives?
- **SQ3:** What are the trade-offs revealed by Pareto-optimal policy alternatives?
- **SQ4:** How do trade-offs differ with respect to alternative hydrology and demand growth scenarios?

## 1.5 ORGANIZATION OF THE REPORT

This introductory chapter is followed by chapter 2 where we dive further into the problem context to identify key actors and their objectives. The methods of the study is presented in chapter 3, which is divided into three sections. Firstly, in section 3.1, we provide an overview of the adopted modelling approach. Following this section in 3.2, we explain the model we built to simulate the system and obtain the outcomes of interest. Lastly, in section 3.3, the experimental strategy is given. Results of the experiments are presented in chapter 4 whereas the discussion based on these results can be found in chapter 5. Finally in chapter 6, research questions are readdressed and the report is concluded with policy recommendations and future work.



## 2

## STUDY AREA

Besides being the longest river in the world (Dumont, 2009), the Nile River Basin hosts more than 257 million people whose livelihood and well-being depend directly on its water (NBI, 2022; Williams and Talbot, 2009). The basin area is densely populated by 54% of the population of the 11 riparian countries, and corresponds to ~10% of the African continent (Dumont, 2009; NBI, 2022). Egypt, Sudan and Ethiopia—three countries that constitute the eastern Nile region (Arsano, 2007)—cover around two thirds of the total basin area (NBI, 2022).

There are three main tributaries furnishing the total annual Nile flow: the White Nile, the Blue Nile and Atbara rivers (Talbot and Williams, 2009). The White Nile, which is the main outlet of Uganda's Lake Victoria (NBI, 2022), provides ~32% contribution to the main flow (Wheeler et al., 2020). Due to the stability of its flow across seasons, this tributary plays a critical role especially during severe drought periods (Talbot and Williams, 2009; Wheeler et al., 2020). The Blue Nile and Atbara rivers, both originating in Ethiopian highlands (NBI, 2022), contribute to the main flow by ~55% and ~13% percent respectively (Wheeler et al., 2020). In contrast to the White Nile, flow from these two tributaries are highly seasonal as a result of the wide variability of rainfall in Ethiopian highlands (Sutcliffe, 2009). Figure 2.1 provides the geographical summary of the Eastern Nile Basin.

The Blue Nile, with its considerable discharge volume and mountainous course, has great hydropower potential (Dumont, 2009; NBI, 2022). This potential has been underlined for decades (Wheeler et al., 2020); nonetheless, it remains mainly untapped and has only recently been materialized by Ethiopia (Block, 2007; Dumont, 2009). The GERD, being constructed near Sudanese-Ethiopian border (Wheeler et al., 2020), is the most remarkable attempt to close this gap; with its 6450 megawatt (MW) electricity generation capacity and 74 billion cubic meters (BCM) total storage, the hydroelectric power plant will be the largest of the continent (Pemunta et al., 2021; Wheeler et al., 2020). However, there are arguments that sizing of the GERD has been determined over-optimistically considering the flow regime of the Blue Nile (Kumagai, 2016).

As filling and operation of the facility will have unpredictable impacts on flow received by downstream riparian countries, the project brought along strong opposition from Egypt and Sudan—the former being more vocal (Falco and Fiorentino, 2022; Pemunta et al., 2021; Wheeler et al., 2020).



Figure 2.1 Geographical view of the study area

## 2.1 ACTOR PERSPECTIVE

We regard Ethiopia, Egypt and Sudan as the main actors in this study. Decision-making authorities are bodies under national governments. They are representing the small stakeholders' interest within geographical border. Unsurprisingly, this set of actors are prevalently preferred across an extensive portion of studies that focus on GERD (Abdelhady et al., 2015; Amer, 2015; Falco and Fiorentino, 2022; Elsayed et al., 2020; King and Block, 2014; Pemunta et al., 2021; Wheeler et al., 2020).

### 2.1.1 Ethiopia

Ethiopia, much like the other two countries considered in this study, has deep historical roots in the Basin (Arsano, 2007). The Ethiopian population is largely rural with over 80% of Ethiopians living in rural areas and agricultural with over 70% of Ethiopians being employed in agriculture (NBI, 2022). Electricity access is not an established standard in the country; only 27% of the population is connected to the grid (NBI, 2022).



Ethiopian government has long been demonstrating ambition towards improving country's water resources management, which is admitted to be a bottleneck for the economic affluence of the country (Arsano, 2007). Nonetheless, steps taken regarding the country's water development challenge the status-quo and hydro-hegemony in the basin (Arsano, 2007). Ethiopia faces strong inertia despite the fact that they hold the upper hand in terms of their riparian position—being located on the upstream—and have growing exploitation potential—having increasing population and consistently demonstrating growing GDP (World Bank, 2021).

Zeitoun and Warner (2006) argue that this inertia is due to the power relations in the basin, which play the decisive role in determining levels of control over water resources that riparian countries can establish. Indeed, these power relations were in effect when the treaties of 1929 and 1959 were signed. The former agreement granted Egypt the right to veto projects influencing their water share whereas the latter concerned allocation of Nile water flow between Egypt and Sudan—by 75% and 25% respectively (Yalew et al., 2021). Ethiopia contests the bindingness of these treaties underlining that they were excluded as a party in both these settings (Arsano, 2007).

Since the late seventies, micro-dams constructed by individual farmers to control water flow constituted an important part of the counter-hegemony strategies adopted by Ethiopia (Berhane et al., 2016; Ibrahim, 2010; Zeitoun and Warner, 2006). These arrangements gained speed around mid-nineties (Berhane et al., 2016), the times that correspond to establishments of the Ministry of Water Resources and complementary institutions (Arsano, 2007). Nonetheless, besides operating in an uncoordinated manner (Ibrahim, 2010), these micro-dams mainly served irrigational purposes and did not target the unrealised hydropower potential of the country.

Initialisation of GERD's construction in 2011, which marked the greatest challenge against the hegemony, was a unilateral action (Pemunta et al., 2021). With the GERD, Ethiopian authorities aim at catalysing economic growth through improved electricity access in the country and promoted trade in the basin and beyond Pemunta et al. (2021); Soliman et al. (2016). Government of Ethiopia communicates the expected annual hydroenergy generation from the GERD as 16 TWh (Wheeler et al., 2020).

### 2.1.2 Egypt

Across riparian countries, Egypt is an exceptional case in terms of electricity and clean water access. Over 99% of the population, regardless of rural-urban distinction, is connected to electricity and clean water networks (NBI, 2022). Egypt also marks the highest GDP per capita among riparian countries with a score of over 3.800\$—which is way above those of Sudan (764.3\$) and Ethiopia (944.0\$) (World Bank, 2021).

Egyptian economy, agriculture in particular, enjoyed the country's position as a main beneficiary of Nile water (Arsano, 2007). Following the Egyptian-Sudanese treaty of 1959, authorities initiated construction of the HAD to further improve security of water supply (Arsano, 2007). With the HAD, Egypt has more control over the Nile flow and manages releases to meet the seasonal demand—which peaks in the summer (Wheeler et al., 2016). Nevertheless, a major downside of the HAD is its large surface, which

causes on average 15 BCM water loss due to evaporation each year (Elba et al., 2014). Diversification—and thereby strengthening—of the economy as well as import of water intensive products are key to Egypt’s water security strategy (Allan, 2009).

Egypt argues that the GERD would cause a considerable decrease in downstream water flow which would hinder food and energy security in the country (Falco and Fiorentino, 2022). Egypt attempted to undercut the project through strategies varying from lobbying financial providers (such as African Development Bank and the World Bank) to threatening with military action (Pemunta et al., 2021). The project was still realised with internal funding and financial support from China (Makonye, 2021; Pemunta et al., 2021).

A relieving aspect of the GERD project in terms of Egypt’s interests is the fact that the reservoir is situated near Sudanese–Ethiopian border. This choice of location emphasizes that Ethiopia is committed to hydropower generation strategy instead of irrigation development—which would cause an increase in Ethiopia’s water withdrawal from Blue Nile (Whittington et al., 2014). Furthermore, since the hydropower plant creates an encouraging factor for Ethiopia to increase water flow into the reservoir, downstream countries can benefit from internal re-direction of water (Whittington et al., 2014). Nonetheless, there is limited discussion over this aspect in the political arena.

### 2.1.3 Sudan

Similar to Egypt and Ethiopia, Sudan’s economy is identified by a strong agricultural focus with around 50% of the population working in agriculture (NBI, 2022). Clean water access in the country is around 86% and 61% in urban and rural areas respectively (NBI, 2022). Similar to Ethiopia, there is large room for improvement in electricity access in the country with only 35% of the population having access currently (NBI, 2022).

Modern agriculture in Sudan goes back to the colonial era, 1920s (Arsano, 2007). Irrigation potential of the country was first explored with the development of Gezira irrigation scheme followed by expansions in other districts (Arsano, 2007). Considering that agriculture is recognized as a competitive advantage for Sudan (Arsano, 2007), decisions influencing the main tributary of the Nile are of crucial importance to Sudan as they are to Egypt.

That being said, position of Sudan on the subject of the GERD is not identical to that of Egypt. Although the Sudanese and Egyptian authorities shared a similar initial reactions to the project by voicing concerns about their national and water supply security, Sudanese opposition weakened over time (Falco and Fiorentino, 2022). Main reason for this change was about the long-lasting battle that Sudan has been fighting against flooding. Field experts and some politicians argued that regulation of highly variable Blue Nile water flow would be beneficial for Sudan (Falco and Fiorentino, 2022).

# 3

## METHODS

### 3.1 EMODPS METHODOLOGY

Considering the evolution of reservoir control methods outlined in the literature review, we chose EMODPS as the core methodology to formulate an optimisation model of the Nile system. To summarise, it entails embedding a nonlinear approximating network as a policy function into the simulation model which calculates release decisions at each time step of a run, based on the state of the system at the particular instance. During the optimisation, parameters of the policy function are improved at each generation of a many objective evolutionary algorithm run (Giuliani et al., 2015). In the ideal scenario, solution set converges to the global optimum of the problem which yields a Pareto-optimal set of objective values. A visual summary of the EMODPS methodology built on top of the XLRM framework is given in figure 3.1.

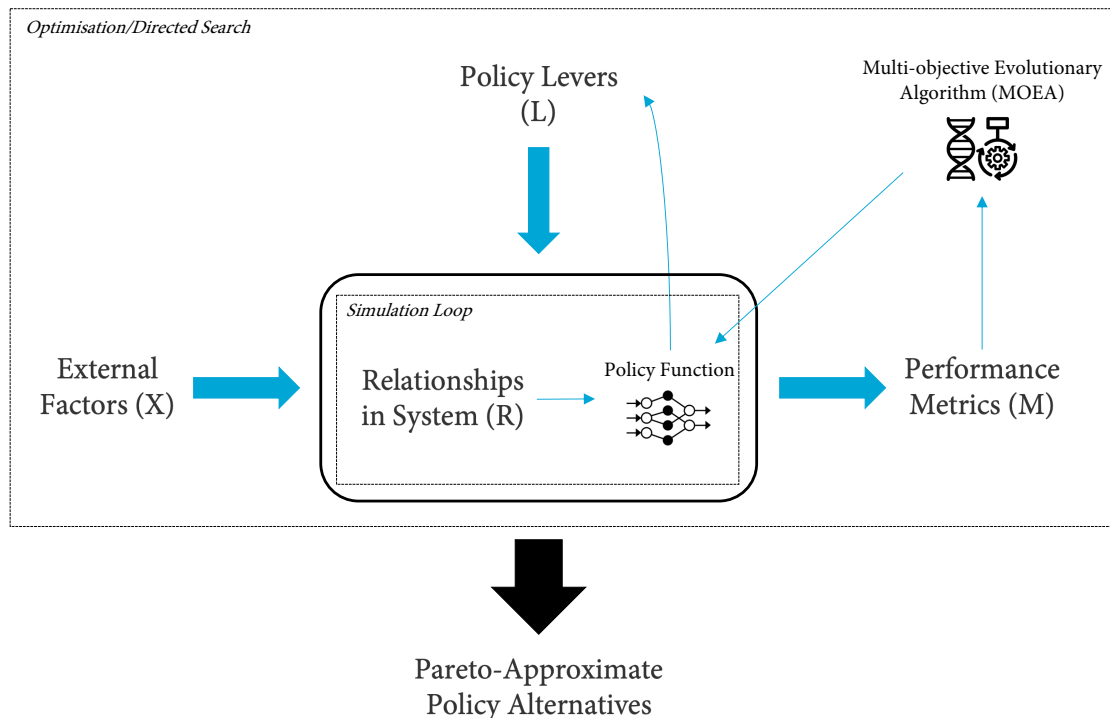


Figure 3.1 Visual summary of the EMODPS methodology

EMODPS was chosen as the core modelling approach because of its following strengths:

- *Flexibility in modelling*: EMODPS leaves great flexibility in formulating and solving many-objective problems (Zatarain Salazar et al., 2016). Since the objective value calculations are done through running a simulation model, any extension to the model is possible as long as an algorithmic description can be made.
- *Less computational burden*: Unlike the exact methods such as SDP, computational cost of EMODPS does not grow uncontrollably with respect to increasing system complexity and it gives an approximation of the Pareto front starting from the first generation of solutions (Giuliani et al., 2015). Therefore, it is a good fit for a multi-reservoir, many-objective system such as the Nile.
- *Adaptive policies*: Since release decisions are conditioned on the system state and hence adaptive, final set of policy alternatives are more robust against changing system conditions compared to the solutions obtained via the optimisation of the equivalent open-loop problem (Giuliani et al., 2015).

Nonetheless, there are few limitations of the methodology:

- *Diversity of solutions*: An important concern about MOEAs is the diversity of the solution set (Laumanns et al., 2002). The more diverse values in the objective space yielded by the set of Pareto-optimal solutions, the more information is available to decision-makers when making judgements on trade-offs (Wang et al., 2017). Unless there is a mechanism to enhance diversity, solutions found by an evolutionary algorithm may not reflect a sufficiently wide range of objective value sets.
- *Convergence to optimality*: Convergence to optimality i.e., a state in the optimisation process where no other solution can strictly dominate any of the solutions in the final Pareto set, is never guaranteed with an evolutionary heuristic (Laumanns et al., 2002). A common approach is to keep track of improvement with respect to the number of function evaluations (NFEs) and end the procedure when the progress curve gets satisfactorily stable. However, this might take too many NFEs and hence too much computational cost.
- *Too many hyper-parameters*: Application of the EMODPS methodology requires determining many hyper-parameters which consist of the ones that are needed to set up the optimisation and the ones that shape the structure of the nonlinear approximating network.

To cope with the first two limitations, we consulted on the literature that tested the performance of different MOEAs regarding these concerns (Reed et al., 2013; Zatarain Salazar et al., 2016). We chose  $\epsilon$ -NSGA-II as the evolutionary algorithm to run the optimisation (Kollat and Reed, 2005). On a different six objective case study in the reservoir control domain, Zatarain Salazar et al. (2016) showed that  $\epsilon$ -NSGA-II is among the best performing algorithms with respect to search diversity and capability to escape from local optima.

In the literature, there is little guidance regarding strategies to cope with the last limitation. There are a few rule of thumbs mentioned on the shape of the policy function (Amaranto et al., 2022; Giuliani et al., 2015). We based hyper-parameter assumptions on such literature when available.

### 3.1.1 Modelling the System

Among the variety of modelling approaches for water systems described by [Castelletti and Soncini-Sessa \(2007\)](#), we adopted the family of *mechanistic models* which can be applied when there exists theories that quantitatively explain how the physical system works. The core mechanism in this case is the mass-balance equations which can be formulated for a single reservoir as follows ([Soncini-Sessa and Weber, 2007](#)):

$$s_{\tau+1} = s_{\tau} + Q_{\tau+1} - E_{\tau+1} - R_{\tau+1} \quad (3.1)$$

where  $s_{\tau}$  is the volume of water in the reservoir in the beginning of decision step  $\tau$ ,  $Q_{\tau+1}$  is the total inflow to the reservoir,  $E_{\tau+1}$  is the total net evaporation and  $R_{\tau+1}$  is the total volume of water released from the reservoir between decision steps  $\tau$  and  $\tau + 1$ . In this study, we selected the decision interval as a month because it is short enough to capture seasonal aspects yet sufficiently large to feasibly run a basin-wide long-term simulation.

Each element in equation 3.1 can be expressed in terms of the factors whose values are known at the instance of calculation. Among these elements, the one that adds most to the computational burden is the calculation of  $R_{\tau}$ . There are two reasons behind this. Firstly, a fresh release decision is calculated at each decision step by the policy function. More notably, within two consecutive decision instances, releases must not violate physical and/or normative constraints of the reservoir. This constraint check usually requires higher time fidelity than the decision interval. Essentially, the actual releases realised in finer time resolution are integrated over the decision interval to calculate  $R_{\tau}$  ([Soncini-Sessa and Weber, 2007](#)). After experimenting with alternatives, we set the integration step to half an hour.

### 3.1.2 Policy Function

There are a couple of alternative functions that are frequently used as policy structure in reservoir control domain. As the aim is to capture the most appropriate mathematical relationship between inputs of the policy function and release decisions, a common choice is to embed a highly flexible non-linear approximating network such as artificial neural networks (ANNs) and radial basis functions (RBFs) ([Giuliani et al., 2015](#)). In this study, our choice is to use a set of RBFs to parametrise the policy function because there is evidence obtained in case studies indicating that they outperform ANNs ([Giuliani et al., 2015](#)). Particularly, the structure adopted by [Giuliani et al. \(2020\)](#)—a weighted sum of Gaussian RBFs—is used as the function that returns the release decisions such as in equation 3.2:

$$u_{\tau}^k = u_{\theta}^k(\bar{z}_{\tau}) = \sum_{i=1}^n (w_i^k \phi_i(\bar{z}_{\tau}) + \alpha_k) \quad (3.2)$$

where  $u_{\tau}^k$  is the  $k^{th}$  release decision at month  $\tau$  and  $\theta$  is the parameter vector for RBFs defined as  $\theta = |c_{j,i}, b_{j,i}, w_i^k|$ .  $\bar{z}_{\tau}$  is the input vector such that  $\bar{z}_t = |z_{\tau,1}, \dots, z_{\tau,m}|$  and  $\alpha_k$  is

the constant adjustment parameter of the  $k^{th}$  release decision. An overview of the RBF network structure is given in figure 3.2

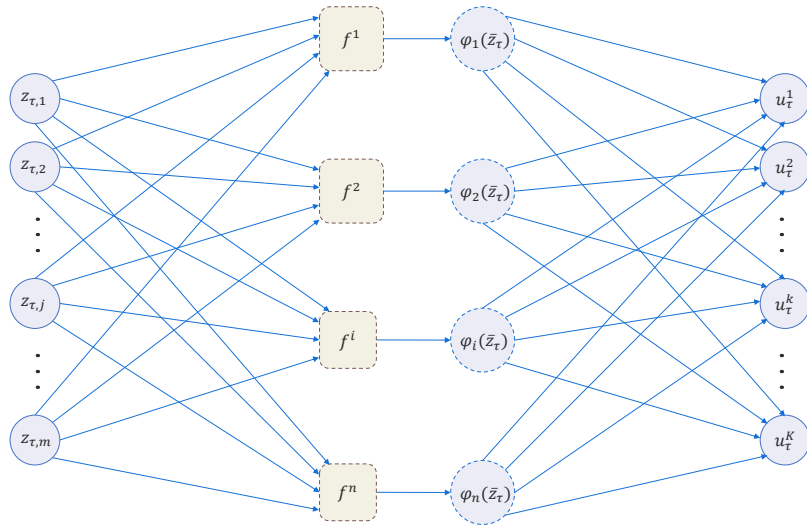


Figure 3.2 Structure of the RBF network. Each input variable  $z_{\tau,j}$  (on the left) feeds into every one of the RBF functions (in the middle) to calculate  $\varphi_i(\bar{z}_\tau)$ . Then weighted sum of all  $\varphi$  values return the release decision  $u_\tau^k$  (on the right).

Calculation in a single Gaussian RBF is done as in equation 3.3:

$$\varphi_i(\bar{z}_\tau) = \exp \left[ - \sum_{j=1}^m \frac{(z_{\tau,j} - c_{j,i})^2}{b_{j,i}^2} \right] \quad (3.3)$$

where  $c_{j,i}$  is the center and  $b_{j,i}$  is the radius parameters corresponding to  $j^{th}$  input and  $i^{th}$  RBF. An illustration of this calculation is given in figure 3.3.

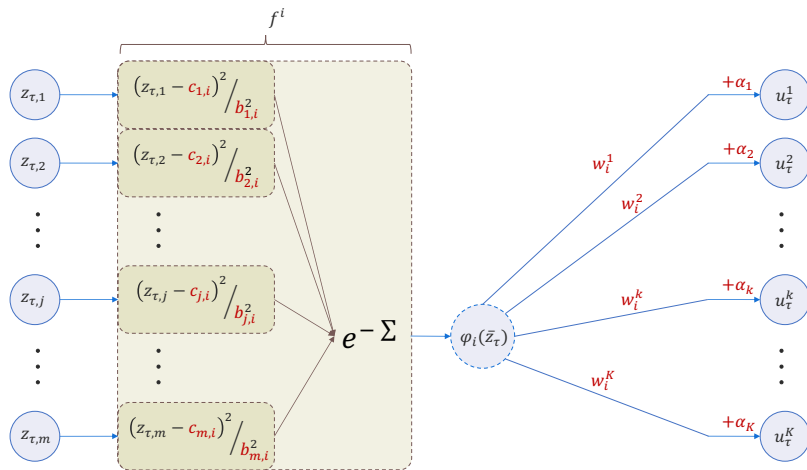


Figure 3.3 Visual representation of a single Gaussian RBF calculation. Free parameters to be optimised are illustrated in red colour. To calculate  $\varphi_i$ , the  $i^{th}$  RBF uses the center and radius parameters ( $c_{j,i}$  and  $b_{j,i}$ ) corresponding to  $j^{th}$  input. Sum of the illustrated calculations made for each input becomes  $\varphi_i$ ; through taking the inverse exponent of the Euler's number,  $e$ .  $u_\tau^k$  values are then calculated as weighted sum of  $\varphi_i$ s (with weight  $w_i^k$  and constant parameter  $\alpha_k$ ).

Specific inputs that pass the system state to the policy function is discussed in model description in the following section. As can be derived from figures 3.2 and 3.3, the total number of free parameters in a Gaussian RBF network is  $(2mn) + (nK) + K$ , where  $m$ ,  $n$ ,  $K$  are the total number of inputs, RBFs and release decisions respectively.

## 3.2 SIMULATION MODEL

Given the knowledge on the study area and the abstract description of the modelling approach, the simulation model that is used to run experiments was formalised. The main goal of this chapter is to present a reproducible and transparent model building process. Expectation from the process of modelling is to explore the system behaviour under varying uncertain conditions and policy alternatives. Therefore, a parametric implementation was made wherever applicable to test the model with different possibilities.

Software implementation of the model was done in the Python programming language because of its ease of use and wide availability of supplementary packages.

### 3.2.1 Model Conceptualisation

#### 3.2.1.1 Scope

The scope of the system that was modelled entails the following dimensions:

- *Geographical boundaries:* Among the three main tributaries of the Nile, Blue Nile is the only one that is thoroughly modelled in this study. There are two reasons for this choice. First, it is the tributary that contributes the most to the total flow of the Nile by far. In addition, the GERD—one of the main motivations of this study—is located on the Blue Nile. The White Nile and Atbara rivers are regarded as exogenous streamflows, the dynamics of which are not calculated via simulation but obtained as time-series inputs to the model. The most upstream element of the system in concern is the inflow of Blue Nile to the GERD. In the farthest downstream, we aggregate the water demand of Egypt and consider that as a single demand zone that the HAD serves.
- *Simulation horizon:* We run the simulation 20 years towards the future, between 2022-2042. We argue that 20 years is the minimum time-span that both covers the filling period of the GERD and leaves enough time to observe possible trade-offs during its operation.

#### 3.2.1.2 Cooperative Setup

A major assumption we made in this study concerns the cooperative setup for managing multiple reservoirs that were governed by different national authorities in reality. What we assume in this study is that a hypothetical central authority has full information over the whole basin and decides on the releases from all reservoirs. This assumption gives the currently non-existing flexibility to coordinate release decisions to the model. Since our aim is to obtain a diverse set of solutions which includes policies that prioritise

individual parties as well as the ones that requires them to make compromises, we decided to keep it free from the constraints of the strategic setup.

### 3.2.1.3 *Model Components*

We modelled the elements that either have an influence on the system state—which is determined by water storage in reservoirs—or are necessary for the calculation of problem objectives. These criteria led to the explicit modelling of four components: reservoirs, hydropower plants, irrigation districts and catchments.

#### **Reservoirs**

Reservoirs can change the system state in three ways. Apart from having the capacity to store and release water, considerable amount of loss occurs from their surface due to evaporation (Elba et al., 2017). We include four reservoirs in the scope of this study. They are the GERD, Roseires, Sennar and the HAD in the order from upstream to downstream. Although having relatively small storage capacities, Roseires (5.9 BCM) and Sennar (0.4 BCM) play important roles in meeting the demand of large agricultural irrigation schemes in Sudan (Wheeler et al., 2020). The HAD, with its large storage capacity (148 BCM), is the major water source of Egypt. Moreover, water level in the HAD is a good indicator of downstream impacts of the GERD as commonly used in the literature (Wheeler et al., 2018).

#### **Hydropower Plants**

Hydropower plants are modelled to calculate the amount of hydro-electric energy generation from dams. Each of the four dams in this study has the capacity to generate hydroenergy. Particularly, electricity generation from the GERD is one major objective from Ethiopia's viewpoint.

#### **Irrigation Districts**

Irrigation Districts are components we use to represent any major source of irreversible water consumption such as an agricultural irrigation scheme or an urban district with freshwater needs. Based on the amount of demand and water availability, part of the water flow is diverted and is lost from the system to meet the demand of an irrigation district. Given the geographical boundaries of the system, we included five irrigation districts located in Sudan and one aggregate irrigation district that represents the demand of Egypt. Using the same demand zone aggregation as in Wheeler et al. (2016), we incorporated the following districts: Upstream Sennar, Gezira-Managil, Downstream Sennar, Tamaniat to Hassanab, Hassanab to Dongola, and Egypt.

#### **Catchments**

A catchment is an area where precipitation is accumulated by the natural topography (Soncini-Sessa and Weber, 2007). Practically, it means an inflow of water to the system and hence a gain. Apart from the points where we treated the three main tributaries as joining to the system delineated in this study, we included five more catchments. Detailed model schematic provided by Wheeler et al. (2018) guided that selection.



## Objectives

Based on the analysis of the study area, we identified several prominent objectives from the perspectives of three countries. For Egypt, reliability of water supply is of fundamental importance; therefore, minimising demand deficits in Egypt is one of their major objectives. Furthermore, they are concerned with the water level in the HAD particularly when there is a risk that it falls below the minimum power generation elevation of 159 meters above sea level (masl) (Wheeler et al., 2018). Similar to Egypt, it is essential to meet the demand of agricultural irrigation schemes in Sudan. Deficits of demand districts in Sudan is aggregated to constitute another objective to be minimised. Although flood risk is also a major concern for Sudan during high flow seasons (Falco and Fiorentino, 2022), we did not consider flooding in this model. We argue that it is not suitable to model flood events reasonably accurately with a model that has a coarse decision interval of a month. Finally, for Ethiopia we only consider maximising hydropower generation as it is their main aim behind constructing the GERD.

### 3.2.1.4 Summary of the Conceptual Model

Figure 3.4 shows the topology of the model components described above. Appendix A.1.1 provides a geographical schematic. Finally, a detailed specification of what individual model components entail is given as a UML class diagram in appendix A.1.2.

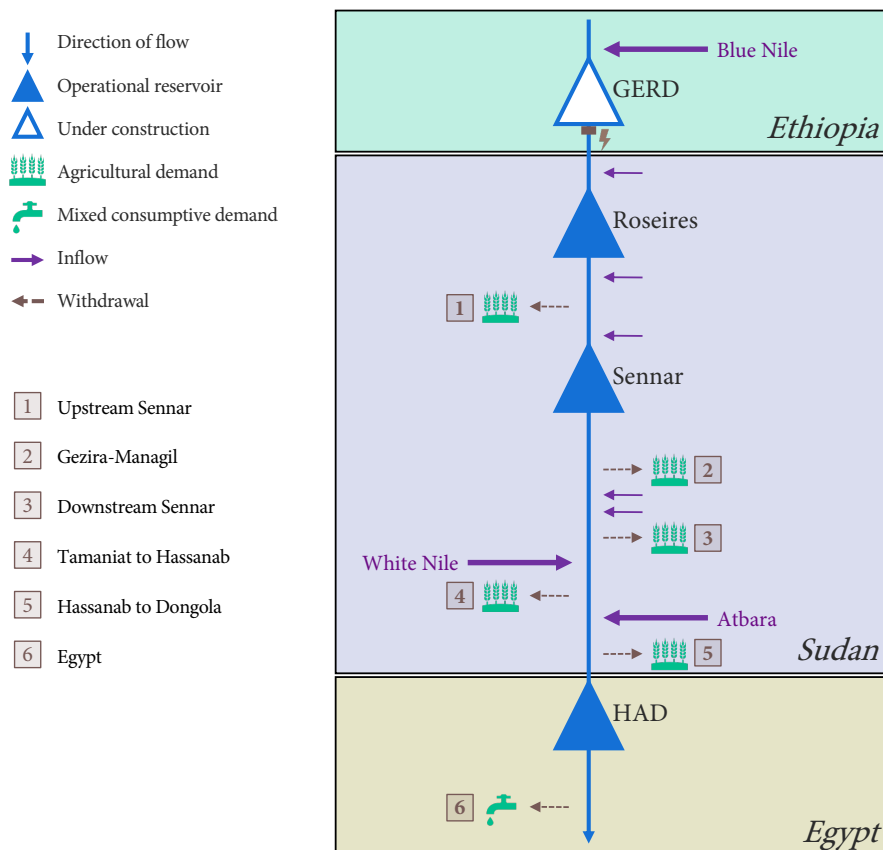


Figure 3.4 Topology of the conceptual model. Components of the system are emphasised. Joining to the flow, main tributaries and other minor catchments are shown in purple colour. Water withdrawal by irrigation districts are illustrated using dashed arrows.

### 3.2.2 Model Formulation

#### 3.2.2.1 Mathematical Formulation

Here we present equations of the model to concretise the abstract formulation introduced in equations 3.1-3.3 along with the formulation of objective functions.

*Release decisions:*

$$u_{\tau}^k = \sum_i [w_i^k \varphi_i(S_{\tau}, \sum_p Q_{\tau-1}^p, \tau \bmod 12) + \alpha_k] \quad (3.4)$$

*Mass-balance equations:*

$$s_{\tau+1}^k = s_{\tau}^k + \int_0^1 f(s_{\tau+t}^k, q_{\tau}^k, e_{\tau}^k, u_{\tau}^k) dt \quad (3.5)$$

*In-month integration:*

$$f = \frac{\Delta s_{\tau+t}^k}{\Delta t} = \underbrace{q_{\tau}^k}_{\text{net inflow}} - \underbrace{A^k(s_{\tau+t}^k)e_{\tau}^k}_{\text{evaporation}} - \underbrace{r^k(s_{\tau+t}^k, u_{\tau}^k)}_{\text{actual release}} \quad (3.6)$$

where  $r$  is defined as follows:

$$r^k(s_{\tau+t}^k, u_{\tau}^k) = \begin{cases} \bar{r}^k(s_{\tau+t}^k), & \text{if } u_{\tau}^k > \bar{r}^k(s_{\tau+t}^k) \\ \underline{r}^k(s_{\tau+t}^k), & \text{if } u_{\tau}^k < \underline{r}^k(s_{\tau+t}^k) \\ u_{\tau}^k, & \text{otherwise} \end{cases} \quad (3.7)$$

in which

- $u_{\tau}^k$  : Release decision for reservoir  $k$  at month  $\tau$
- $w_i^k$  : Weight of the  $i^{\text{th}}$  radial basis function for the release of reservoir  $k$
- $S_{\tau}$  : Vector of all reservoir storages at the beginning of month  $\tau$
- $Q_{\tau}^p$  : Inflow rate of catchment  $p$  at month  $\tau$
- $\alpha_k$  : Constant adjustment parameter of the  $k^{\text{th}}$  release decision
- $s_{\tau}^k$  : Storage in reservoir  $k$  at the beginning of month  $\tau$
- $q_{\tau}^k$  : Rate of net inflow incoming to reservoir  $k$  at month  $\tau$
- $e_{\tau}^k$  : Rate of evaporation occurring from the surface of reservoir  $k$  at month  $\tau$
- $A^k(s)$  : Function that calculates the surface area of reservoir  $k$  based on storage  $s$
- $r^k(s, u)$  : Function that calculates the actual release decision of reservoir  $k$  based on storage  $s$  and policy output  $u$
- $\bar{r}^k(s)$  : Maximum possible release from reservoir  $k$  when the storage is  $s$
- $\underline{r}^k(s)$  : Minimum possible release from reservoir  $k$  when the storage is  $s$
- $k$  : Index that represents one of the four reservoirs of the problem
- $\tau$  : Time index used to represent discrete months in simulation horizon
- $t$  : Time index used to represent small time steps for in-month integration
- $i$  : Index for RBFs

Equation 3.4 shows the calculation of release decision as a weighted sum of RBFs. It is calculated at the beginning of each month  $\tau$  for each reservoir  $k$ . This equation also shows the specific inputs given to the policy function as the state of system at a particular instance. The first input ( $S_\tau$ ) is a vector which holds the storage values of all reservoirs. The second input ( $\sum_n Q_{\tau-1}^n$ ) is the sum of catchment inflows—total gain to the system—in the previous month. In addition, the policy function is also informed about the current month of the year ( $\tau \bmod 12$ ) to account for seasonal factors before deciding on the release.

Equation 3.5 is a high-level representation of how the storage in reservoir  $k$  changes when moving from month  $\tau$  to  $\tau + 1$ . As discussed in section 3.1.1, determining actual releases requires finer time resolution. Exact evaporation and release values are calculated dynamically based on the most up-to-date storage values within a month. They are integrated over time to calculate the total addition to or subtraction from reservoir storage. Integration function ( $f$ ) receives the most recent storage value ( $s_{\tau+t}^k$ ) along with the inputs of net inflow ( $q_\tau^k$ ), evaporation rate ( $e_\tau^k$ ) and release decision ( $u_\tau^k$ ) for the month.

In equation 3.6, integration function ( $f$ ) is further decomposed. There are three elements causing reservoir storage to change. Net inflow ( $q_\tau^k$ ) is the water flow per second that is received from the model components prior to the reservoir  $k$  on the model topology. The function that converts reservoir storage to corresponding surface area ( $A^k(s)$ ) is multiplied by the evaporation rate of the month ( $e_\tau^k$ ) to calculate water loss due to evaporation per second. Finally, calculation of the actual release with respect to the constraints of a reservoir is shown in equation 3.7. Actual release is bounded by the minimum and maximum possible releases given the storage in the reservoir at the time instance.

Equations that show the input-output relations between specific model components are given in appendix A.2.

### Objective Functions

For the many-objective optimisation phase of the methodology, we operationalise six objective functions based on the conceptual description given in section 3.2.1 and considering rival risk aversion framings (Quinn et al., 2017). The first five objectives are to be minimised whereas the last one is to be maximised in the optimisation run.

**Egypt average yearly demand deficit (minimisation)** is the yearly average value of unmet demand in Egypt expressed in BCM/year throughout the 20 years the model is simulated. Its mathematical formulation is as follows:

$$\frac{1}{20} \sum_{\tau=1}^{240} \max(0, D_\tau^{Egypt} - V_\tau^{Egypt}) \quad (3.8)$$

where  $D_\tau^{Egypt}$  is the water demand of and  $V_\tau^{Egypt}$  is the received water flow by the irrigation district *Egypt* in month  $\tau$ .

**Egypt 90<sup>th</sup> percentile worst monthly demand deficit (minimisation)** is an objective formulated to minimise the adversity of a possible disastrous month. Among the deficit values of all 240 months calculated as in  $\max(0, D_{\tau}^{Egypt} - V_{\tau}^{Egypt})$ , this objective function returns the 90<sup>th</sup> percentile when the 100<sup>th</sup> percentile corresponds to the highest deficit value.

**HAD frequency of months below minimum power generation level (minimisation)** is an indicator of water level reliability in the HAD. It is calculated as follows:

$$\frac{1}{240} \sum_{\tau=1}^{240} HAD_{\tau} \quad (3.9)$$

where  $HAD_{\tau}$  is an indicator variable defined as:

$$HAD_{\tau} = \begin{cases} 1, & \text{if } h^{HAD}(s_{\tau}) < 159 \\ 0, & \text{otherwise} \end{cases} \quad (3.10)$$

where  $h^{HAD}(s)$  is the function that calculates the water level in HAD in masl when the storage is  $s$ .

**Sudan average yearly demand deficit (minimisation)** is calculated in a similar manner to the same objective of Egypt. The only difference is that it is an aggregation of deficits faced by multiple irrigation districts in Sudan.

$$\frac{1}{20} \sum_{\tau=1}^{240} \sum_{j \in SD} \max(0, D_{\tau}^j - V_{\tau}^j) \quad (3.11)$$

where  $SD$  is the set of all irrigation districts in Sudan and  $j$  is the index for expressing one such district.

**Sudan 90<sup>th</sup> percentile worst monthly demand deficit (minimisation)** is calculated in the same way as the same objective of Egypt.

**Ethiopia yearly hydroenergy generation from GERD (maximisation)**

$$\frac{1}{20} \sum_{\tau=1}^{240} \underbrace{P_{\tau}^{GERD}}_{\text{power output}} \cdot \underbrace{d(\tau \bmod 12) \cdot 24}_{\text{hours in month}} \quad (3.12)$$

$$P_{\tau}^{GERD} = \min(r_{\tau}^{GERD}, r_{max}^{GERD}) \cdot g \cdot \max(0, h^{GERD}(s_{\tau}) - h_{turbine}^{GERD}) \cdot \eta^{GERD} \quad (3.13)$$

in which

- $r_{max}^{GERD}$  : Flow that corresponds to the maximum rotational speed of the turbine
- $g$  : Gravitational constant
- $h_{turbine}^{GERD}$  : Height of the turbines in GERD
- $\eta^{GERD}$  : Efficiency of the hydropower generation process in GERD

Objective formulations are summarised in table 3.1

Country	Objective	Aggregation level	Unit	Direction
Egypt	Demand deficit	Yearly average	BCM/year	minimise
Egypt	Demand deficit	90 <sup>th</sup> percentile worst month	BCM/month	minimise
Egypt	HAD level reliability	Frequency over 20 years	%	minimise
Sudan	Demand deficit	Yearly average	BCM/year	minimise
Sudan	Demand deficit	90 <sup>th</sup> percentile worst month	BCM/month	minimise
Ethiopia	Hydroenergy generation	Yearly average	TWh/year	maximise

Table 3.1 Overview of optimisation objectives

### 3.2.2.2 Algorithmic Formulation

The equations that make up the mathematical formulation were expressed in Python programming language. Execution sequence of a single simulation run is described as a flowchart in figure 3.5.

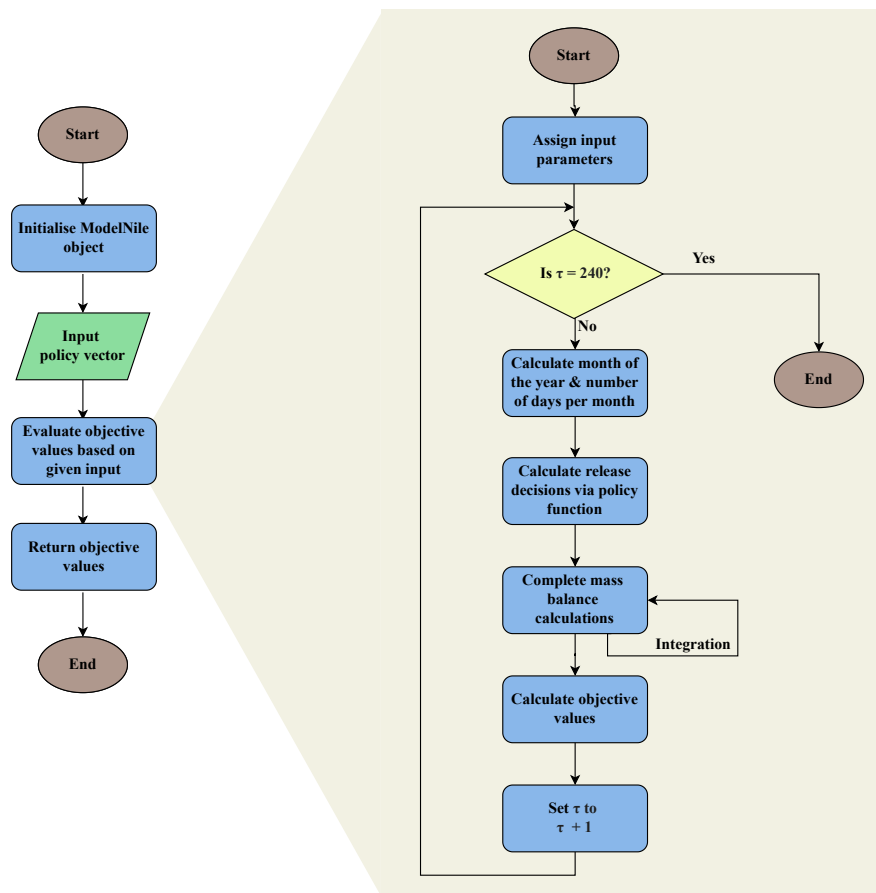


Figure 3.5 Flowchart of simulation run time

### 3.2.3 Data Requirements

We distinguish three types of data that are required. The first category is physical system quantities. It entails quantitative data about dam operations. Secondly, we have a set of hydro-climatic data. It concerns the flow rate of streamflows joining the system from catchments as well as the rates of evaporation from or precipitation to reservoirs. Finally, we present a third category for the water demand of irrigation districts.

#### 3.2.3.1 Physical System Quantities

Data for the following variables are needed regarding the reservoir operations. Specific values used for each variable are given in appendix A.3.

- *Storage-level-surface conversions*: Although the main variable that describes the state of a reservoir is the volume of water stored, elevation of water surface and dynamic surface area of the reservoir are also needed for calculations. Particularly, the former is used for the calculation of hydroenergy generation and the latter is a multiplier for the calculation of evaporation. We use the data points given in the supplementary material of [Wheeler et al. \(2016\)](#) for conversion among the three quantities. During a simulation run, it is common that a conversion from a variable value which does not have an exact match in the data set is needed. In such cases, we use linear interpolation between the closest existing data points.
- *Minimum and maximum release constraints*: [Soncini-Sessa and Weber \(2007\)](#) identify two types of release constraints: physical and normative. The former concerns instantaneous release capacity of the dam given its elevation. For the reservoirs in this study, only the minimum and maximum operational levels were accessible from the literature. Based on these levels, we assumed zero or maximum possible releases for the constraints corresponding to certain elevations. If the water level in a dam is below minimum operational level, no release can be made until the dam is operational again. On the contrary, to prevent undesired spillage, releases are increased to the maximum capacity when the water level approaches the full supply level. Normative constraints are any additional rules imposed on top of the physical constraints. They may include minimum obligatory flows required for environmental services ([Soncini-Sessa and Weber, 2007](#)). Due to lack of data, we left such requirements out of the modelling scope. In addition, we did not impose any predetermined constraints because our aim is to discover a wide policy range and explore what release patterns they correspond to through a post-optimisation trade-off analysis.
- *Hydropower plant parameters*: Variables that are used to calculate hydroenergy generation are the elevation of turbines, maximum turbine flow, plant capacity and plant efficiency. These values are well documented for the three dams other than the GERD. The values in [Wheeler et al. \(2016\)](#) were used for the three dams. Since there is not sufficiently established data for the GERD yet, we based the choice of values on information in the literature and our own assumptions.

### 3.2.3.2 Hydroclimatic Data

- *Streamflows of major tributaries:* There are gauging stations at the points where the White Nile and Atbara rivers join the Main Nile. UN Global Runoff Data Centre provides measurements from these stations (Fekete et al., 2002). For the Mogren gauging station which is just before the White Nile-Main Nile junction, this data set includes summary statistics in the form of minimum, mean and maximum flows per month between the years 1973-1982. We used this information and assumed a separate triangular distribution for the flow variable of each month. Likewise, we found mean and standard deviation values for the gauging station before the Atbara-Main Nile junction. Those are used to assume a separate normal distribution for the flow variable of each month. Finally, average monthly values from the gauging station just before the GERD on the Blue Nile was found from El-dardiry and Hossain (2021). To account for the volatility across simulated years, a uniform distribution with plus and minus 30% upper and lower limit with respect to the mean value is used to generate Blue Nile inflow data points. Summary of the input data is given in table 3.2. Average monthly flows of the three tributaries under baseline conditions are visualised in figure 3.6.

Month	White Nile			Atbara		Blue Nile
	min	mean	max	mean	std	mean
January	735.0	1010.8	1254.0	7.7	11.6	301.6
February	624.0	776.3	1101.0	3.0	8.1	195.6
March	705.0	793.3	1015.0	0.4	1.5	152.2
April	1033.0	1160.6	1369.0	1.5	7.3	149.4
May	686.0	1045.7	1306.0	3.0	11.9	233.7
June	659.0	763.4	902.0	28.3	38.7	690.2
July	333.0	569.1	802.0	592.8	299.7	2733.5
August	300.0	535.0	1000.0	1979.0	740.5	5869.2

Table 3.2 Summary statistics used to generate streamflows of major tributaries. All values are in m<sup>3</sup>/s.

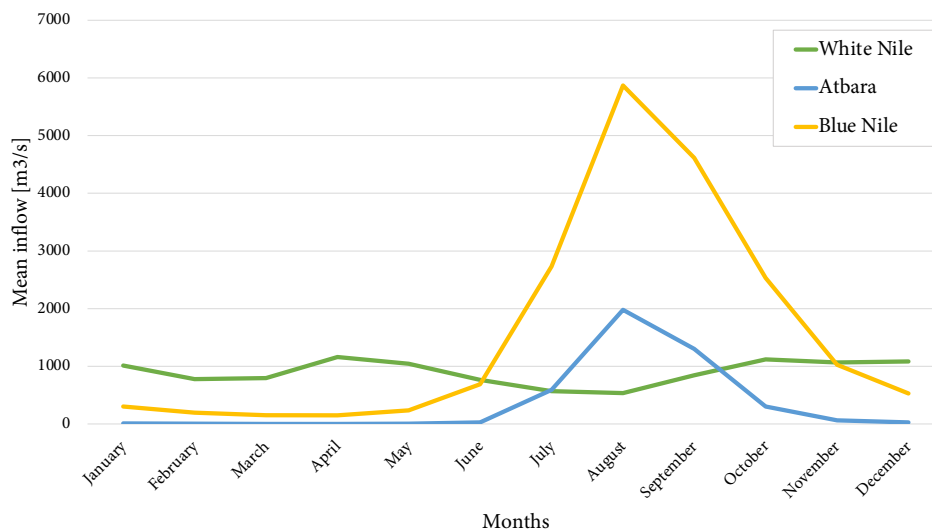


Figure 3.6 Average monthly inflow of three main tributaries under baseline conditions

- *Streamflows of minor catchments:* Wheeler et al. (2018) provided artificially generated streamflow values for all minor inflows joining the Nile from various locations. Under baseline conditions, the authors generated 100 sets of stochastic future data. Depending on the seed of the simulation experiment, we used one such set for the minor inflows that reside in the scope of this study.
- *Monthly evaporation rates:* Wheeler et al. (2016) provided monthly evaporation rates per surface area for each of the four reservoirs in this study. We used the values given in that study.

### 3.2.3.3 Demand

Wheeler et al. (2016) provided monthly demand figures for the irrigation districts in this study which can be found in appendix A.4. However, those figures entail a single value per month which would lead to static water demand over the simulated years. With the growing population and economic activity in the basin, water demand is also expected to rise. As we argue that growing demand is a crucial factor which has an impact on the realisation of objectives, particularly demand deficits, we modelled demand growth in a parametric manner. We assumed a constant water demand growth equal to the population growth in the three countries of this study. A weighted average of population growth in Egypt, Sudan and Ethiopia based on the NBI (2022) is calculated as 2.12% per year. We consider this value as the baseline demand growth. Assuming that the figures given by (Wheeler et al., 2016) are from the year of publication, we expanded the water demand with respect to the growth rate parameter for the years in the simulation horizon.

### 3.2.4 Key Assumptions

- *Lag time between components:* We could not find a reliable source which measures the time it takes water to move from one model component to the other. Wheeler et al. (2018) approximated the travel time between the GERD and the HAD as 15 to 25 days. We decided to regard every transition between two model components to occur within the same month except for one. To account for the long distance between the irrigation districts of Tamaniat and Hassanab, we introduced one-month travel time between these two components.
- *Filling of GERD:* Although there is a lot of debate over the filling strategy of the GERD to be adopted by Ethiopian authorities, we decided not to impose any particular filling rule on the model. Essentially, filling is achieved through not releasing a proportion of inflow from Blue Nile. The ideal filling strategy for Ethiopia is expected to maximise the hydroenergy generated from the GERD. Since this concept as well as the interests of the downstream countries were already formulated as the objectives of the optimisation, various filling patterns were left to be explored from the solution set.
- *Policy function hyper-parameters:* Giuliani et al. (2015) showed that the policy function which attained the highest performance had a total number of RBFs in the proximity of  $(m + K)$ , the number of inputs plus outputs of the control problem. Amaranto et al. (2022), referring to the same study, stated the heuristic for the



ideal number of RBFs as  $(m + K + 1)$ . Following the footsteps of both studies, we determined the number of RBFs as  $(m + K)$ . Since we have six input variables in total (storage values of four dams, total inflow of the previous month and index of the current month) and four output variables (release decisions for each of the four dams), this logic resulted in 10 RBFs. Following the calculation shown in section 3.1.2, we ended up with  $(2 * 10 * 6) + (10 * 4) + 4 = 164$  free parameters to be optimised.

## 3.3 EXPERIMENTAL SETUP

### 3.3.1 Baseline Optimisation

After formulating the simulation model and gaining confidence in its fitness for purpose we ran an evolutionary optimisation in the policy lever space. As explained in section 3.2.4, we have 164 parameters which constitute our decision variable space. We ran the  $\epsilon$ -NSGA-II algorithm for 50,000 NFEs and kept track of the metrics of epsilon progress and hypervolume to test convergence. Epsilon values for all objectives can be found in appendix A.5.

We connected our model to the open source Python library Exploratory Modelling and Analysis (EMA) Workbench and ran its implementation of the  $\epsilon$ -NSGA-II optimisation algorithm (Kwakkel, 2017). A 48-CPU computing node from the Delft High Performance Computing Centre was utilized to run the experiments in parallel (Delft High Performance Computing Centre, DHPC).

### 3.3.2 Uncertainty Analysis

Although the model includes uncertain hydro-climatic and socioeconomic factors, to run an optimisation, the analyst must set a value for every variable that is not included in the optimisation search space. For this reason, the optimisation run is conditioned on a reference scenario and hence likely to be sub-optimal under other scenarios (Watson and Kasprzyk, 2017). Therefore, it is also possible that trade-offs found in one scenario might not be significant if the procedure is repeated under different SOWs.

To cope with this limitation, we conducted three additional analyses building on the results of the baseline optimisation. The core idea at the foundation of these analyses is sampling over the uncertainty space to generate alternative SOWs and re-evaluating the optimised solutions under each scenario. Uncertain variables considered in this study along with their sampling ranges are presented in table 3.3.

Uncertain Variable	Baseline Value	Range
Yearly Demand Growth Rate	0.0212	0.01 - 0.03
Blue Nile Mean Coefficient	1	0.75 - 1.25
White Nile Mean Coefficient	1	0.75 - 1.25
Atbara Mean Coefficient	1	0.75 - 1.25
Blue Nile Deviation Coefficient	1	0.5 - 1.5
White Nile Deviation Coefficient	1	0.5 - 1.5
Atbara Deviation Coefficient	1	0.5 - 1.5

Table 3.3 Overview of uncertain variables and ranges

The baseline value for the *yearly demand growth rate* parameter was determined as 2.12% with respect to the population growth trend in the basin. There are agricultural expansion projections for the Nile Basin including scenarios that correspond to 1.72% and 1.43% yearly growth until 2050 (IWMI, 2021). Nonetheless, these scenarios are formulated based on expansion of irrigation schemes and do not consider urban freshwater needs. When the population growth is taken into account, there are projections expecting Egypt and Ethiopia to be among the top eight countries where the global population growth until 2050 is concentrated (UN, 2022). To account for both extremes, we set the range for the yearly demand growth values as [0.01 – 0.03].

Among the seven uncertain variables, all six except for the *yearly demand growth rate* parameter concerns the hydrology of the major tributaries of the Nile River. Probability distributions that generate monthly flow values were conjectured in section 3.2.3.2. Although parameters of these distributions were estimated based on available historical data, they are subject to deep uncertainty. On the one hand, Nile’s well-known inter-annual variability along with potential extreme events exacerbated by climate change add to the uncertainty. On the other hand, water consumption in the parts of the Nile Basin that we left out of the system scope may change. In case consumptive water uses in Ethiopia and countries upstream the White Nile start growing, mean inflow from major tributaries would decrease and vice versa. To incorporate alternative inflow realisations, we used multiplicative adjustment factors for mean and standard deviation of the probability distributions that generate monthly streamflows for the three main tributaries. It was assumed that  $\pm 25\%$  for mean and  $\pm 50\%$  for standard deviation with respect to the baseline values provide sufficiently wide ranges to capture possible realisations.

5000 alternative SOWs were created by jointly sampling values for the uncertain variables using the Latin hypercube sampling technique due to its efficiency in covering the uncertainty space uniformly (Helton and Davis, 2003). This sampling provided the basis for the following analyses.

### 3.3.2.1 Global Sensitivity Analysis

We investigated the influence of uncertainty variables and policy selection in explaining the variability in the outcomes of interest. To that end, we conducted a global sensitivity analysis. Objective values were evaluated through resimulation of a set of selected policies under the SOWs obtained from Latin hypercube sampling. To obtain an estimation of significance of each uncertainty variable as well as the policy selection, we used the

extra trees algorithm which is based on fitting multiple regression trees (Geurts et al., 2006). This analysis quantified the influence of each input on each outcome of interest.

### *3.3.2.2 Robustness of Policy Alternatives*

We also explored how the performances of the selected policies change under different SOWs. Particularly, we quantified the robustness of policy alternatives using 90<sup>th</sup> percentile maximum regret metric (McPhail et al., 2018). Based on the regret scores of policies, we examined possible trade-offs and synergies among objectives. In essence, our procedure slightly diverges from the MORDM framework of Kasprzyk et al. (2013) as we reduced the set of policy alternatives based on judgment instead of resimulating the full Pareto-optimal set. Additionally, we used a visual approach to inspect which policy maximises the performance of each objective in all possible regions of the uncertainty space.

### *3.3.2.3 Trade-offs under Alternative Scenarios*

To investigate how trade-offs vary with respect to uncertain conditions, we adopted a scenario discovery approach (Bryant and Lempert, 2010). There are several algorithmic methods for scenario discovery in the literature (Kwakkel and Jaxa-Rozen, 2016). We adopted a visual approach proposed by Suzuki et al. (2015). The aim is to identify the uncertainty combinations which lead to interesting realisations of an outcome of interest based on the inspection of a high-dimensional visual where the occurrence frequency is colour-coded. With the guidance of this method, we selected four scenarios in addition to the baseline scenario. We tested the full Pareto-optimal solution set obtained through the baseline optimisation by simulating those policies under discovered scenarios and obtaining a set of objective values for each policy-scenario combination. We reflected on how objective trade-offs play out under those five scenarios.

# 4 | RESULTS

## 4.1 BASELINE OPTIMISATION

The optimisation run under the baseline scenario resulted in 340 Pareto-optimal solution alternatives. Convergence analysis for this optimisation run can be found in appendix [B.1](#).

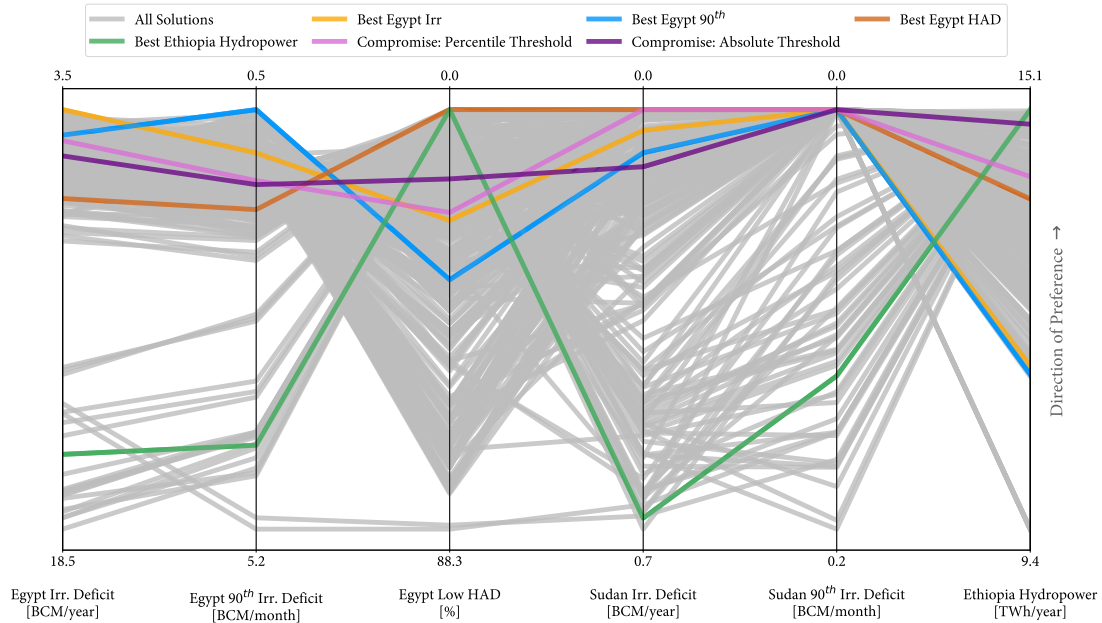
### 4.1.1 Objective Trade-offs

Figure 4.1 is the parallel coordinates representation of the optimisation results. In this figure, six specific policies were colour-coded. A policy label that starts with the word "best" corresponds to the policy which leads to the most desirable value for the particular objective. We added two compromise solutions to the colour-coded policy set. Both were obtained through imposing a constraint on the objective value sets. The policy *Compromise: Percentile Threshold* makes all objectives attain a value that is more desirable than 45<sup>th</sup> percentile where the 100<sup>th</sup> percentile corresponds to the most desirable objective value. Similarly, the policy *Compromise: Absolute Threshold* makes all objectives attain a value that is higher than 0.82 on the normalised scale where the best objective value corresponds to 1.

It is worth noting that the most desirable value for an objective can be yielded by more than one policy alternative. This is the case for the objectives of Sudan irrigation deficit, Sudan 90<sup>th</sup> percentile irrigation deficit and Egypt low HAD. We observed that value ranges for Sudan's objectives are much narrower compared to those of Egypt. A large number of policies including the *Compromise: Percentile Threshold* brings zero deficit for Sudan. For this reason, we did not include any additional policies that minimise those objectives. A distinct policy which yields 0% for the Egypt low HAD objective was colour-coded. Moreover, it was observed that the *Best Ethiopia Hydropower* policy also achieves the 0% outcome for the HAD. This hints a synergy between two objectives.

Considering the irrigation deficit objectives of Egypt, we saw a different picture. The *Best Ethiopia Hydropower* policy leads to objective values in the proximity of the worst outcomes for the two Egypt objectives. It results in 15.8 BCM/year for average yearly and 4.2 BCM/month for 90<sup>th</sup> percentile worst month deficits, unacceptably large outcomes from Egypt's point of view. Likewise, policy alternatives that optimise the objectives of Egypt have a similar effect on the hydroenergy generation objective of Ethiopia. These

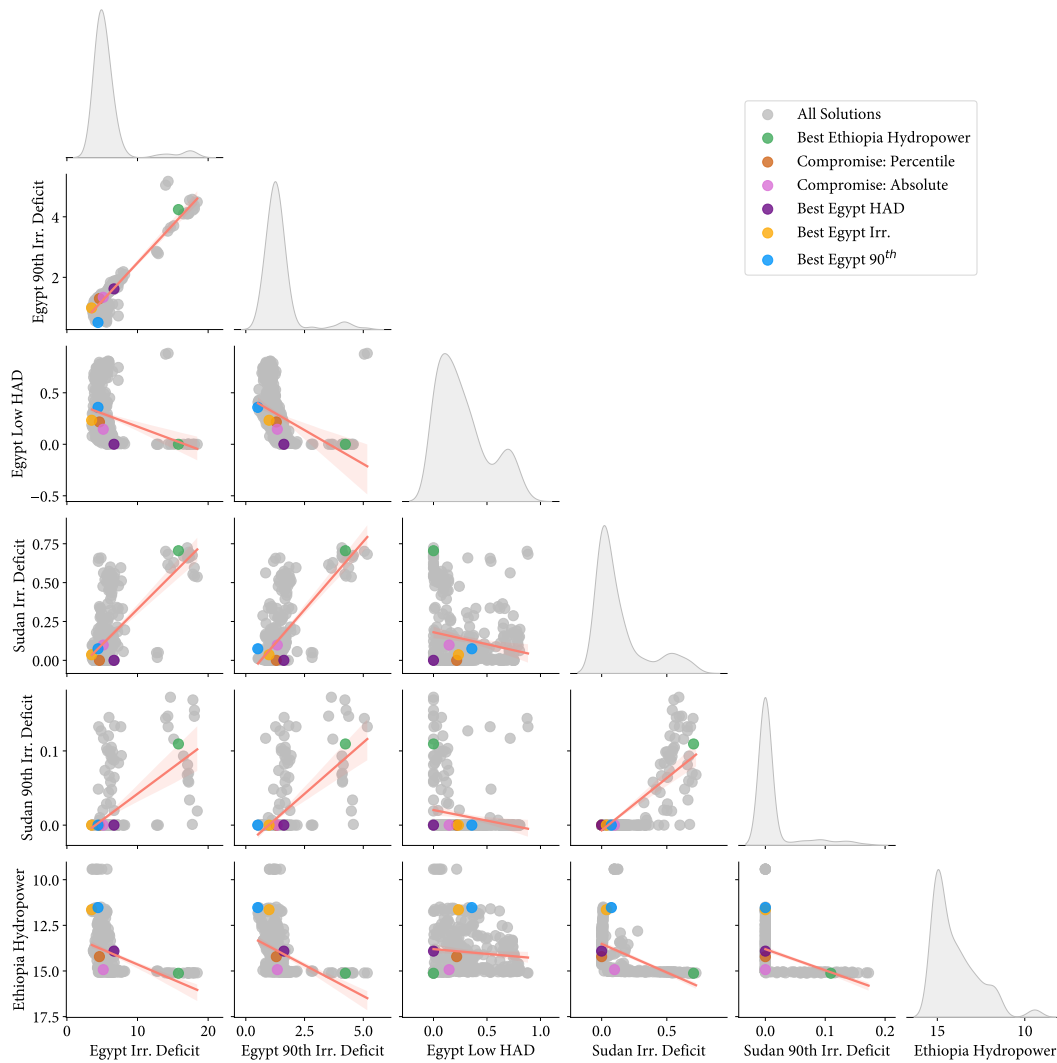
policies lead to 2.4 TWh/year less hydroenergy for Ethiopia compared to its average realisation with the Pareto-optimal set.



**Figure 4.1** Parallel coordinates plot of Pareto-optimal solutions of baseline optimisation. Minimum and maximum levels attained by objective values are given on the ends of each parallel axis. Extremes are positioned such that an upper value is always more desirable for each objective.

To examine the overall trade-off patterns within the full Pareto front in addition to the differences between individual performance maximising policies, we visualised two-way comparisons between objectives using a pair plot as shown in figure 4.2a. Each scatter plot is fitted a regression line. The slope of this regression line informs us about the trend between two objectives. When the angle between the regression line and the x-axis is around  $45^\circ$  in the positive direction, it is an indication that there is an alignment between two objectives i.e., policies which maximise the performance of one objective also tend to yield desirable outcomes for the other. On the contrary, when the angle is around  $-45^\circ$ , it signals a trade-off in the similar manner. Table in figure 4.2b provides the slope of the regression lines fitted for each objective pair.

Nonetheless, slope itself is not enough to draw conclusions about the significance of such a relation. If the points are scattered dispersedly and there is no substantial accumulation around the regression line, slope might be misleading. In this regard, we used Pearson correlation coefficient to quantify the significance of the relation between two objectives. We argue that the closer the coefficient becomes to  $-1$  or  $+1$ , the more stable the relation is. Pearson correlation coefficients calculated for objective pairs can be found in table in figure 4.2c.



(a) Pair plot for objective values. Pair-wise scatter plots are given along with a fitted regression line. Policies selected from figure 4.1 were colour-coded using the same legend. Histogram of individual objectives are visible on the diagonal. The axes of Ethiopia Hydropower objective (maximisation) is reversed such that all objective values get more desirable towards the left on the x-axis and bottom on the y-axis.

	Egypt Irr. Deficit	Egypt 90 <sup>th</sup> Irr. Deficit	Egypt Low HAD	Sudan Irr. Deficit	Sudan 90 <sup>th</sup> Irr. Deficit	Ethiopia Hydropower
Egypt Irr. Deficit	1.00	0.81	-0.43	0.95	0.62	-0.43
Egypt 90 <sup>th</sup> Irr. Deficit	0.81	1.00	-0.69	0.89	0.75	-0.56
Egypt Low HAD	-0.43	-0.69	1.00	-0.19	-0.15	-0.08
Sudan Irr. Deficit	0.95	0.89	-0.19	1.00	0.60	-0.40
Sudan 90 <sup>th</sup> Irr. Deficit	0.62	0.75	-0.15	0.60	1.00	-0.35
Ethiopia Hydropower	-0.43	-0.56	-0.08	-0.40	-0.35	1.00

(b) Regression slopes between objectives. Fit was done based on normalised objective values. +1 and -1 correspond to 45° and -45° angles respectively. Whenever the absolute value of slope turns out to be bigger than 1, it is replaced with 1/ slope as it only means swapping the dependent and independent variables of the regression line.

	Egypt Irr. Deficit	Egypt 90 <sup>th</sup> Irr. Deficit	Egypt Low HAD	Sudan Irr. Deficit	Sudan 90 <sup>th</sup> Irr. Deficit	Ethiopia Hydropower
Egypt Irr. Deficit	1.00	0.93	-0.30	0.65	0.58	-0.36
Egypt 90 <sup>th</sup> Irr. Deficit	0.93	1.00	-0.42	0.68	0.60	-0.39
Egypt Low HAD	-0.30	-0.42	1.00	-0.19	-0.20	-0.09
Sudan Irr. Deficit	0.65	0.68	-0.19	1.00	0.80	-0.47
Sudan 90 <sup>th</sup> Irr. Deficit	0.58	0.60	-0.20	0.80	1.00	-0.31
Ethiopia Hydropower	-0.36	-0.39	-0.09	-0.47	-0.31	1.00

(c) Pearson correlation coefficient between objectives

Figure 4.2 Overall trade-off patterns within the full Pareto front

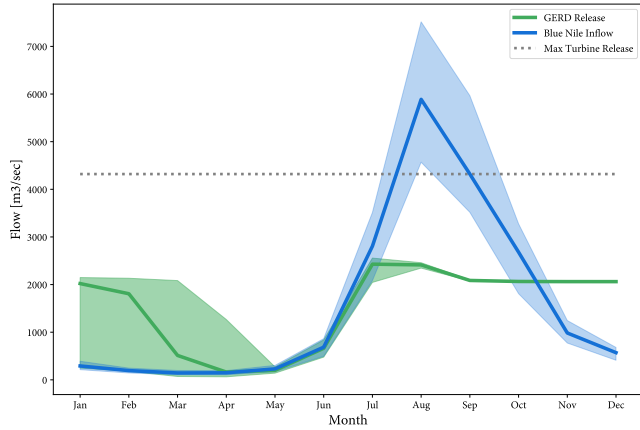
The most prominent relation among all objective pairs is the alignment between the two irrigation deficit objectives of Egypt. Tables 4.2b and 4.2c show slope and correlation coefficients that are fairly close to 1. We observe a similar trend between the two objectives of Sudan despite being not as strong as those of Egypt. This result suggests that, under the baseline scenario, rival objective formulations from different risk aversion perspectives do not lead to diverging interests.

Another pattern that is visible from figure 4.2 is that the hydroenergy generation objective of Ethiopia overall has negative relations with irrigation deficit objectives of Egypt and Sudan, the former being more pronounced considering the exact objective values. Looking at the bottom-most row of figure 4.2a, a group of policies that maximise Ethiopia's hydropower can be identified. Although these policies overall yield above average irrigation deficits for Egypt and Sudan, deficit outcomes spread over a wide range of values. This finding is emphasised by the horizontal distance between the *Compromise: Absolute Threshold* (pink) and *Best Ethiopia Hydropower* (green) policies on the bottom-most row. This observation hints at the possibility of finding acceptable terms for all parties.

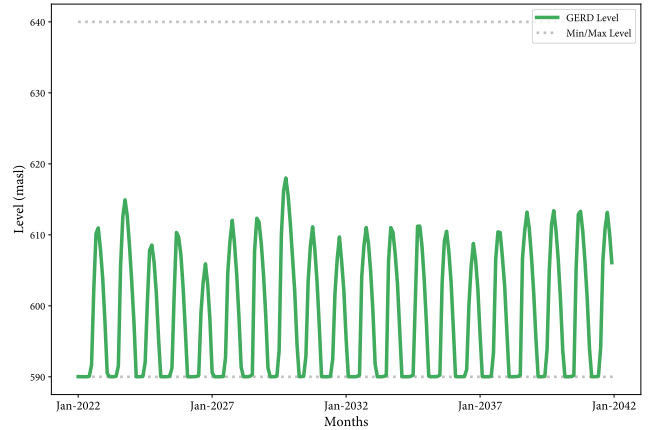
Although individual colour-coded policies suggest an alignment between Ethiopia Hydropower and Egypt low HAD, these two objectives are uncorrelated when the full Pareto-optimal set is considered. We assert that this is because these two objectives are directly influenced by two major decision points—releases from the GERD and the HAD—and the Pareto-approximate set flexibly represent a variety of possibilities for both decision points. Consider the case when the GERD does not release desirably high from Egypt's perspective. The solution space covers both possibilities of the HAD keeping water at the cost of irrigation deficits downstream and releasing water at the cost of being unoperational. This phenomenon not only points to the lack of dependence between Ethiopia Hydropower and Egypt low HAD objectives, but also signals potential internal trade-off for Egypt. Despite not being very strong, this internal trade-off is also visible from figure 4.2.

#### 4.1.2 Physical System Implications

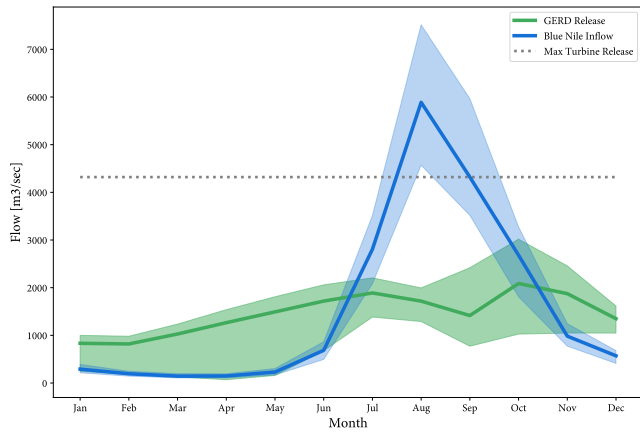
We re-ran the simulation model with all colour-coded policies under the baseline conditions. To inspect the implications of these policies on the operations of the GERD, we visualised releases from the GERD and its elevation over time. Here in figure 4.3, to concisely illustrate the extremes and a compromise, we present the results from the *Best Egypt Irrigation*, *Compromise: Percentile Threshold* and *Best Ethiopia Hydropower* policies. Using the same three policies, in figure 4.4, we show the implications on Egypt's irrigation demand and elevation of the HAD. Appendix B.2 includes these visuals for the other policies.



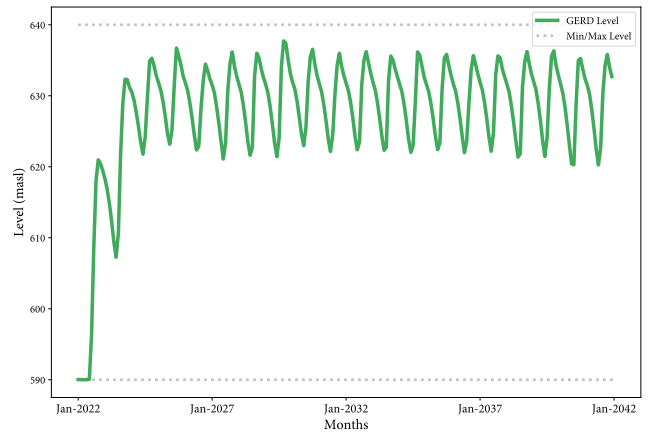
(a) The GERD inflow versus release with Best Egypt Irr. policy



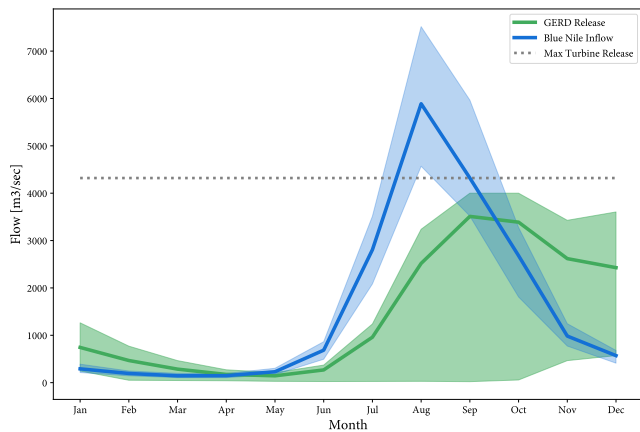
(b) The GERD elevation with Best Egypt Irr. policy



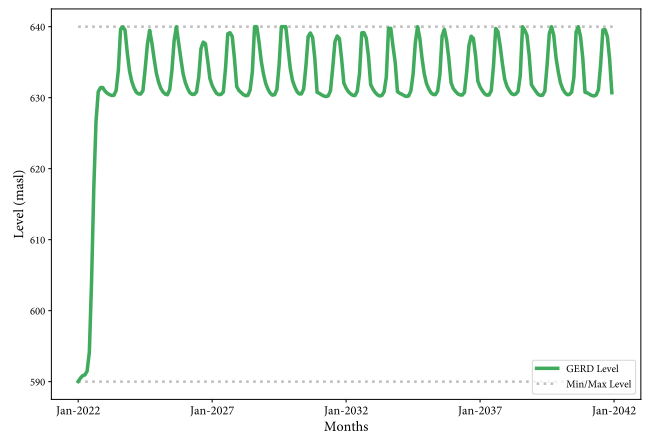
(c) The GERD inflow versus release with Compromise: Percentile Threshold policy



(d) The GERD elevation with Compromise: Percentile Threshold policy



(e) The GERD inflow versus release with Best Ethiopia Hydropower policy



(f) The GERD elevation with Best Ethiopia Hydropower policy

**Figure 4.3** Physical system implications of different policies on the GERD. Figures on the left summarise inflow to and release from the GERD over the whole simulation horizon. The line graph shows the mean value corresponding to the month in the x-axis over twenty years. Shaded area covers the range of values in each month. Figures on the right show the monthly time series of reservoir elevation over the simulation horizon.



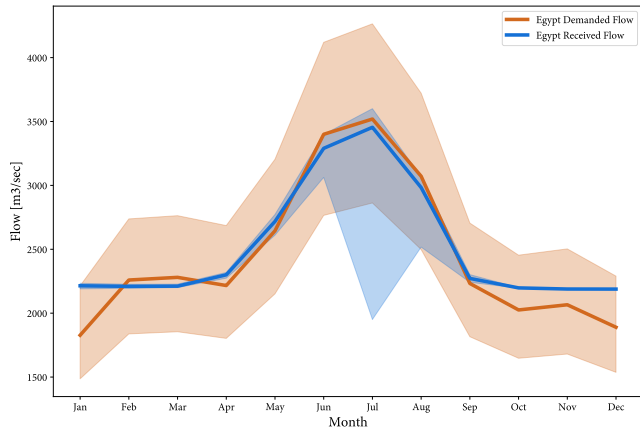
A distinct difference among the three policies is the dynamics of the elevation of the GERD. The *Best Ethiopia Hydropower* policy rapidly fills up the reservoir to the full supply level and stably maintains the level at high. On the contrary with the *Best Egypt Irrigation* policy, the GERD never gets close to the full capacity. Moreover, volatility of elevation dynamics is significantly larger in figure 4.3b compared to 4.3f. On the other hand, *Compromise: Percentile Threshold* policy attains a balance both in terms of the initial filling and over time level variance. Under this policy, filling is extended over a duration of a few years and the GERD never reaches its full supply level. Finally, amplitude of oscillation in the GERD's level is in-between those of the other two policies.

The *Best Egypt Irrigation* policy imposes high and stable releases from the GERD between the months July and January. This release pattern supports meeting the peak irrigation demand in Egypt over summer months. Nonetheless, releases from the GERD do not necessarily follow the exact demand pattern because of other storage, diversion, inflow possibilities between the GERD and Egypt. For instance, Egypt also utilises the storage capacity of the HAD. In fact, figure 4.4b shows that with the *Best Egypt Irrigation* policy, the elevation of the HAD consistently declines over time to satisfy increasing downstream demand.

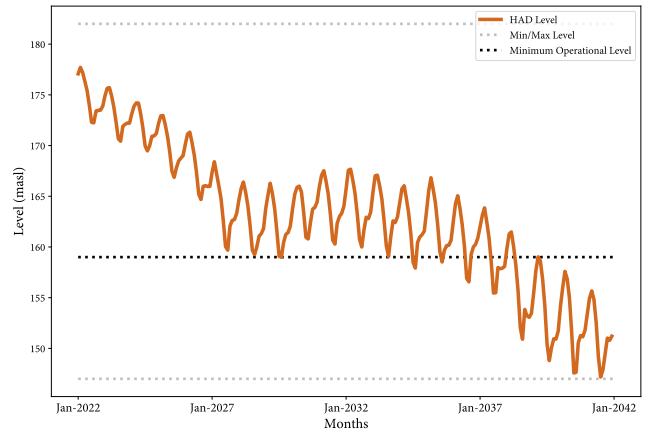
The *Best Ethiopia Hydropower* policy seeks for a balance between the GERD's elevation and release because hydroenergy generation is a multiplicative function of the two. Releasing too much in a month leads to lower water levels whereas to keep higher water levels at all costs, the GERD must reduce its release. Both these strategies result in sub-optimal hydropower. We see from figures 4.3e and 4.3f that the *Best Ethiopia Hydropower* policy matches the high release periods with Blue Nile inflow and stabilises the GERD's level. It is worth noting that even during the high release periods, maximum releases stay below the turbine capacity of the GERD. Finally, the *Compromise: Percentile Threshold* policy brings a balanced release over a year.

Figure 4.4a shows that the *Best Egypt Irrigation* policy arranges the releases so that the flow received by Egypt closely follows up the demand pattern. On the other extreme, as can be observed from figure 4.4e, the *Best Ethiopia Hydropower* policy ignores the demand regime in Egypt. The *Compromise: Percentile Threshold* policy yields received releases for Egypt in line with the demand seasonality although not as strictly as the *Best Egypt Irrigation* does. Another point to note is that none of the three policies simultaneously achieve optimal system performance with respect to Egypt irrigation deficit and low HAD objectives. From figure 4.4f, we see that the policy which disregards Egypt's irrigation deficit objectives leads to the HAD never falling below the power generation level. On the other hand, the policies which incorporate concerns about demand deficits result in low levels in the HAD towards the end of the simulation horizon inevitably with the growing demand.

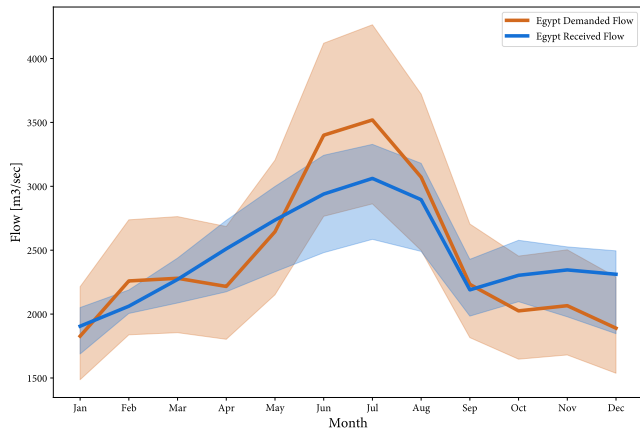
In addition, evaporation from the HAD varies according to the water level in the reservoir. We calculated average yearly water loss due to evaporation from the HAD's surface as 9.2, 8.9 and 14.5 BCM/year with the policies *Best Egypt Irrigation*, *Compromise: Percentile Threshold* and *Best Ethiopia Hydropower* respectively. With the same policies, yearly average evaporation from the GERD was realised as 0.9, 1.7 and 1.8 BCM/year.



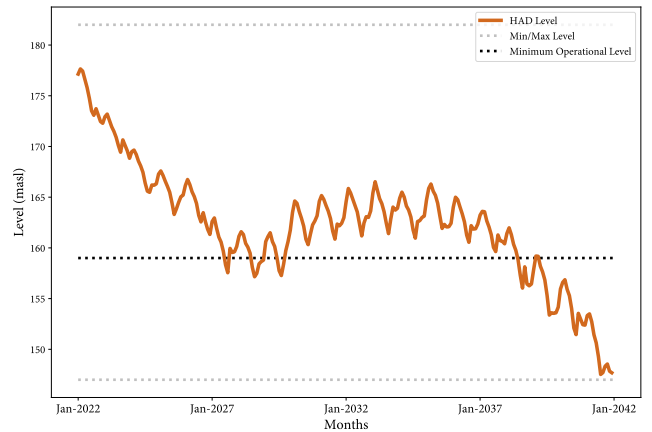
(a) Egypt demanded versus received flow with Best Egypt Irr. policy



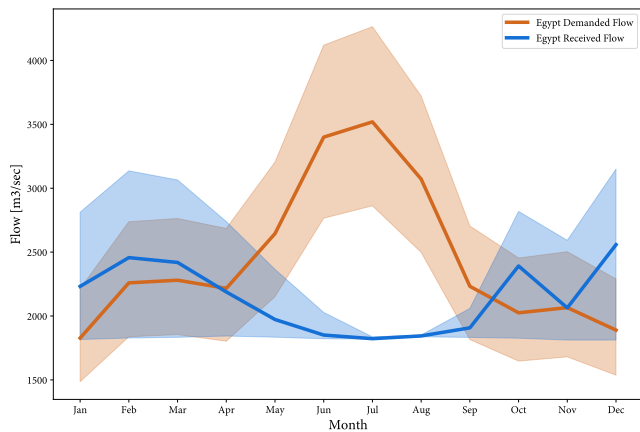
(b) The HAD elevation with Best Egypt Irr. policy



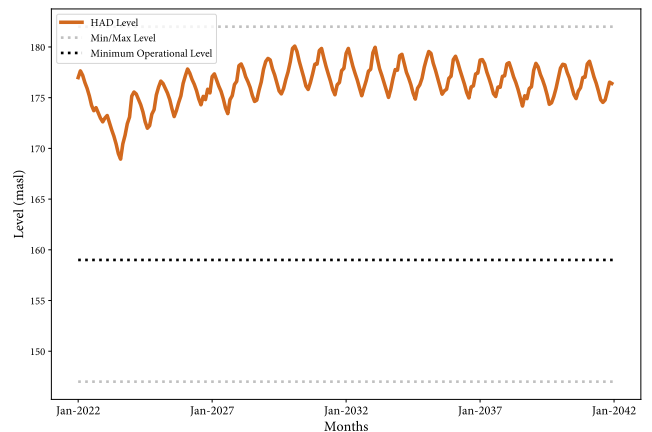
(c) Egypt demanded vs. received flow with Compromise: Percentile Threshold



(d) The HAD elevation with Compromise: Percentile Threshold



(e) Egypt demanded vs. received flow with Best Ethiopia Hydropower



(f) The HAD elevation with Best Ethiopia Hydropower

**Figure 4.4** Physical system implications of different policies on Egypt. Figures on the left summarise demanded and received water flow over the whole simulation horizon. The line graph shows the mean values corresponding to the month in the x-axis over twenty years. Shaded area covers the range of values in each month. Figures on the right show the monthly time series of the HAD elevation over the simulation horizon.

The last physical system implication that we visualised is the dynamics of the water demanded and received by the irrigation district of Gezira-Managil—the largest agricultural irrigation scheme in Sudan. In figure 4.5, we chose to present these variables only with the *Best Ethiopia Hydropower* policy because no other policy displays considerable demand deficits. Resulting figures with other policies can be found in appendix B.2.

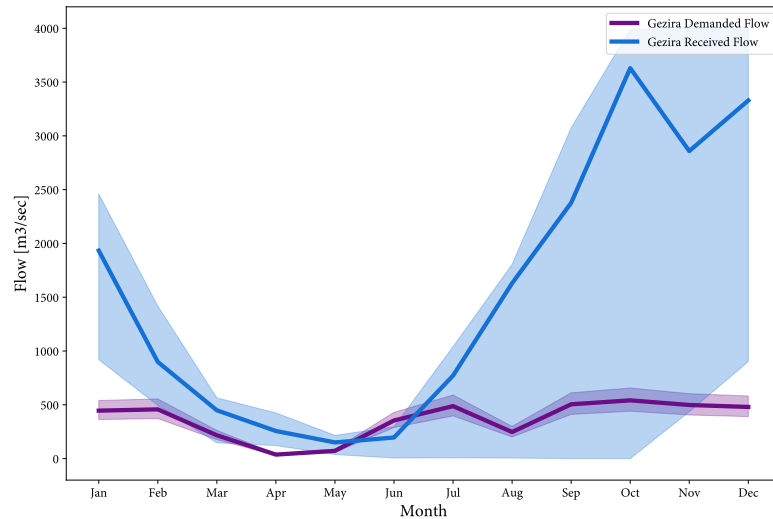


Figure 4.5 Gezira received flow versus demand with Best Ethiopia Hydropower policy

Sudan suffers from a small amount of deficit during the aggressive filling of the GERD that the *Best Ethiopia Hydropower* policy prescribes. In the long run, irrigation demand in Gezira-Managil is satisfied by a large margin as the mean lines in figure 4.5 confirm. It is likely that the trade-off between Sudan irrigation deficit and Ethiopia Hydropower objective discussed in section 4.1.1 stems from rapid filling strategies.

## 4.2 UNCERTAINTY ANALYSIS

### 4.2.1 Global Sensitivity Analysis

In table 4.1, we have the importance of uncertain factors in explaining the variability in outcomes of interest. These values were calculated using the extra trees algorithm and fitting 1000 regression trees for each objective.

Table 4.1 indicates that the selected policy is influential on the outcome for all objectives, particularly for Sudan. The mean Blue Nile inflow is of utmost importance for hydroenergy generation in Ethiopia. Likewise, average inflows of tributaries have large impact on the elevation of the HAD, Blue Nile being the most prominent. Irrigation deficit in Egypt is greatly influenced by the demand growth rate. Inflow deviations of major tributaries did not turn out to be impactful for any of the objectives. This can be attributed to high level of storage and regulation provided by the four reservoirs in the system.

	Egypt Irr. Deficit	Egypt 90th Irr. Deficit	Egypt Low HAD	Sudan Irr. Deficit	Sudan 90th Irr. Deficit	Ethiopia Hydropower
<b>Policy</b>	0.19	0.20	0.22	0.83	0.68	0.23
<b>Atbara Deviation</b>	0.01	0.01	0.01	0.00	0.00	0.00
<b>Atbara Mean</b>	0.01	0.02	0.03	0.00	0.00	0.00
<b>Blue Nile Deviation</b>	0.01	0.01	0.01	0.00	0.01	0.00
<b>Blue Nile Mean</b>	0.13	0.25	0.54	0.11	0.23	0.75
<b>White Nile Deviation</b>	0.01	0.01	0.01	0.00	0.00	0.00
<b>White Nile Mean</b>	0.06	0.11	0.16	0.00	0.00	0.01
<b>Demand Growth</b>	0.58	0.39	0.02	0.05	0.06	0.00

Table 4.1 Feature scores of uncertain parameters on each outcome calculated using extra trees algorithm

#### 4.2.2 Robustness of Policies

In table 4.2, 90<sup>th</sup> percentile maximum regret scores of the policy selection are given.

	Egypt Irr. Deficit	Egypt 90th Irr. Deficit	Egypt Low HAD	Sudan Irr. Deficit	Sudan 90th Irr. Deficit	Ethiopia Hydropower
<b>Best Egypt Irr.</b>	0.04	0.42	0.80	0.17	0.00	3.87
<b>Best Egypt 90th</b>	4.04	2.61	0.80	0.23	0.02	4.10
<b>Best Egypt HAD</b>	7.58	2.00	0.75	0.03	0.00	2.84
<b>Best Ethiopia Hydropower</b>	11.97	3.35	0.00	1.00	0.37	0.00
<b>Compromise: Percentile</b>	7.64	2.58	0.83	0.01	0.00	2.65
<b>Compromise: Absolute</b>	3.08	0.93	0.88	0.11	0.00	0.21

Table 4.2 90th percentile maximum regret scores of policies on each objective. Colour-coding was done column-wise such that darker shades of red (blue) represent high (low) regret for an objective. All values are given in terms of the unit of the corresponding objective.

Based on table 4.2, the *Compromise: Absolute Threshold* policy looks promising in the sense that it yields low regret scores for all objectives except for the Egypt low HAD. The only policy that minimises the regret for the Egypt low HAD objective is the *Best Ethiopia Hydropower*. This policy also achieves high level of robustness with respect to Ethiopia's hydropower objective. An exact opposite robustness pattern was obtained with the *Best Egypt Irrigation* policy. This policy is highly robust with respect to irrigation deficits whereas it attains poor regret scores for Egypt low HAD and Ethiopia's hydropower objectives. This finding suggests a robustness trade-off between objectives concerning maximising water level in the two major dams and minimising irrigation demand deficits.

Figure 4.6 summarises how the best performing policies for each objective change with respect to varying SOWs. We compiled this figure in two steps:

1. Using the algorithm for the dimensional stacking analysis of EMA Workbench (Kwakkel, 2017) as a basis, we divided the uncertainty space into segments of low, medium and high values of four most influential uncertain variables—demand

growth rate and mean inflows of three tributaries. This selection was guided by the feature scores given in section 4.2.1. Three levels in four variables resulted in  $3^4 = 81$  regions in the uncertainty space.

2. For every objective, each uncertainty region was coloured based on the policy that performs the best under the highest number of scenarios. Marker size in the region indicates how much improvement the best performer policy makes compared to the second best alternative on average. The region is empty if multiple policies yield maximum performance in all scenarios.

Figure 4.6 contains the illustration for all objectives but Sudan's 90<sup>th</sup> percentile worst deficit which resulted in multiple best performer policies under all scenarios, therefore an empty figure.

We see from figures 4.6a and 4.6e that two policies, the *Best Egypt Irrigation* and *Best Ethiopia Hydropower* dominantly optimise their targeted objectives in almost all SOWs. This observation is especially prominent in the regions corresponding to extreme stress scenarios—low Blue Nile flow for Ethiopia, high demand growth rate and low Blue Nile flow for Egypt.

Another interesting result appears for Egypt's 90<sup>th</sup> percentile worst deficit objective under highly stressed scenarios. While the two deficit objectives of Egypt are aligned in a large portion of the uncertainty space, the top-right segment of figure 4.6b exhibits solid performance gains by the *Best Ethiopia Hydropower* policy. This region of high pressure scenarios paves the way for diverging interests between different risk aversion levels in deficit objectives. When demand deficits are concerned, consistent mediocre performance brought by *Best Ethiopia Hydropower* policy becomes more desirable for the 90<sup>th</sup> percentile objective compared to sacrificing a number of months to achieve less overall deficit.

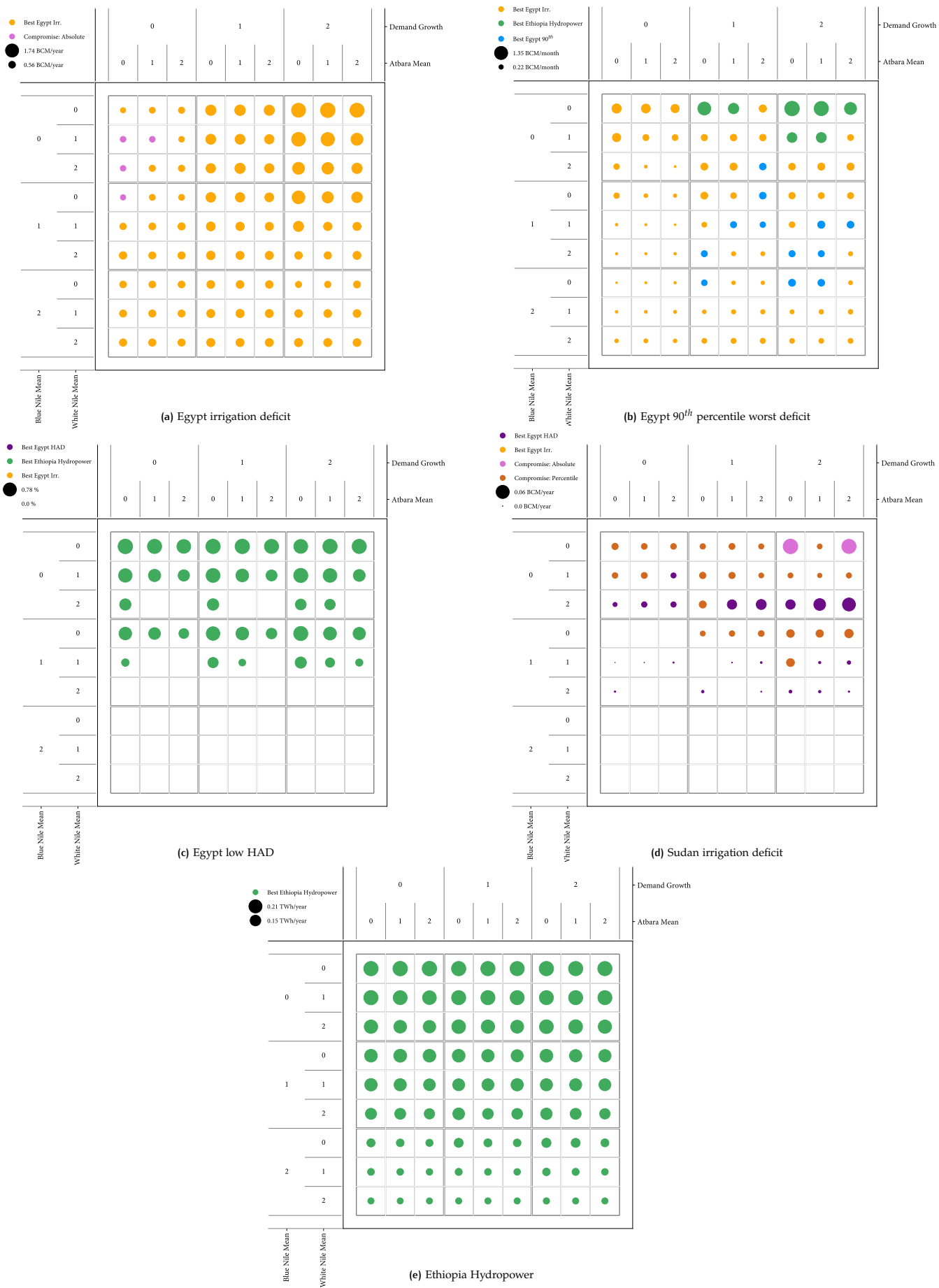


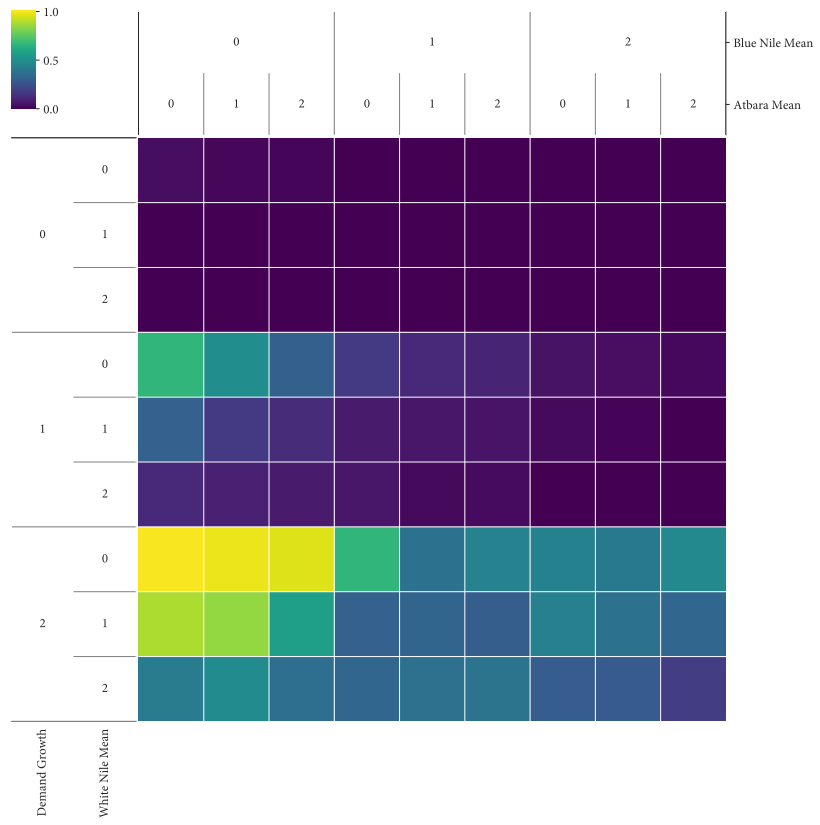
Figure 4.6 Best performers for each objective in the uncertainty space.

### 4.2.3 Scenario Discovery

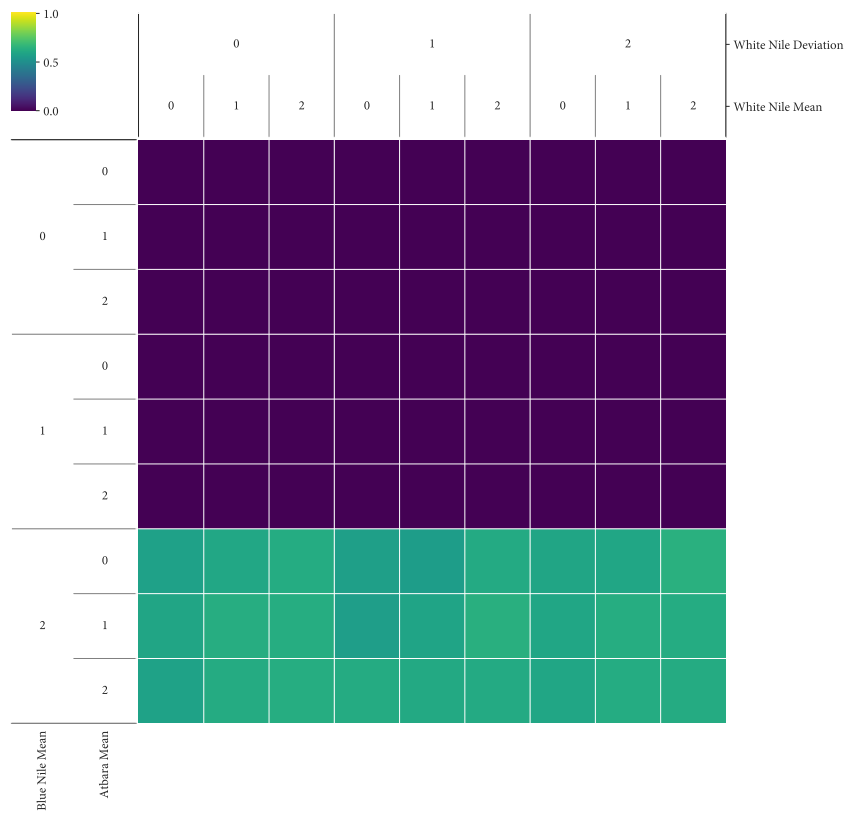
We performed dimensional stacking analyses for all objectives. This entails making binary classifications of experiments based on whether or not they yield outcomes in the top or bottom 20% across all experiments. Then, partitioned regions in the uncertainty space are colour-coded according to the proportion of cases of interest. Six objectives and two binary classifications (top and bottom 20%) resulted in 12 dimensional stacking plots. In figure 4.7, we present the results from two outcomes of interest: worst 20% Egypt irrigation deficit and best 20% GERD hydroenergy generation. Plots for the rest of the outcomes can be found in appendix B.3. We did not observe different trends in addition to what 4.7a and 4.7b exhibit.

In figure 4.7a, colour-coding basis is the lowest 20% performance region for the yearly irrigation deficit of Egypt. High demand growth, low Blue Nile flow and to a lesser extent low White Nile flow describes the high-density boxes. In figure 4.7b, cases in which the performance of hydropower from the GERD is in the top 20% were categorised as the cases of interest. All of the best hydroenergy generation cases stand in the region where the mean flow of the Blue Nile is higher than the baseline.

In light of the graphs as well as the analyses in sections 4.2.1 and 4.2.2, we defined two scenarios in addition to the baseline: *Extreme Stress Scenario* and *High Blue Nile Scenario*. Parameter values for these scenarios are provided in appendix B.4. *Extreme Stress Scenario*, in which demand growth rate is high and mean inflows of tributaries are low, is the subspace where all objectives attained the most undesirable outcomes. Furthermore, section 4.2.2 hints the exacerbation of trade-offs between objectives under this scenario. *High Blue Nile Scenario*, is the scenario in which all uncertainty variables except for the mean Blue Nile flow are at their baseline value. The mean flow of Blue Nile was set at its upper limit in the considered range. In figure 4.7b, this scenario is shown to lead Ethiopia to desirable outcomes regarding hydroenergy generation. Another motivation was Ethiopia's potential strategy of reducing water withdrawal from the Blue Nile in regions upstream the GERD to achieve near full hydroenergy generation capacity as discussed in the literature (Whittington et al., 2014).



(a) Worst 20<sup>th</sup> percentile Egypt irrigation deficit



(b) Best 20<sup>th</sup> percentile GERD hydropower generation

Figure 4.7 Dimensional stacking performed for different outcomes of interest.



#### 4.2.4 Trade-offs under Scenarios

Pareto-optimal policy set was re-simulated under selected scenarios. Table 4.3 provides summary statistics regarding the objective value realisations. Results of the re-simulation under the *Extreme Stress Scenario* is illustrated in figure 4.8. We used the pair plot, regression slope and correlation tables as in section 4.1.1.

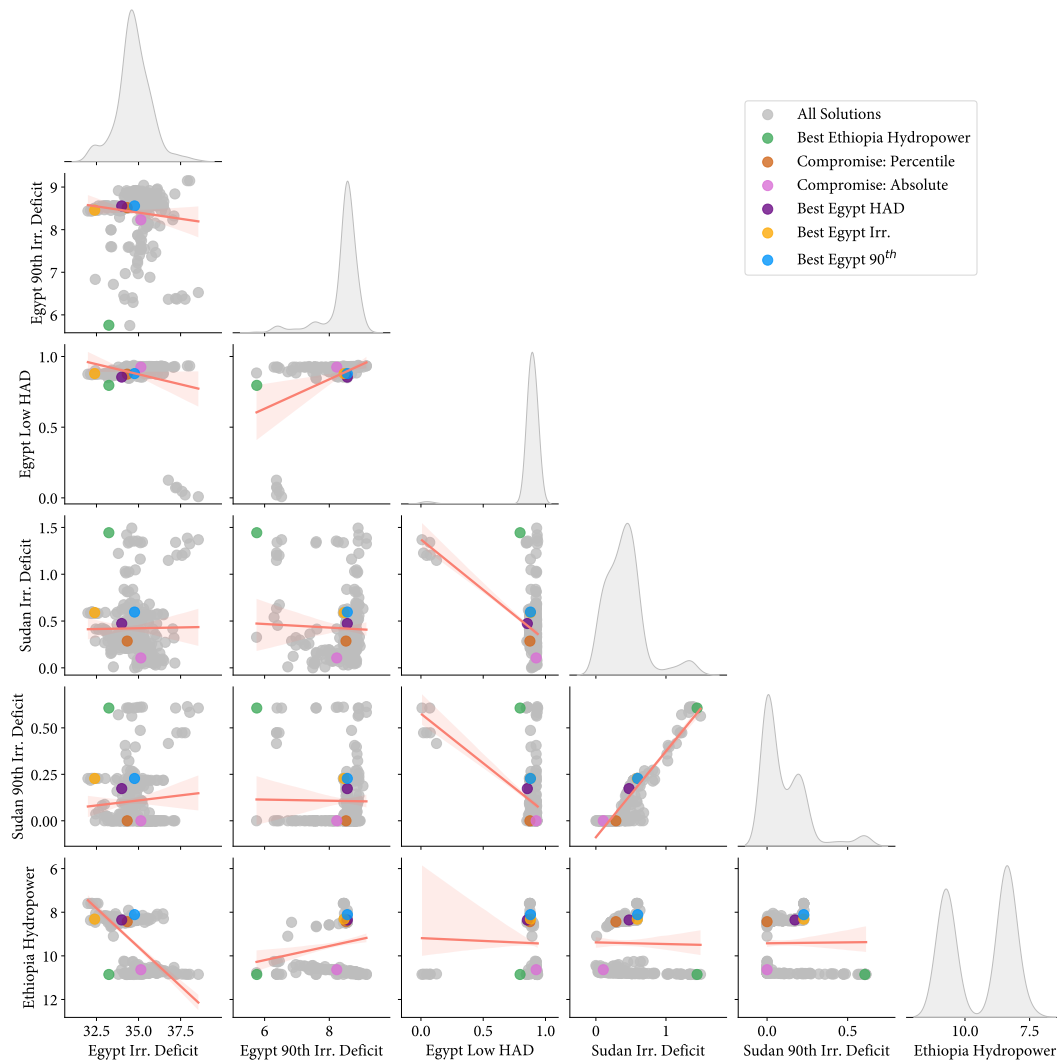
Scenario	Statistic	Objectives					
		Egypt Irr. Deficit [BCM/year]	Egypt 90 <sup>th</sup> Irr. Deficit [BCM/month]	Egypt Low HAD [%]	Sudan Irr. Deficit [BCM/year]	Sudan 90 <sup>th</sup> Irr. Deficit [BCM/month]	Ethiopia Hydropower [TWh/year]
Baseline	mean	5.80	1.43	28	0.14	0.01	13.94
	min	3.50	0.51	0	0.00	0.00	9.42
	max	18.46	5.17	88	0.72	0.17	15.13
Extreme Stress	mean	34.72	8.41	88	0.42	0.11	9.41
	min	31.99	5.75	1	0.00	0.00	7.60
	max	38.55	9.15	94	1.49	0.61	10.86
High Blue Nile	mean	8.04	2.44	0	0.09	0.00	18.63
	min	3.08	1.01	0	0.00	0.00	10.81
	max	13.43	3.97	52	0.42	0.00	19.26

Table 4.3 Ranges of objectives achieved by optimized policy set under different scenarios

In comparison to the trade-offs under the baseline scenario, alignment between Egypt's two deficit objectives clearly diminishes. Interestingly, Sudan's deficit objectives appear even more aligned resembling the results for Egypt under the baseline given in figure 4.2. This indicates an interesting phenomenon about risk aversion levels of objective formulations. Considering that the deficit values consistently increase with the growing demand, the system gets pressured to a point where policies that optimise aggregate objectives tend to sacrifice a period towards the end of the simulation horizon when water is no longer available in accessible dams. The higher the pressure, the longer the period of observations that are sacrificed. When the outcome that corresponds to the 90<sup>th</sup> percentile joins the set of sacrificed observations, facing consistent mediocre deficits becomes more preferable for the 90<sup>th</sup> percentile objective. Therefore, its alignment with the aggregate deficit objective disappears. This emphasises that such internal trade-off conclusions are sensitive to the risk aversion level of objective formulations.

Distribution of Ethiopia's hydroenergy generation becomes distinctly bi-modal. Policies that leads high and low hydropower are clearly separated. Group of selected policies that yield desirable outcomes under the baseline scenario remains the same. Tables 4.8b and 4.8c suggest relatively strong trade-off between Ethiopia hydropower and Egypt irrigation deficit.

Figure 4.9 illustrates the results from the re-simulation runs that were taken under the *High Blue Nile Scenario*. Expectedly, under this scenario, higher levels of energy generation from the GERD were achieved by several policy alternatives. Moreover, colour-coding of tables 4.9b and 4.9c is lighter, indicating milder trade-offs.



(a) Pair plot for objective values

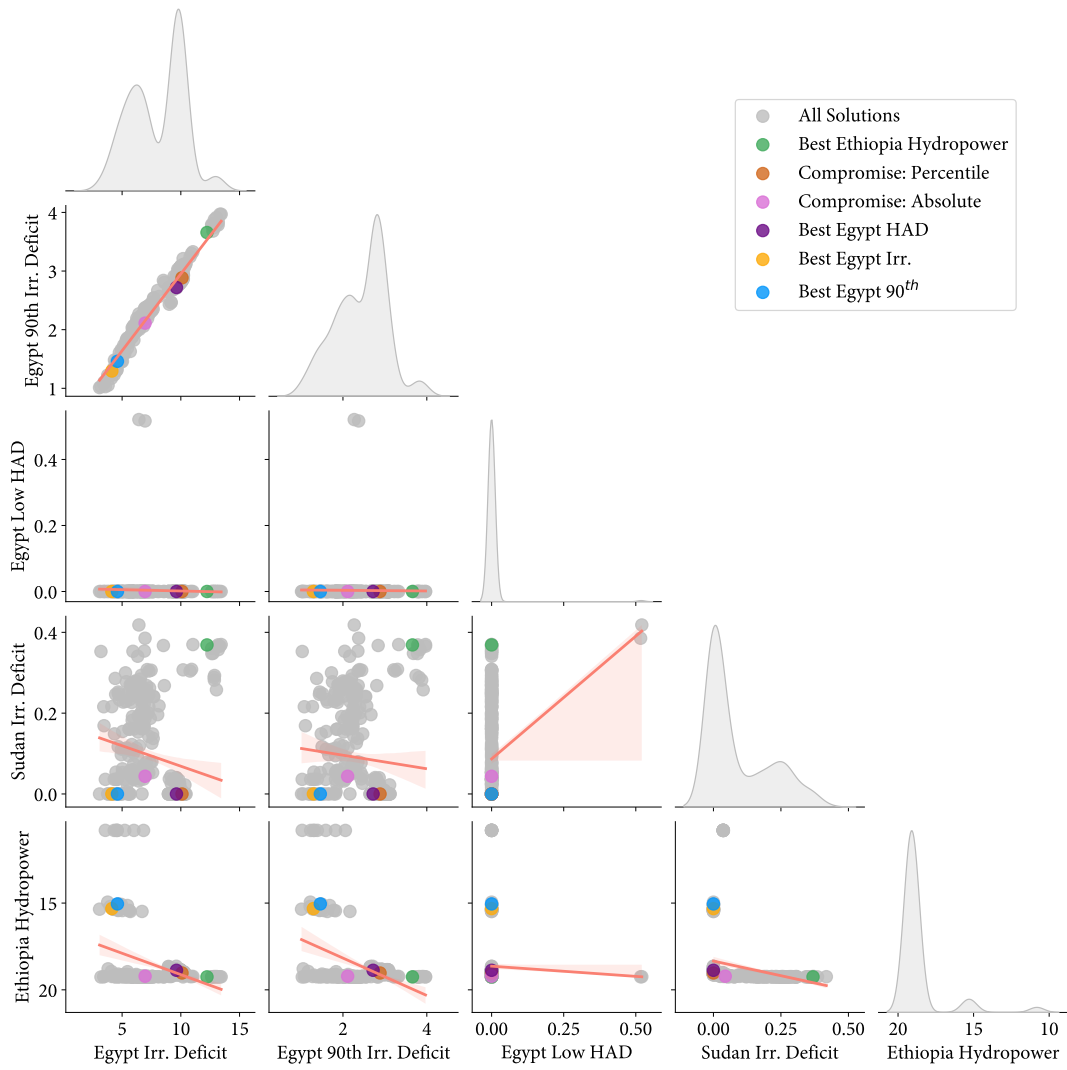
	Egypt Irr. Deficit	Egypt 90 <sup>th</sup> Irr. Deficit	Egypt Low HAD	Sudan Irr. Deficit	Sudan 90 <sup>th</sup> Irr. Deficit	Ethiopia Hydropower
Egypt Irr. Deficit	1.00	-0.09	-0.19	-0.01	0.08	-0.71
Egypt 90 <sup>th</sup> Irr. Deficit	-0.09	1.00	0.36	-0.10	-0.08	0.36
Egypt Low HAD	-0.19	0.36	1.00	-0.68	-0.82	-0.07
Sudan Irr. Deficit	-0.01	-0.10	-0.68	1.00	0.89	-0.05
Sudan 90 <sup>th</sup> Irr. Deficit	0.08	-0.08	-0.82	0.89	1.00	0.01
Ethiopia Hydropower	-0.71	0.36	-0.07	-0.05	0.01	1.00

(b) Regression slopes between objectives

	Egypt Irr. Deficit	Egypt 90 <sup>th</sup> Irr. Deficit	Egypt Low HAD	Sudan Irr. Deficit	Sudan 90 <sup>th</sup> Irr. Deficit	Ethiopia Hydropower
Egypt Irr. Deficit	1.00	-0.09	-0.24	-0.01	0.05	-0.60
Egypt 90 <sup>th</sup> Irr. Deficit	-0.09	1.00	0.48	-0.08	-0.06	0.16
Egypt Low HAD	-0.24	0.48	1.00	-0.43	-0.42	-0.02
Sudan Irr. Deficit	-0.01	-0.08	-0.43	1.00	0.93	-0.02
Sudan 90 <sup>th</sup> Irr. Deficit	0.05	-0.06	-0.42	0.93	1.00	0.00
Ethiopia Hydropower	-0.60	0.16	-0.02	-0.02	0.00	1.00

(c) Correlation between objectives

Figure 4.8 Overall trade-off patterns under the *Extreme Stress Scenario*



(a) Pair plot for objective values

	Egypt Irr. Deficit	Egypt 90 <sup>th</sup> Irr. Deficit	Egypt Low HAD	Sudan Irr. Deficit	Ethiopia Hydropower
Egypt Irr. Deficit	1.00	0.92	-0.02	-0.22	-0.31
Egypt 90 <sup>th</sup> Irr. Deficit	0.92	1.00	-0.01	-0.09	-0.39
Egypt Low HAD	-0.02	-0.01	1.00	0.76	-0.07
Sudan Irr. Deficit	-0.22	-0.09	0.76	1.00	-0.17
Ethiopia Hydropower	-0.31	-0.39	-0.07	-0.17	1.00

(b) Regression slopes between objectives

	Egypt Irr. Deficit	Egypt 90 <sup>th</sup> Irr. Deficit	Egypt Low HAD	Sudan Irr. Deficit	Ethiopia Hydropower
Egypt Irr. Deficit	1.00	0.98	-0.05	-0.18	-0.37
Egypt 90 <sup>th</sup> Irr. Deficit	0.98	1.00	-0.01	-0.07	-0.43
Egypt Low HAD	-0.05	-0.01	1.00	0.21	-0.03
Sudan Irr. Deficit	-0.18	-0.07	0.21	1.00	-0.26
Ethiopia Hydropower	-0.37	-0.43	-0.03	-0.26	1.00

(c) Correlation between objectives

Figure 4.9 Overall trade-off patterns under the *High Blue Nile Scenario*

# 5

## DISCUSSION

### 5.1 PRACTICAL IMPLICATIONS

#### 5.1.1 Fillings and Operations of the GERD

In view of the individual performance maximising policies for each objective under the baseline scenario, we found evident trade-offs between the hydroenergy generation objective of Ethiopia and consumptive uses of Egypt as well as Sudan. Physical system implications of candidate policies revealed that a major cause behind this trade-off is filling strategies for the GERD prescribed by alternative policies. One extreme is the aggressive filling of the GERD to an extent that leads to the blockage of the Blue Nile flow for multiple years, hence water shortages downstream. On the other extreme, the GERD never fills up near its full supply level and generates mediocre levels of hydroenergy. Having said that, there is a wide range of alternative solutions between these two extremes. The compromise solutions that we analysed are promising in the sense that they imply slower cooperative filling approaches. In that regard, our results support the agreed annual release solution proposed by [Wheeler et al. \(2016\)](#).

The average annual hydroenergy production that we calculated for the GERD under the baseline conditions varies between 9.4 and 15.1 TWh, averaging 13.9 TWh. This average is similar to the findings of earlier studies ([Abdelazim et al., 2020](#); [Eldardiry and Hossain, 2021](#)). Yet, it is significantly below the 16 TWh ambition that the Ethiopian government has announced ([Wheeler et al., 2020](#)). This signifies that unless mean inflow from the Blue Nile increases substantially, large hydropower capacity of the GERD will be underutilised.

#### 5.1.2 Challenge of Demand Growth

While filling of the GERD stands as a reason for trade-offs in the near future, another clash of interests occurs towards the end of the simulation horizon due to inevitable water shortage concerns with increasing demand. This brings up the fundamental trade-off between keeping dams operational and effective versus satisfying growing consumptive demand. Under every scenario tested in this analysis, the selection of adaptive policy alternatives exhibit such trade-offs in varying degrees. Being the country with the highest water consumption in the basin, Egypt is expected to face this major challenge. Although the nature of demand deficit varies according to the risk aversion and time aggregation logic of objective formulations, achieving zero deficit is not possible given

overall water balance of the Nile system. Acquiring more storage capacity by means of dam construction is not a systemic solution for the water shortage problem. Furthermore, it brings the additional issue of water loss due to evaporation which is particularly prominent in the case of the HAD.

### 5.1.3 Impacts on Sudan

In almost all of the experiments we conducted, the aggregate water demand in Sudan is satisfied with little or no deficit. One reason behind this observation can be that Sudan is located in the junction of all main tributaries; therefore, the water flow in the country is significantly higher compared to the average water demand. Unless aggressive filling of the GERD imposes complete blockage of the Blue Nile flow, Sudan's irrigation objectives are fulfilled.

Lastly, even though flood protection objective was left beyond the scope of our modelling, discrepancy between received flow and demand hints at flood risk which is indeed relevant for Sudan.

### 5.1.4 Room for Cooperation

Our results highlight the potential of compromise policies in managing the objectives of all stakeholders without imposing heavy sacrifices. Besides performing well under the baseline scenario, these compromise policies achieve high robustness scores for multiple objectives under varying socioeconomic and hydro-climatic conditions. They represent an opportunity for cooperative operating of the dams in the basin through which additional benefits are to be obtained. One such benefit can be about high evaporation losses from the HAD. The GERD, due to the more favourable bathymetric and climatic characteristics of the reservoir, experiences lower evaporation losses compared to the HAD. The more the water storage is concentrated upstream, the less amount of water is lost due to evaporation.

Our experiments in the uncertainty space suggest that under highly stressed scenarios, policies that target a specific objective tend to achieve more improvement for their objective compared to alternative policies. This implies that it could get more difficult to create space for negotiation when the pressure from external factors rises. On the contrary, magnitude of trade-offs becomes milder under the *HighBlueNileScenario*. Favourable hydrology of the Blue Nile flow can reduce the tension between parties.

## 5.2 LIMITATIONS

### 5.2.1 Conceptual Limitations

To keep our scope focused, we examined the trade-offs between six objectives from the perspectives of the three countries. Nonetheless, the Nile River basin covers a larger area than our system scope and communities within the borders of 11 countries depend on the Nile's flow. Therefore, there are many stakeholder activities and interests that

we did not incorporate in our study. For instance, water diversion in the rest of the basin was only superficially modelled as adjustable parameters of inflow distributions. A more comprehensive scope would let us model the system more accurately.

Moreover, we formulated the objectives as aggregated within a country and from a utilitarian perspective. Therefore, even within the current system scope, there are stakeholder interests that were not taken into account. People and ecosystems that depend on the environmental services provided by the Nile are not represented. An example is the flood-recession agriculture in Sudan, which is expected to be hit by the regulated release regime by the GERD (Taye et al., 2016). Due to lack of reliable data, we could not consider such interests. Expanding the objective set would enable a richer trade-off analysis.

### 5.2.2 Methodological Limitations

Trusting in the adaptive quality of Pareto-optimal policy alternatives and considering the computational cost, we performed optimisation only under the baseline scenario. Still, policy functions may have biases towards system conditions under which they were trained. Extending the analysis with an approach similar to multi-scenario MORDM (Watson and Kasprzyk, 2017) could yield sharper trade-offs under discovered scenarios.

Simplifications made to cope with the lack of available data cause few limitations to the model. For instance, yearly demand growth was assumed to be proportional to population growth and same for Egypt and Sudan. Streamflows of major tributaries were generated following simple probability distribution assumptions. These assumptions overlook characteristics of the hydro-climatic data such as autocorrelation and cyclic behaviour in the form of flood and drought periods. With detailed time-series data, statistical models could be fitted to better capture characteristics of these variables.

# 6

## CONCLUSION

### 6.1 ADDRESSING THE RESEARCH QUESTION

In this study, we set out to answer the question “*How can the trade-offs between different water uses in the Eastern Nile Basin be explored under changing socioeconomic and hydro-climatic uncertainties adopting many-objective optimisation approach?*”. To that end, we developed a simulation model of the Nile system and coupled it with a many-objective optimisation algorithm. We selected a set of policies from the Pareto-front generated by the optimisation and carried out simulations under varying uncertain scenarios. There are four sub-questions that led us in addressing the main research question. Here, we briefly present the answers to those questions.

#### **SQ1: What are the key water related objectives of stakeholders in the Eastern Nile Basin?**

The Nile is at the centre of the life for all three countries considered in this study. Egypt depends on Nile’s flow to fulfill almost all their fresh water need which includes urban consumption and agricultural irrigation. The HAD, a large dam located in Egypt, grants Egyptian authorities means to regulate water flow to meet the demand. Elevation of the HAD is not only regarded as an indicator of water security in the country but also determines hydropower generation. Similar to Egypt, agriculture has a major share in Sudan’s economy. Several Sudanese irrigation schemes scattered across the basin withdraw water from the Nile system. Ethiopia differs from these two countries with regard to their interaction with the Nile. Being motivated by the suitable topography and poor electricity access in the country, Ethiopia recently started to exploit their hydroenergy potential. The GERD has been an emblematic of this ambition.

#### **SQ2: How can the system of reservoirs be modelled in order to optimise release decisions for problem objectives?**

A simulation model of a multi-reservoir system can be built around the mechanism of mass-balance equations. This mechanism is a specification of the mathematical relationship between consecutive reservoir storages over time. Topology of the system in concern is represented through integrating components such as reservoirs, hydropower plants, irrigation districts and catchments. By inserting a flexible policy function in the simulation model, release decisions can be conditioned on dynamic system information. Parameters for the policy function can be optimised by MOEAs with respect to problem objectives. This complete procedure corresponds to the EMODPS methodology.

**SQ3: What are the trade-offs revealed by Pareto-optimal policy alternatives?**

Prominent trade-offs exist between Ethiopia's hydropower maximisation and deficit minimisation objectives of Egypt and Sudan. There are two major drivers of these trade-offs. On the one hand, potential aggressive filling of the GERD by Ethiopia at the cost of blocking the flow downstream clashes with the interests of Egypt and Sudan in the short-term. On the other hand, growing demand in the long-term brings the dilemma of maintaining dams operational versus satisfying the demand. This dilemma poses a common challenge for both the GERD and the HAD.

**SQ4: How do trade-offs differ with respect to alternative hydrology and demand growth scenarios?**

Extreme stress scenarios, in which the rate of demand growth is high and average inflows are low, reinforce the trade-offs between Egypt's aggregate deficit minimisation and Ethiopia's hydropower maximisation. Under such scenarios, the cost of not prioritising their objectives rise for the parties. Therefore, the room for negotiation becomes smaller. Furthermore, clashing interests also occur between different risk aversion framings for the objectives of the same country. On the contrary, tension between objectives decrease when the system conditions evolve in a favourable direction.

## 6.2 POLICY RECOMMENDATION

Trans-boundary collaboration is needed for addressing multiple challenges in the basin. The first and the most urgent challenge is filling of the GERD. The dam is already operational and Ethiopian authorities desire to boost hydroenergy generation without losing any time. However, there is no settlement among the three countries concerning the filling scheme and duration. This contributes to the escalation of tension among parties—between Egypt and Ethiopia in particular. If Ethiopia chooses to quickly fill the dam by ignoring downstream interests, both Sudan and Egypt can face dire consequences which would hinder the trust in the basin and damage the cooperation potential in the future. Therefore, a peaceful compromise solution is needed. It is possible to find alternatives which require parties to make minor sacrifices for the good of all. Parties should make binding agreements to delineate the exact strategy concerning filling duration and scheme. This strategy should be adaptive, accounting for dynamic hydro-climatic conditions.

Another serious challenge facing Egypt particularly is the growing water demand. A status-quo strategy cannot respond to this challenge sustainably. With the current demand growth trends, overall water balance in the Nile system gets tilted in the shortage direction within the following two decades. To both keep the HAD operational and minimise deficits, Egypt has to stabilise their demand. Consider two distinct strategies when the risk of shortage is on the horizon. The first option is to use all available storage to release water as much as it is pulled by the demand. This strategy leads to decreasing water availability and eventually drastic shortages. The second option is to maintain some buffer water supply in the reservoirs with the sight of future risks. This strategy accepts an amount of deficit consistently. Comparing these alternatives, the second one can provide more incentive for the water consuming social system to adapt to the "new



normal” through behavioural changes.

Basin-wide cooperation can be effective also to cope with this challenge. Moving water intensive agricultural products from Egypt to the water-rich upstream countries can be beneficial for all parties. This way, the water is concentrated more in the regions with lower evaporation rates and is kept in the system to a larger degree. This change necessitates higher levels of trust which can be facilitated through efficient trade agreements. Egypt can further specialise in its industrial production capabilities and play a pioneering role in producing win-win opportunities for the whole basin.

Sudan has interest alignments with both Egypt and Ethiopia. On one hand, they share concerns with Egypt regarding the GERD’s filling. On the other hand, regulation of the Blue Nile flow by the GERD reduces flood risk. The ruling out of cooperation potential by the escalation between Egypt and Ethiopia is therefore not desirable for Sudan. Having a common ground with both of the strained parties, they can play a mediator role in bolstering cooperation. Sudan can formulate and propose trade deals with Egypt for the readjustment of water intensive economic activities. Moreover, given their strategic geographical position, they can take part in the transmission of hydro-electricity generated in Ethiopia, facilitating their export. It is worth noting that with the growing demand pressure, the zero-sum characteristic of the strategic setup in the basin becomes more prominent. Therefore, the quicker the mediating action is taken, the more likely it is to achieve cooperative solutions.

Lastly, it is not feasible to sustainably operate the GERD at its full design capacity. High hydroenergy ambitions of Ethiopian authorities can be achieved only if the average flow reaching the GERD increases. The average flow depends on two factors. One is the Blue Nile flow and essentially rainfall in Ethiopian highlands, which is bounded by natural constraints. The second is water withdrawal from the flow in Ethiopia prior to the GERD. There are speculations about Ethiopia’s intentions of reducing water withdrawal to adopt a full capacity hydroenergy strategy. Although reduced diversion decreases overall tension among parties considering growing demand, it would encourage water-intensive activities in downstream instead of upstream. Concerning the overall water balance in the system, this strategy does not fit well with a cooperative economic arrangement.

### 6.3 FUTURE RESEARCH

The Nile River Basin is not limited to the countries and objectives considered in this study. Problem framings that are formulated to include different stakeholder interests could bring broader perspective to academic and political discussion. Future research can begin with incorporating the elements of environmental services and flood risk mitigation. Moreover, our study adopted a utilitarian approach in formulating stakeholder objectives. Different ethical theories would provide more insight into the distribution of benefits and damages across disaggregate units of communities.

We investigated the system in a full cooperation setup in this study. This choice was to ensure that the trade-offs are caused by the system description rather than the indepen-

dent individual management strategies of the national authorities For future research, alternative cooperation settings can be formulated reflecting on the strategic structure of the political arena.

On a more methodological point, we did not experiment with alternative sets of variables that pass the dynamic system information to adaptive policies. Expanding the input set with demand prediction could increase flexibility of the policy function in capturing water shortage dilemmas.

## BIBLIOGRAPHY

- N. Abdelazim, H. Bekhit, and M. N. Allam. Operation of the Grand Ethiopian Renaissance Dam: Potential Risks and Mitigation Measures. *Journal of Water Management Modeling*, 2020. doi: 10.14796/jwmm.c469.
- D. Abdelhady, K. Aggestam, D.-E. Andersson, O. Beckman, R. Berndtsson, K. B. Palmgren, K. Madani, U. Ozkirimli, K. M. Persson, P. Pilesjö, and et al. The Nile and the Grand Ethiopian Renaissance Dam: Is there a meeting point between nationalism and hydrosolidarity? *Journal of Contemporary Water Research & Education*, 155(1): 73–82, 2015. doi: 10.1111/j.1936-704x.2015.03197.x.
- M. A. Abu-Zeid and A. K. Biswas. Some major implications of climatic fluctuations on water management. *International Journal of Water Resources Development*, 7(2):74–81, June 1991. doi: 10.1080/07900629108722497.
- J. A. Allan. *Nile Basin Asymmetries: A Closed Fresh Water Resource, Soil Water Potential, the Political Economy and Nile Transboundary Hydropolitics*, pages 749–770. Springer Netherlands, Dordrecht, 2009. doi: 10.1007/978-1-4020-9726-3\_35.
- A. Amaranto, D. Juizo, and A. Castelletti. Disentangling sources of future uncertainties for water management in sub-Saharan river basins. *Hydrology and Earth System Sciences*, 26(2):245–263, Jan. 2022. doi: 10.5194/hess-26-245-2022.
- R. M. T. Amer. Revisiting hydro-hegemony from a benefitsharing perspective: the case of the Grand Ethiopian Renaissance Dam. Discussion Paper 5/2015, Bonn, 2015. URL <http://hdl.handle.net/10419/199455>.
- A. Ansar, B. Flyvbjerg, A. Budzier, and D. Lunn. Should we build more large dams? The actual costs of hydropower megaproject development. *Energy Policy*, 69:43–56, June 2014. doi: 10.1016/j.enpol.2013.10.069.
- Y. Arsano. *Ethiopia and the Nile: Dilemmas of national and regional hydropolitics*. PhD thesis, 2007.
- R. Barnes. Ethiopia’s US\$ 5bn Grand Renaissance Dam Project Updates, May 2022. URL <https://constructionreviewonline.com/project-timelines/ethiopias-us-5bn-grand-renaissance-dam-project-updates>.
- M. Basheer, K. G. Wheeler, N. A. Elagib, M. Etichia, E. A. Zagona, G. M. Abdo, and J. J. Harou. Filling Africa’s Largest Hydropower Dam Should Consider Engineering Realities. *One Earth*, 3(3):277–281, Sept. 2020. doi: 10.1016/j.oneear.2020.08.015.
- G. Berhane, T. Gebreyohannes, K. Martens, and K. Walraevens. Overview of micro-dam reservoirs (MDR) in Tigray (northern Ethiopia): Challenges and benefits. *Journal of African Earth Sciences*, 123:210–222, Nov. 2016. doi: 10.1016/j.jafrearsci.2016.07.022.

- F. Bertoni, A. Castelletti, M. Giuliani, and P. M. Reed. Discovering dependencies, trade-offs, and robustness in joint dam design and operation: An ex-post assessment of the Kariba Dam. *Earth's Future*, 7(12):1367–1390, Dec. 2019. doi: 10.1029/2019ef001235.
- P. J. Block. Integrated Management of the Blue Nile Basin in Ethiopia: Hydropower and Irrigation Modeling. 2007. doi: 10.22004/AG.ECON.42413.
- B. P. Bryant and R. J. Lempert. Thinking inside the box: A participatory, computer-assisted approach to scenario discovery. *Technological Forecasting and Social Change*, 77(1):34–49, Jan. 2010. doi: 10.1016/j.techfore.2009.08.002.
- A. Castelletti and R. Soncini-Sessa. Chapter 4 Systems, models and indicators. In R. Soncini-Sessa, editor, *Integrated and Participatory Water Resources Management: Theory*, volume 1 of *Developments in Integrated Environmental Assessment*, pages 95–136. Elsevier, 2007. doi: 10.1016/S1574-101X(07)01104-0.
- K. Deb, A. Pratap, S. Agarwal, and T. Meyarivan. A fast and elitist multiobjective genetic algorithm: NSGA-II. *IEEE Transactions on Evolutionary Computation*, 6(2):182–197, Apr. 2002. doi: 10.1109/4235.996017.
- Delft High Performance Computing Centre (DHPC). DelftBlue Supercomputer (Phase 1). <https://www.tudelft.nl/dhpc/ark:/44463/DelftBluePhase1>, 2022.
- H. J. Dumont. A description of the Nile basin, and a synopsis of its history, ecology, biogeography, hydrology, and natural resources. In *The Nile : origin, environments, limnology and human use*, pages 1–21. Springer Netherlands, 2009. doi: 10.1007/978-1-4020-9726-3\_1.
- E. Elba, D. Farghaly, and B. Urban. Modeling High Aswan Dam Reservoir Morphology Using Remote Sensing to Reduce Evaporation. *International Journal of Geosciences*, 05(02):156–169, 2014. doi: 10.4236/ijg.2014.52017.
- E. Elba, B. Urban, B. Ettmer, and D. Farghaly. Mitigating the Impact of Climate Change by Reducing Evaporation Losses: Sediment Removal from the High Aswan Dam Reservoir. *American Journal of Climate Change*, 06(02):230–246, 2017. doi: 10.4236/ajcc.2017.62012.
- H. Eldardiry and F. Hossain. Evaluating the hydropower potential of the Grand Ethiopian Renaissance Dam. *Journal of Renewable and Sustainable Energy*, 13(2):024501, Mar. 2021. doi: 10.1063/5.0028037.
- H. Elsayed, S. Djordjević, D. A. Savić, I. Tsoukalas, and C. Makropoulos. The Nile Water-Food-Energy Nexus under Uncertainty: Impacts of the Grand Ethiopian Renaissance Dam. *Journal of Water Resources Planning and Management*, 146(11):04020085, Nov. 2020. doi: 10.1061/(asce)wr.1943-5452.0001285.
- S. D. Falco and G. Fiorentino. The GERD dam in the water dispute between Ethiopia, Sudan and Egypt. A scenario analysis in an ecosystem approach between physical and geopolitical geography. *AIMS Geosciences*, 8(2):233–253, 2022. doi: 10.3934/geosci.2022014.

- B. M. Fekete, C. J. Vörösmarty, and W. Grabs. Nile Basin, Mogren Station, 2002. URL <https://www.compositerunoff.sr.unh.edu/html/Polygons/P1673100.html>.
- P. Geurts, D. Ernst, and L. Wehenkel. Extremely randomized trees. *Machine Learning*, 63(1):3–42, Mar. 2006. doi: 10.1007/s10994-006-6226-1.
- M. Giuliani, J. D. Herman, A. Castelletti, and P. Reed. Many-objective reservoir policy identification and refinement to reduce policy inertia and myopia in water management. *Water Resources Research*, 50(4):3355–3377, Apr. 2014. doi: 10.1002/2013WR014700.
- M. Giuliani, A. Castelletti, F. Pianosi, E. Mason, and P. M. Reed. Curses, Tradeoffs, and Scalable Management: Advancing Evolutionary Multiobjective Direct Policy Search to Improve Water Reservoir Operations. *Journal of Water Resources Planning and Management*, 142(2):04015050, Aug. 2015. doi: 10.1061/(ASCE)WR.1943-5452.0000570.
- M. Giuliani, M. Zaniolo, P. Block, and A. Castelletti. Data-driven control of water reservoirs using an emulator of the climate system. *IFAC-PapersOnLine*, 53(2):16531–16536, 2020. doi: 10.1016/j.ifacol.2020.12.771.
- M. Giuliani, J. R. Lamontagne, P. M. Reed, and A. Castelletti. A State-of-the-Art Review of Optimal Reservoir Control for Managing Conflicting Demands in a Changing World. *Water Resources Research*, 57(12), Dec. 2021. doi: 10.1029/2021WR029927.
- G. Guariso and M. Sangiorgio. Performance of Implicit Stochastic Approaches to the Synthesis of Multireservoir Operating Rules. *Journal of Water Resources Planning and Management*, 146(6):04020034, June 2020. doi: 10.1061/(ASCE)WR.1943-5452.0001200.
- M. Hakimi-Asiabar, S. H. Ghodsypour, and R. Kerachian. Deriving operating policies for multi-objective reservoir systems: Application of self-learning genetic algorithm. *Applied Soft Computing*, 10(4):1151–1163, Sept. 2010. doi: 10.1016/j.asoc.2009.08.016.
- J. Helton and F. Davis. Latin hypercube sampling and the propagation of uncertainty in analyses of complex systems. *Reliability Engineering & System Safety*, 81(1):23–69, 2003. doi: 10.1016/S0951-8320(03)00058-9.
- J. D. Herman, P. M. Reed, H. B. Zeff, and G. W. Characklis. How should robustness be defined for water systems planning under change? *Journal of Water Resources Planning and Management*, 141(10), oct 2015. doi: 10.1061/(asce)wr.1943-5452.0000509.
- A. M. Ibrahim. The Nile Basin Cooperative Framework Agreement: the beginning of the end of Egyptian hydro-political hegemony. *Missouri Environmental Law and Policy Review*, 18:282, 2010.
- IWMI. Water availability concerns surface as irrigation area in Nile basin projected to increase significantly by 2050, Oct 2021. URL <https://www.iwmi.cgiar.org/2021/10>.
- J. R. Kasprzyk, P. M. Reed, B. R. Kirsch, and G. W. Characklis. Managing population and drought risks using many-objective water portfolio planning under uncertainty. *Water Resources Research*, 45(12), Dec. 2009. doi: 10.1029/2009wro08121.

- J. R. Kasprzyk, S. Nataraj, P. M. Reed, and R. J. Lempert. Many objective robust decision making for complex environmental systems undergoing change. *Environmental Modelling & Software*, 42:55–71, Apr. 2013. doi: 10.1016/j.envsoft.2012.12.007.
- M. Keskinen, J. Guillaume, M. Kattelus, M. Porkka, T. Räsänen, and O. Varis. The Water-Energy-Food Nexus and the Transboundary Context: Insights from Large Asian Rivers. *Water*, 8(5):193, May 2016. doi: 10.3390/w8050193.
- A. King and P. Block. An assessment of reservoir filling policies for the Grand Ethiopian Renaissance Dam. *Journal of Water and Climate Change*, 5(2):233–243, Jan. 2014. doi: 10.2166/wcc.2014.043.
- J. B. Kollat and P. M. Reed. The value of online adaptive search: A performance comparison of NSGAI,  $\epsilon$ -NSGAI and  $\epsilon$ MOEA. In *Lecture Notes in Computer Science*, pages 386–398. Springer Berlin Heidelberg, 2005. doi: 10.1007/978-3-540-31880-4\_27.
- D. Koutsoyiannis and A. Economou. Evaluation of the parameterization-simulation-optimization approach for the control of reservoir systems. *Water Resources Research*, 39(6), June 2003. doi: 10.1029/2003WR002148.
- J. Kumagai. The Grand Ethiopian Renaissance Dam gets set to open, Dec 2016. URL <https://spectrum.ieee.org/the-grand-ethiopian-renaissance-dam-gets-set-to-open>.
- J. H. Kwakkel. The Exploratory Modeling Workbench: An open source toolkit for exploratory modeling, scenario discovery, and (multi-objective) robust decision making. *Environmental Modelling & Software*, 96:239–250, 2017. doi: 10.1016/j.envsoft.2017.06.054.
- J. H. Kwakkel and M. Jaxa-Rozen. Improving scenario discovery for handling heterogeneous uncertainties and multinomial classified outcomes. *Environmental Modelling & Software*, 79:311–321, May 2016. doi: 10.1016/j.envsoft.2015.11.020.
- M. Laumanns, L. Thiele, K. Deb, and E. Zitzler. Combining convergence and diversity in evolutionary multiobjective optimization. *Evolutionary Computation*, 10(3):263–282, Sept. 2002. doi: 10.1162/106365602760234108.
- R. Lempert, S. Popper, and S. Bankes. *Shaping the Next One Hundred Years: New Methods for Quantitative, Long-Term Policy Analysis*. RAND Corporation, 2003. doi: 10.7249/MR1626.
- J. Liu, A. Dorjderem, J. Fu, X. Lei, and D. Macer. *Water Ethics and Water Resource Management*. UNESCO, 2011.
- H. Maier, Z. Kapelan, J. Kasprzyk, J. Kollat, L. Matott, M. Cunha, G. Dandy, M. Gibbs, E. Keedwell, A. Marchi, A. Ostfeld, D. Savic, D. Solomatine, J. Vrugt, A. Zecchin, B. Minsker, E. Barbour, G. Kuczera, F. Pasha, A. Castelletti, M. Giuliani, and P. Reed. Evolutionary algorithms and other metaheuristics in water resources: Current status, research challenges and future directions. *Environmental Modelling & Software*, 62:271–299, Dec. 2014. doi: 10.1016/j.envsoft.2014.09.013.
- F. Makonye. The Grand Ethiopian Renaissance Dam (GERD) as a Solution for Sustainable Hydro-electricity Generation: Tensions and Threats with Egypt and the Sudan, journal = *Journal of African Foreign Affairs*. 8(2):61–74, Aug. 2021. doi: 10.31920/2056-5658/2021/v8n2a4.

- V. A. W. J. Marchau, W. E. Walker, P. J. T. M. Bloemen, and S. W. Popper, editors. *Decision Making under Deep Uncertainty*. Springer International Publishing, 2019. doi: 10.1007/978-3-030-05252-2.
- C. McPhail, H. R. Maier, J. H. Kwakkel, M. Giuliani, A. Castelletti, and S. Westra. Robustness Metrics: How are they calculated, when should they be used and why do they give different results? *Earth's Future*, 6(2):169–191, Feb. 2018. doi: 10.1002/2017ef000649.
- NBI. Nile Basin, 2022. URL <http://atlas.nilebasin.org/start/>.
- R. Oliveira and D. P. Loucks. Operating rules for multireservoir systems. *Water Resources Research*, 33(4):839–852, Apr. 1997. doi: 10.1029/96WR03745.
- N. V. Pemunta, N. V. Ngo, C. R. F. Djomo, S. Mutola, J. A. Seember, G. A. Mbong, and E. A. Forkim. The Grand Ethiopian Renaissance Dam, Egyptian National Security, and human and food security in the Nile River Basin. *Cogent Social Sciences*, 7(1), Jan. 2021. doi: 10.1080/23311886.2021.1875598.
- J. D. Quinn, P. M. Reed, M. Giuliani, and A. Castelletti. Rival framings: A framework for discovering how problem formulation uncertainties shape risk management trade-offs in water resources systems. *Water Resources Research*, 53(8):7208–7233, Aug. 2017. doi: 10.1002/2017wr020524.
- P. Reed, D. Hadka, J. Herman, J. Kasprzyk, and J. Kollat. Evolutionary multiobjective optimization in water resources: The past, present, and future. *Advances in Water Resources*, 51:438–456, Jan. 2013. doi: 10.1016/j.advwatres.2012.01.005.
- Rédaction AfricaNews. Ethiopia completes second phase of filling of the “Grand Renaissance” dam, Jul 2021. URL <https://www.africanews.com/2021/07/19/ethiopia-completes-second-phase-of-refill-on-controversial-mega-dam-on-the-nile>.
- M. Sangiorgio and G. Guariso. NN-Based Implicit Stochastic Optimization of Multi-Reservoir Systems Management. *Water*, 10(3):303, Mar. 2018. doi: 10.3390/w10030303.
- A. M. Sharaky, K. H. Hamed, and A. B. Mohamed. Model-Based Optimization for Operating the Ethiopian Renaissance Dam on the Blue Nile River. In A. M. Negm and S. Abdel-Fattah, editors, *Grand Ethiopian Renaissance Dam Versus Aswan High Dam: A View from Egypt*, pages 119–148. Springer International Publishing, Cham, 2019. doi: 10.1007/698\_2017\_188.
- G. Soliman, H. Soussa, and S. Elsayed. Assessment of Grand Ethiopian Renaissance Dam Impacts Using Decision Support System. 10 2016. doi: 10.9790/0661-1805060818.
- R. Soncini-Sessa and E. Weber. Chapter 5 Modelling the components. In R. Soncini-Sessa, editor, *Integrated and Participatory Water Resources Management: Theory*, volume 1 of *Developments in Integrated Environmental Assessment*, pages 137–184. Elsevier, 2007. doi: 10.1016/S1574-101X(07)01105-2.
- A.-T. Stamou and P. Rutschmann. Pareto Optimization of Water Resources Using the Nexus Approach. *Water Resources Management*, 32(15):5053–5065, Dec. 2018. doi: 10.1007/s11269-018-2127-x.

- J. R. Stedinger, B. F. Sule, and D. P. Loucks. Stochastic dynamic programming models for reservoir operation optimization. *Water Resources Research*, 20(11):1499–1505, Nov. 1984. doi: 10.1029/wr020i011p01499.
- J. V. Sutcliffe. The Hydrology of the Nile Basin. In *The Nile*, pages 335–364. Springer Netherlands, 2009. doi: 10.1007/978-1-4020-9726-3\_17.
- S. Suzuki, D. Stern, and T. Manzocchi. Using association rule mining and high-dimensional visualization to explore the impact of geological features on dynamic flow behavior. SPE, Sept. 2015. doi: 10.2118/174774-ms.
- A. Swain. The Nile River Basin Initiative: Too many cooks, too little broth. *SAIS Review*, 22(2):293–308, 2002. doi: 10.1353/sais.2002.0044.
- M. R. Talbot and M. A. Williams. *Cenozoic Evolution of the Nile Basin*, pages 37–60. Springer Netherlands, Dordrecht, 2009. ISBN 978-1-4020-9726-3. doi: 10.1007/978-1-4020-9726-3\_3.
- M. T. Taye, P. Willems, and P. Block. Implications of climate change on hydrological extremes in the blue Nile basin: A review. *Journal of Hydrology: Regional Studies*, 4: 280–293, Sept. 2015. doi: 10.1016/j.ejrh.2015.07.001.
- M. T. Taye, T. Tadesse, G. B. Senay, and P. Block. The grand Ethiopian renaissance dam: Source of cooperation or contention? *Journal of Water Resources Planning and Management*, 142(11):02516001, 2016.
- UN. World population prospects - population division, 2022. URL <https://population.un.org/wpp/publications>.
- J. Verhagen, P. van der Zaag, and E. Abraham. Operational planning of WEF infrastructure: quantifying the value of information sharing and cooperation in the eastern Nile basin. *Environmental Research Letters*, 16(8):085006, July 2021. doi: 10.1088/1748-9326/ac1194.
- W. E. Walker, V. Marchau, and J. H. Kwakkel. Uncertainty in the Framework of Policy Analysis. In *Public Policy Analysis: New Developments*, volume 179 of *International Series in Operations Research & Management Science*. Springer, New York, 2013. ISBN 978-1-4614-4601-9.
- H. Wang, Y. Jin, and X. Yao. Diversity assessment in many-objective optimization. *IEEE Transactions on Cybernetics*, 47(6):1510–1522, Jun 2017. doi: 10.1109/tcyb.2016.2550502.
- A. A. Watson and J. R. Kasprzyk. Incorporating deeply uncertain factors into the many objective search process. *Environmental Modelling & Software*, 89:159–171, Mar. 2017. doi: 10.1016/j.envsoft.2016.12.001.
- K. G. Wheeler and R. Caplan. How natural resource (mis-)management in the Nile River basin may threaten stability, May 2020. URL <https://gjia.georgetown.edu/2020/05/20/natural-resource-mis-management-in-nile-river-basin-may-threaten-stability>.
- K. G. Wheeler, M. Basheer, Z. T. Mekonnen, S. O. Eltoum, A. Mersha, G. M. Abdo, E. A. Zagana, J. W. Hall, and S. J. Dadson. Cooperative filling approaches for the



- Grand Ethiopian Renaissance Dam. *Water International*, 41(4):611–634, June 2016. doi: 10.1080/02508060.2016.1177698.
- K. G. Wheeler, J. W. Hall, G. M. Abdo, S. J. Dadson, J. R. Kasprzyk, R. Smith, and E. A. Zagona. Exploring Cooperative Transboundary River Management Strategies for the Eastern Nile Basin. *Water Resources Research*, 54(11):9224–9254, Nov. 2018. doi: 10.1029/2017WR022149.
- K. G. Wheeler, M. Jeuland, J. W. Hall, E. Zagona, and D. Whittington. Understanding and managing new risks on the Nile with the Grand Ethiopian Renaissance Dam. *Nature Communications*, 11(1):5222, Dec. 2020. doi: 10.1038/s41467-020-19089-x.
- D. Whittington, J. Waterbury, and M. Jeuland. The grand renaissance dam and prospects for cooperation on the eastern Nile. *Water Policy*, 16(4):595–608, Mar. 2014. doi: 10.2166/wp.2014.011b.
- M. A. Williams and M. R. Talbot. *Late Quaternary Environments in the Nile Basin*, pages 61–72. Springer Netherlands, Dordrecht, 2009. doi: 10.1007/978-1-4020-9726-3\_4.
- M. A. J. Williams. Human Impact on the Nile Basin: Past, Present, Future. In *The Nile : origin, environments, limnology and human use*, pages 771–779. Springer Netherlands, 2009. doi: 10.1007/978-1-4020-9726-3\_36.
- World Bank. World Bank Open Data, 2021. URL <https://data.worldbank.org>.
- World Bank. *Directions In Hydropower : Scaling up for Development*. World Bank, 2010. URL <http://hdl.handle.net/10986/11702>.
- S. G. Yalew, J. Kwakkel, and N. Doorn. Distributive Justice and Sustainability Goals in Transboundary Rivers: Case of the Nile Basin. *Frontiers in Environmental Science*, 8, Feb. 2021. doi: 10.3389/fenvs.2020.590954.
- C. Zarfl, A. E. Lumsdon, J. Berlekamp, L. Tydecks, and K. Tockner. A global boom in hydropower dam construction. *Aquatic Sciences*, 77(1):161–170, Oct. 2014. doi: 10.1007/s00027-014-0377-0.
- J. Zatarain Salazar, P. M. Reed, J. D. Herman, M. Giuliani, and A. Castelletti. A diagnostic assessment of evolutionary algorithms for multi-objective surface water reservoir control. *Advances in Water Resources*, 92:172–185, June 2016. doi: 10.1016/j.advwatres.2016.04.006.
- M. Zeitoun and J. Warner. Hydro-hegemony – a framework for analysis of transboundary water conflicts. *Water Policy*, 8(5):435–460, Oct. 2006. doi: 10.2166/wp.2006.054.

### A.1 CONCEPTUAL MODEL

#### A.1.1 Model Components in Geographical Context

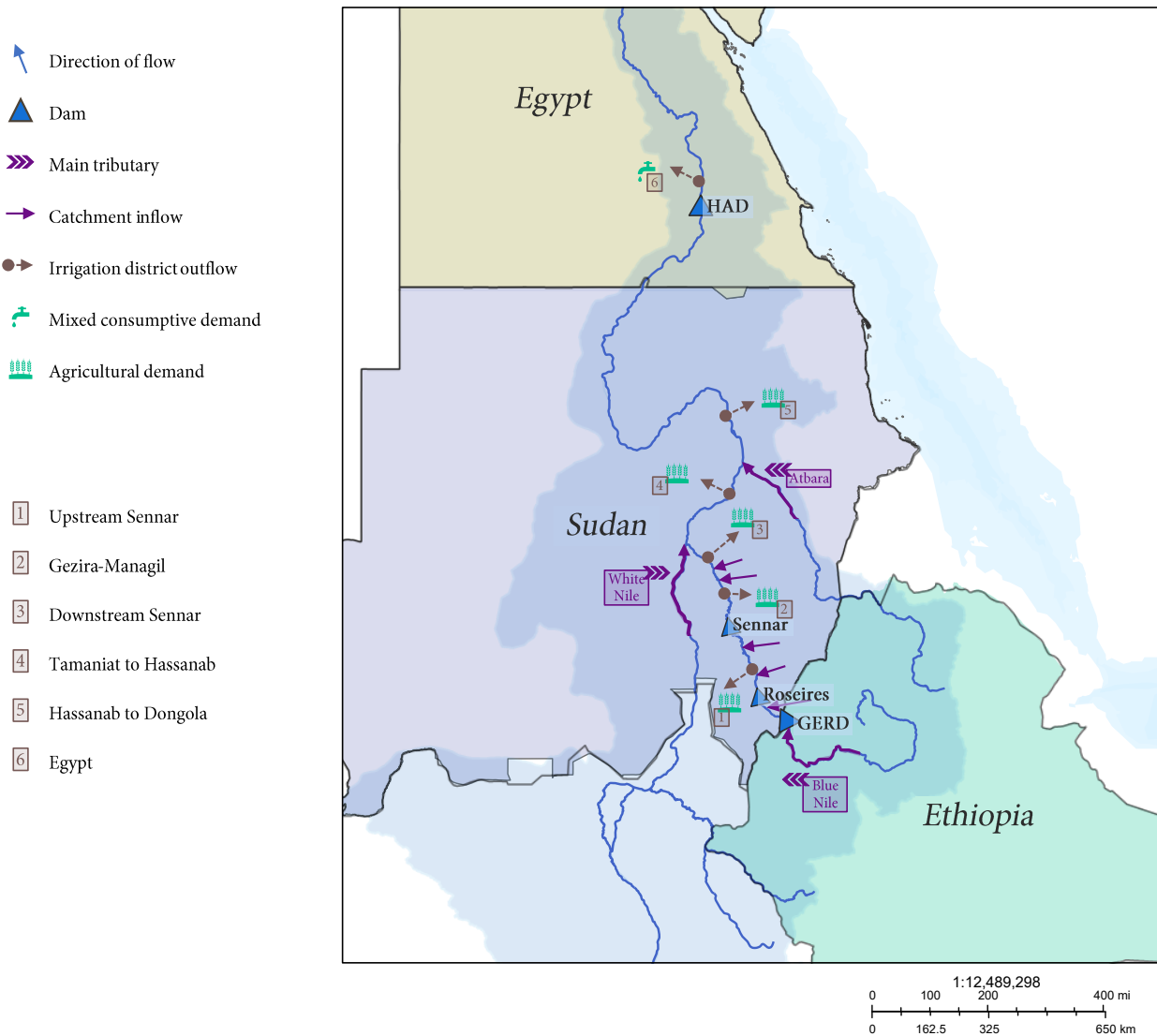


Figure A.1 Geographical schematic of the scope

### A.1.2 Component Specification

Each component type corresponds to a class in the Python implementation of the model. In addition, there are three more classes that represent the features and methods of the model, policy and RBF classes.

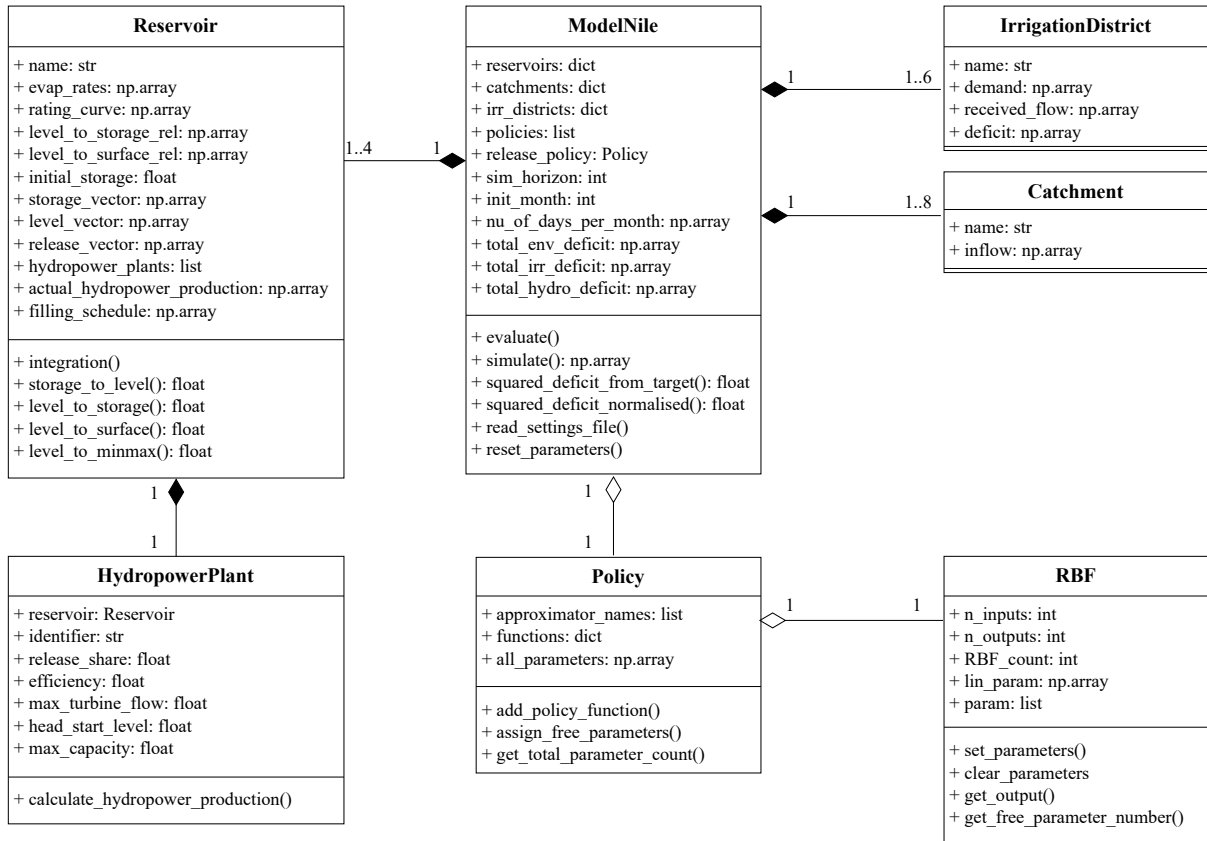


Figure A.2 UML class diagram representation of model objects

## A.2 SPECIFIC MODEL EQUATIONS

### A.2.1 GERD Inflow

$$q_{\tau}^{GERD} = \hat{Q}_{\tau}^{BlueNile} \quad (A.1)$$

where  $\hat{Q}_{\tau}^{BlueNile}$  is the average secondly flow from Blue Nile.

### A.2.2 Roseires Inflow

$$q_{\tau}^{Roseires} = \hat{R}_{\tau}^{GERD} + \hat{Q}_{\tau}^{Catch1} \quad (A.2)$$

where  $\hat{R}_{\tau}^{GERD}$  is the actual average secondly release from GERD and  $\hat{Q}_{\tau}^{Catch1}$  is the sum of average secondly flows from catchments that join the flow between GERD and Roseires.

### A.2.3 Upstream Sennar Received Flow

$$v_{\tau}^{USSennar} = \hat{R}_{\tau}^{Roseires} + \hat{Q}_{\tau}^{Catch2} \quad (A.3)$$

where  $\hat{R}_{\tau}^{Roseires}$  is the actual average secondly release from Roseires and  $\hat{Q}_{\tau}^{Catch2}$  is the sum of average secondly flows from catchments that join the flow between Roseires and Abu Na'ama.

### A.2.4 Sennar Inflow

$$q_{\tau}^{Sennar} = \max(0, v_{\tau}^{USSennar} - d_{\tau}^{USSennar}) + \hat{Q}_{\tau}^{Catch3} \quad (A.4)$$

where  $\max(0, v_{\tau}^{USSennar} - d_{\tau}^{USSennar})$  is the leftover flow from Upstream Sennar and  $\hat{Q}_{\tau}^{Catch3}$  is the sum of average secondly flows from catchments that join the flow between Suki and Sennar.

### A.2.5 Gezira Received Flow

$$v_{\tau}^{Gezira} = \hat{R}_{\tau}^{Sennar} \quad (A.5)$$

where  $\hat{R}_{\tau}^{Sennar}$  is the actual average secondly flow released from Sennar.

### A.2.6 Downstream Sennar Received Flow

$$v_{\tau}^{DSSennar} = \max(0, v_{\tau}^{Gezira} - d_{\tau}^{Gezira}) + \hat{Q}_{\tau}^{Dinder} + \hat{Q}_{\tau}^{Rahad} \quad (A.6)$$

where  $\max(0, v_{\tau}^{Gezira} - d_{\tau}^{Gezira})$  is the leftover flow from Gezira and  $\hat{Q}_{\tau}^{Dinder}$  and  $\hat{Q}_{\tau}^{Rahad}$  are the average secondly flows from Dinder and Rahad tributaries respectively.

### A.2.7 Taminiat Received Flow

$$v_{\tau}^{Taminiat} = \max(0, v_{\tau}^{DSSennar} - d_{\tau}^{DSSennar}) + \hat{Q}_{\tau}^{WhiteNile} \quad (A.7)$$

where  $\max(0, v_{\tau}^{DSSennar} - d_{\tau}^{DSSennar})$  is the leftover flow from Downstream Sennar and  $\hat{Q}_{\tau}^{WhiteNile}$  is the average secondly flow from White Nile.

#### A.2.8 Hassanab Received Flow

$$v_{\tau}^{Hassanab} = \max(0, v_{\tau-1}^{Taminiat} - d_{\tau-1}^{Taminiat}) + \hat{Q}_{\tau}^{Atbara} \quad (A.8)$$

where  $\max(0, v_{\tau-1}^{Taminiat} - d_{\tau-1}^{Taminiat})$  is the leftover flow from Taminiat in previous month and  $\hat{Q}_{\tau}^{Atbara}$  is the average secondly flow from Atbara.  $v_0^{Taminiat} - d_0^{Taminiat}$  is assumed to be  $934.2 \text{ m}^3/\text{s}$ , which is the average of the latest five years available at the Dongola gauging station (Fekete et al., 2002).

#### A.2.9 HAD Inflow

$$q_{\tau}^{HAD} = \max(0, v_{\tau}^{Hassanab} - d_{\tau}^{Hassanab}) \quad (A.9)$$

where  $\max(0, v_{\tau}^{Hassanab} - d_{\tau}^{Hassanab})$  is the leftover flow from Hassanab.

#### A.2.10 Egypt Received Flow

$$v_{\tau}^{Egypt} = \hat{R}_{\tau}^{HAD} \quad (A.10)$$

where  $\hat{R}_{\tau}^{HAD}$  is the actual average secondly flow released from HAD.

## A.3 RESERVOIR DATA

### A.3.1 Hydro-power Generation Data

Reservoir	Variable	Value	Reference
GERD	Initial Storage ( $m^3$ )	15 BCM	Barnes (2022); Rédaction AfricaNews (2021)
	Max Turbine Flow ( $m$ )	4320	Abdelazim et al. (2020)
	Efficiency (%)	93%	Abdelazim et al. (2020)
	Head Start Level ( $m$ )	507	Eldardiry and Hossain (2021)
	Max Capacity (MW)	6000	Wheeler et al. (2016)
Roseires	Initial Storage ( $m^3$ )	4.57 BCM	Assumption
	Max Turbine Flow ( $m$ )	1031.65	Wheeler et al. (2016)
	Efficiency (%)	80%	Assumption
	Head Start Level ( $m$ )	467	Wheeler et al. (2016)
	Max Capacity (MW)	280	Wheeler et al. (2016)
Sennar	Initial Storage ( $m^3$ )	0.43 BCM	Assumption
	Max Turbine Flow ( $m$ )	117	Wheeler et al. (2016)
	Efficiency (%)	80%	Assumption
	Head Start Level ( $m$ )	417.2	Wheeler et al. (2016)
	Max Capacity (MW)	15	Wheeler et al. (2016)
HAD	Initial Storage ( $m^3$ )	137 BCM	Assumption
	Max Turbine Flow ( $m$ )	4211	Wheeler et al. (2016)
	Efficiency (%)	90%	Assumption
	Head Start Level ( $m$ )	147	Wheeler et al. (2016)
	Max Capacity (MW)	2100	Wheeler et al. (2016)

Table A.1 Overview of hydropower generation data

Three reservoirs other than the GERD were assumed to be 75% full from the start. Initial storage level of the GERD as of the simulation starting date (January 2022) is controversial. We assumed an initial storage of 15 BCM which corresponds to 590 masl, minimum operational level of the GERD.

### A.3.2 Elevation-Area-Storage Curves

GERD			Roseires			Sennar			HAD		
Level (m)	Stor- age (BCM)	Sur- face (km <sup>2</sup> )	Level (m)	Stor- age (BCM)	Sur- face (km <sup>2</sup> )	Level (m)	Stor- age (BCM)	Sur- face (km <sup>2</sup> )	Level (m)	Stor- age (BCM)	Sur- face (km <sup>2</sup> )
500	0	3	465	0	5	411	0	0	110	0	0
510	0.01	11	467	0.027	10	412	0.001	0.9	120	5.2	450
520	0.02	29	467.7	0.046	13	412.6	0.002	2.1	125	7.8	600
530	0.05	61	468	0.056	15	413	0.002	3.2	130	11.3	749
540	0.75	111	470	0.156	33	413.6	0.005	5.7	135	15.6	988
550	2	180	472	0.321	58	414	0.007	7.8	140	21.2	1242
560	3	272	473	0.429	74	414.6	0.013	11.7	145	28.3	1589
570	6	387	475	0.699	111	415	0.018	15.6	150	37.2	1962
580	9.8	531	477	1.044	156	415.6	0.028	20.8	155	48.1	2414
590	15	703	478	1.246	181	416	0.037	25.3	160	61.5	2950
600	21.5	905	480	1.708	238	416.6	0.054	33	165	77.9	3581
610	31	1133	482	2.29	302	417	0.068	38.8	170	97.6	4308
620	42.5	1380	483	2.645	335	417.6	0.094	48.6	175	121	5168
630	57	1638	485	3.461	403	418	0.114	55.8	180	150	6118
640	74	1904	487	4.415	466	418.6	0.151	67.8	183	169	6752

Table A.2 Elevation-Area-Storage curves for reservoirs

### A.3.3 Evaporation Rates

	GERD	Roseires	Sennar	HAD
Jan	13.50	17.98	17.98	10.38
Feb	13.60	18.48	18.48	13.00
Mar	17.10	22.66	22.66	20.30
Apr	15.70	22.11	22.11	25.20
May	10.60	18.91	18.91	31.71
Jun	4.20	6.27	6.27	32.49
Jul	-0.40	-2.79	-2.79	32.40
Aug	0.10	-2.60	-2.60	31.50
Sept	1.40	1.95	1.95	27.00
Oct	9.10	12.49	12.49	21.51
Nov	11.40	15.69	15.69	14.01
Dec	11.50	16.74	16.74	10.60

Table A.3 Evaporation rates for reservoirs per month of the year (*cm*)



### A.3.4 Minimum and Maximum Release Constraints

#### A.3.4.1 GERD

Level (masl)	590	591	630	640
Min. release (m <sup>3</sup> /s)	0	0	0	4000
Max. release (m <sup>3</sup> /s)	0	10000	10000	10000

Table A.4 Minimum and maximum release for the GERD

#### A.3.4.2 Roseires

Level (masl)	467	475	481	490
Min. release (m <sup>3</sup> /s)	0	0	1000	4000
Max. release (m <sup>3</sup> /s)	0	10000	10000	10000

Table A.5 Minimum and maximum release for the Roseires

#### A.3.4.3 Sennar

Level (masl)	417.2	418	420	421.7
Min. release (m <sup>3</sup> /s)	0	0	0	4000
Max. release (m <sup>3</sup> /s)	0	6000	6000	10000

Table A.6 Minimum and maximum release for the Sennar

#### A.3.4.4 HAD

Level (masl)	147	148	175	182
Min. release (m <sup>3</sup> /s)	0	0	1000	4000
Max. release (m <sup>3</sup> /s)	0	4000	4000	4000

Table A.7 Minimum and maximum release for the HAD

#### A.4 DISTRICT DEMAND DATA

	Upstream Sennar	Gezira	Down-stream Sennar	Taminiat	Hassanab to Dongola	Egypt
Jan	67.58	319.59	7.47	18.67	28.38	1310.48
Feb	66.14	328.21	8.27	12.81	19.84	1620.37
Mar	44.80	155.32	10.45	5.23	8.21	1635.30
Apr	34.72	26.62	11.57	4.63	6.94	1589.51
May	35.10	51.52	12.32	7.09	10.83	1896.65
Jun	77.16	254.24	12.73	14.66	22.38	2438.27
Jul	97.45	349.84	8.96	13.44	20.16	2523.89
Aug	93.71	176.97	7.09	10.83	16.05	2202.81
Sept	132.33	361.88	10.42	20.45	30.48	1601.08
Oct	148.22	388.29	11.20	25.01	37.71	1452.36
Nov	141.98	357.25	10.03	25.85	38.97	1481.48
Dec	82.89	344.24	7.09	23.15	35.10	1355.29

Table A.8 District demand data

## A.5 EPSILON VALUES

We had determined the epsilon value for each objective by doing several trial simulations and observing the range of objective values.

Objective	Epsilon
Egypt average yearly demand deficit	0.1
Egypt 90 <sup>th</sup> percentile worst demand deficit	0.01
Egypt HAD level reliability	0.01
Sudan average yearly demand deficit	0.1
Sudan 90 <sup>th</sup> percentile worst demand deficit	0.01
Ethiopia hydro-energy generation	0.1

Table A.9 Epsilon values used in the optimisation for each objective

# B | APPENDICES: RESULTS

## B.1 CONVERGENCE ANALYSIS

While the  $\epsilon$ -progress curve on the left shows that there is still room for improvement, the hypervolume graph on the right seems to be in a stabilising trend. Given the time and computational constraints of the project, we deemed the status of convergence as sufficient with 50,000 NFEs.

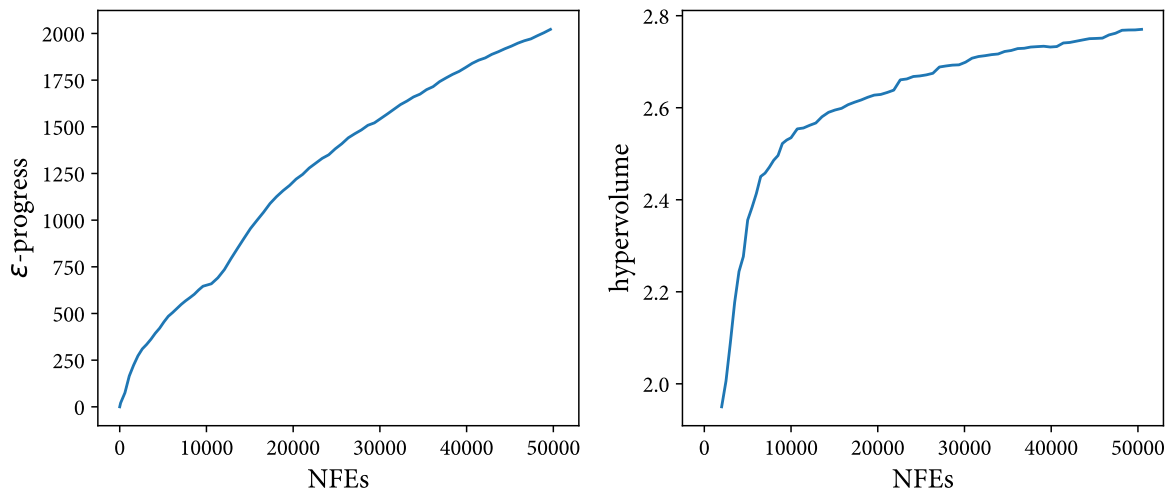
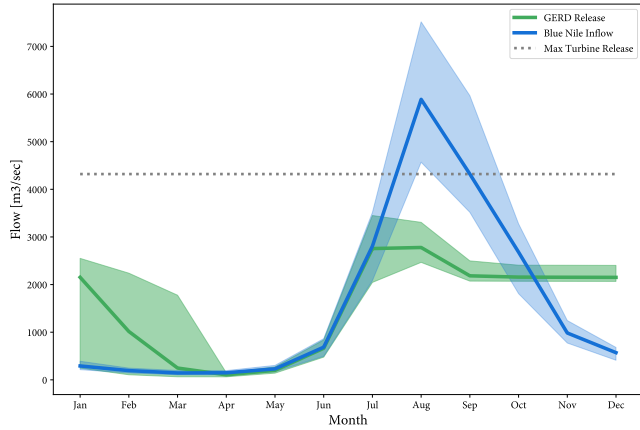


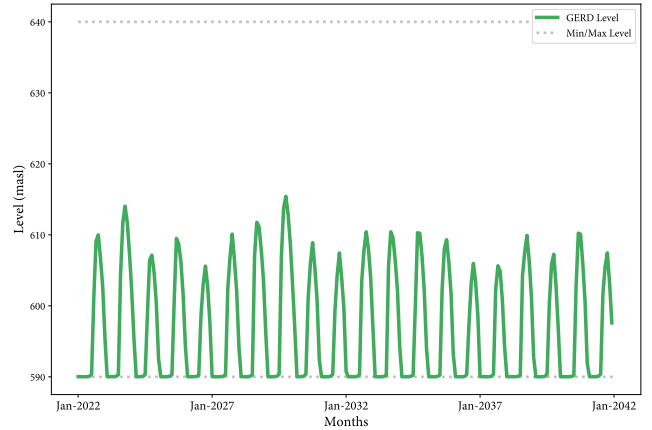
Figure B.1  $\epsilon$ -progress and hypervolume convergence

## B.2 PHYSICAL SYSTEM IMPLICATIONS

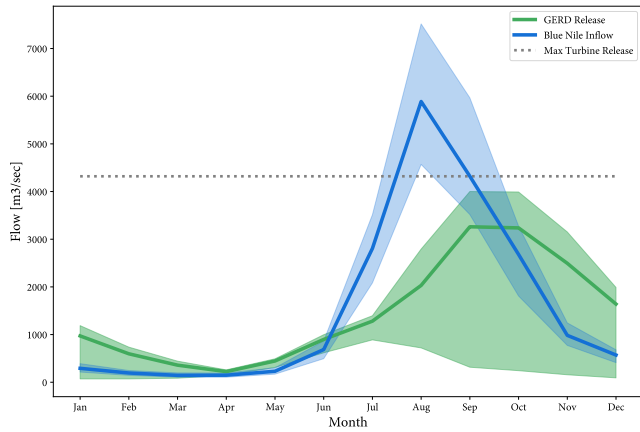
In this section, we present physical system changes imposed by policies—particularly those that were not explicitly discussed in [4.1.2](#).



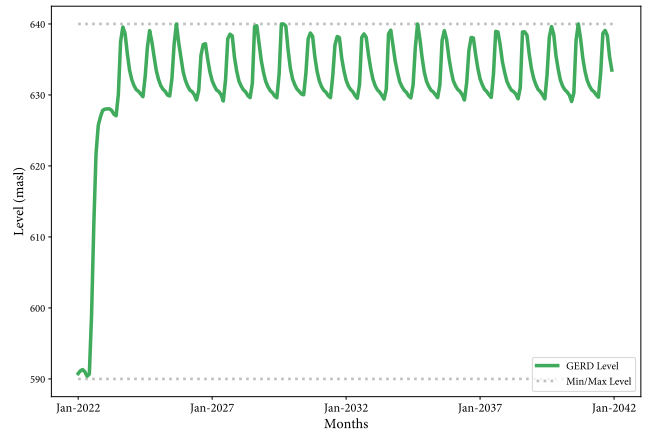
(a) The GERD inflow versus release with Best Egypt 90<sup>th</sup> Percentile policy



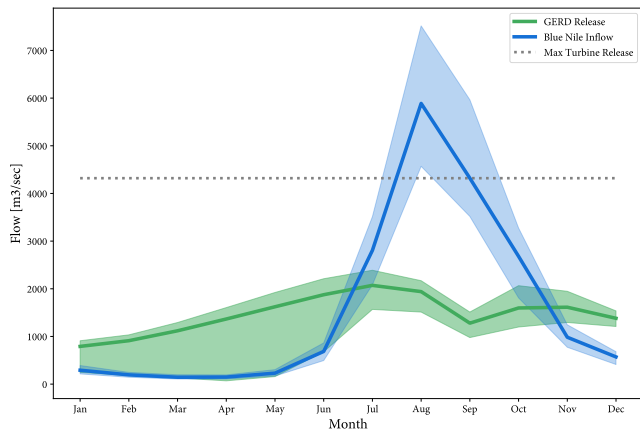
(b) The GERD elevation with Best Egypt 90<sup>th</sup> Percentile policy



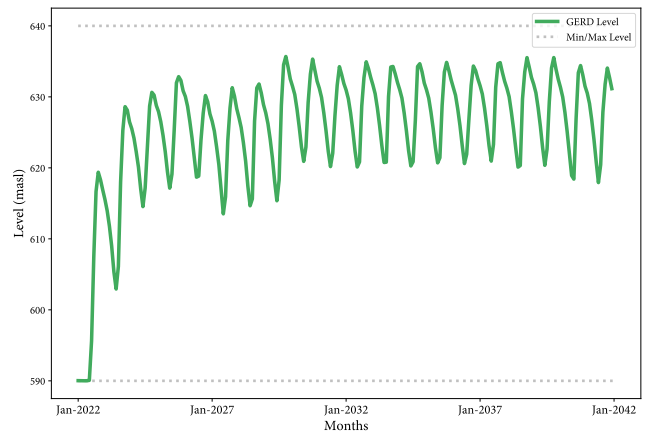
(c) The GERD inflow versus release with Compromise: Absolute Threshold policy



(d) The GERD elevation with Absolute: Percentile Threshold policy

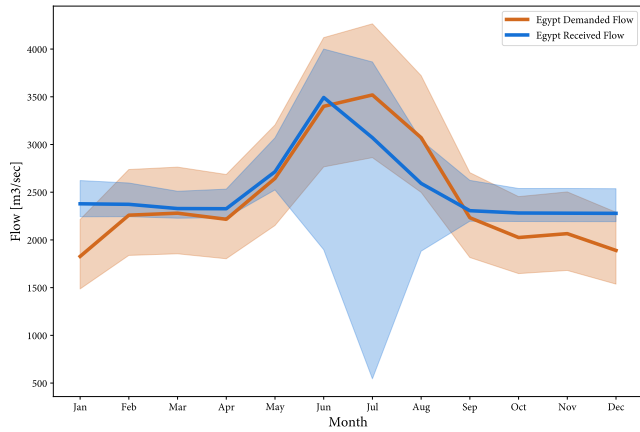


(e) The GERD inflow versus release with Best Egypt Low HAD policy

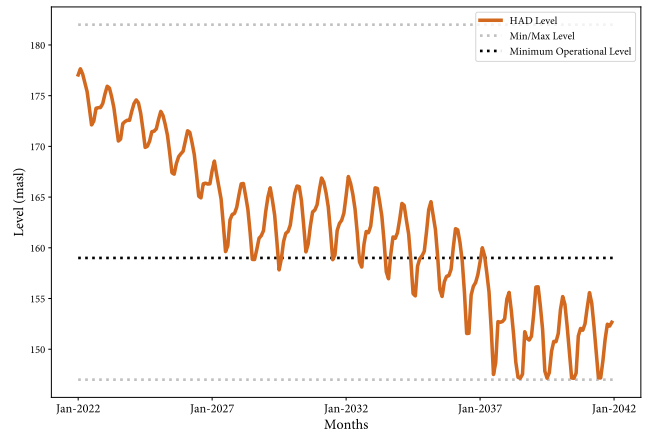


(f) The GERD elevation with Best Egypt Low HAD policy

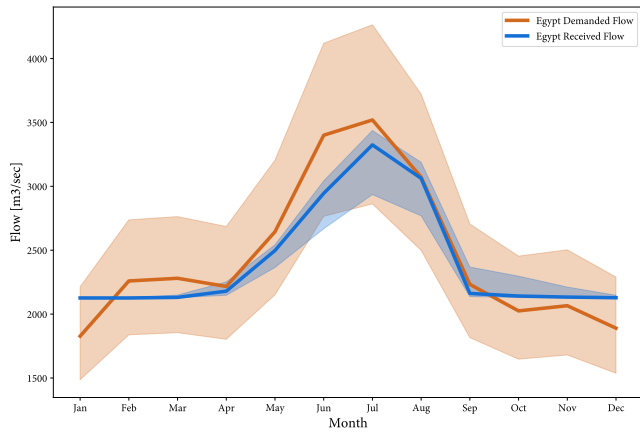
**Figure B.2** Physical system implications of different policies on the GERD. Figures on the left summarise inflow to and release from the GERD over the whole simulation horizon. Shaded area covers the range of values in each month. Figures on the right show the monthly time series of reservoir elevation over the simulation horizon.



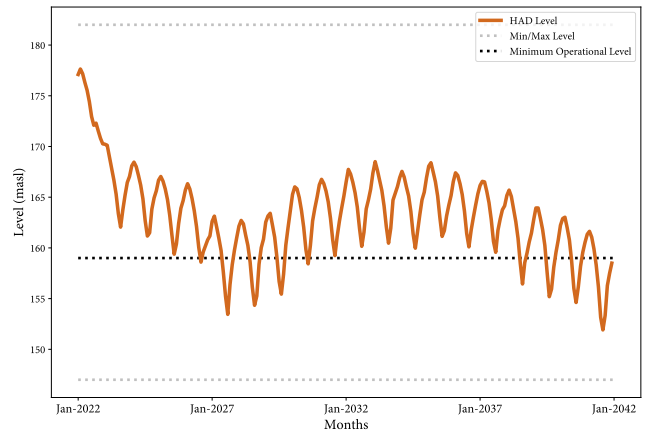
(a) Egypt demanded versus received flow with Best Egypt 90<sup>th</sup> Percentile policy



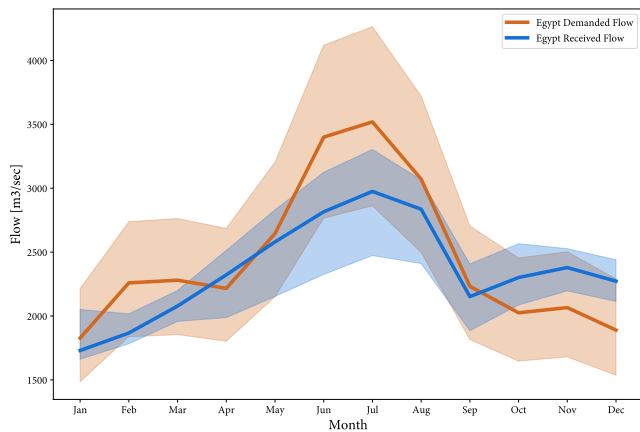
(b) The HAD elevation with Best Egypt 90<sup>th</sup> Percentile policy



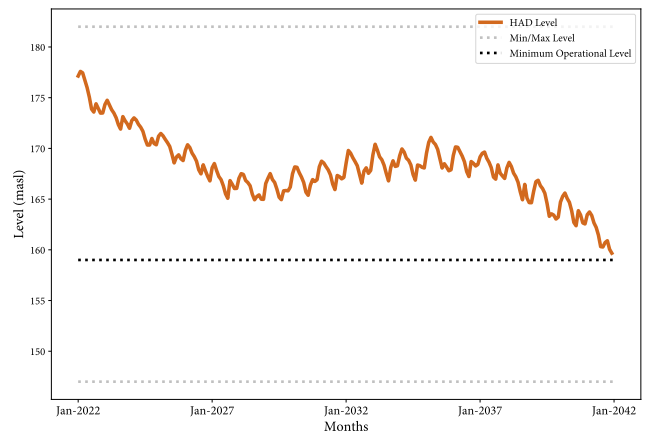
(c) Egypt demanded vs. received flow with Compromise: Absolute Threshold



(d) The HAD elevation with Compromise: Absolute Threshold

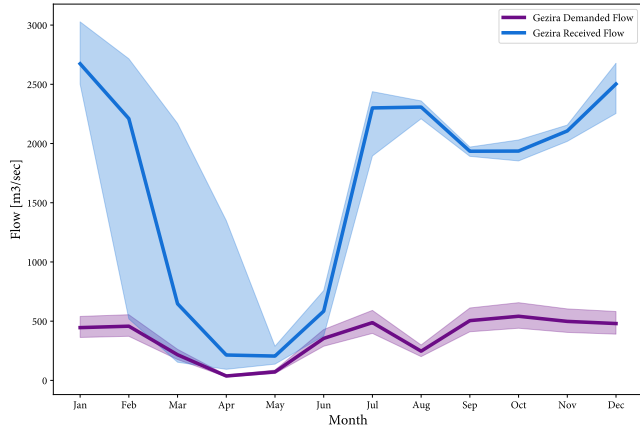


(e) Egypt demanded vs. received flow with Best Egypt Low HAD

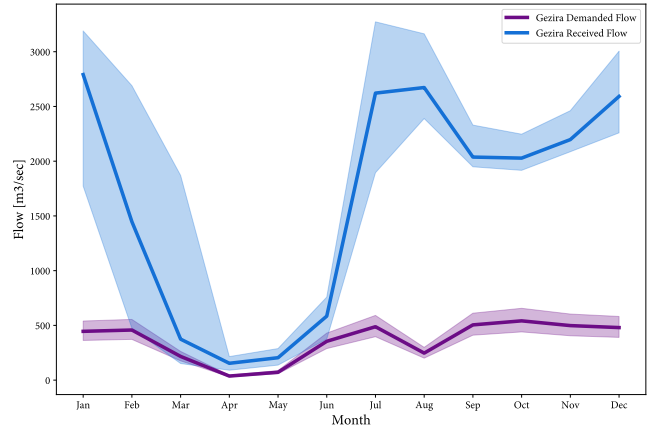


(f) The HAD elevation with Best Egypt Low HAD

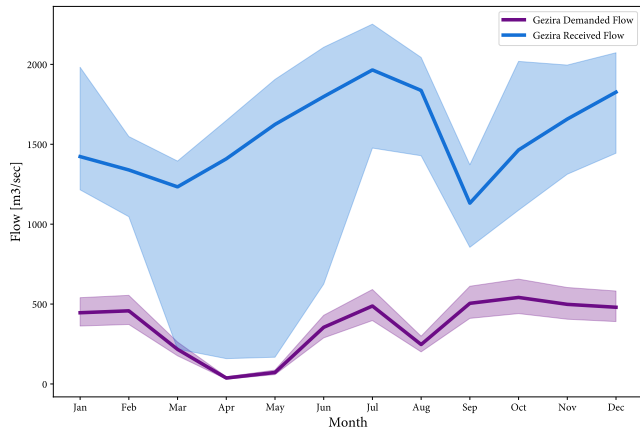
**Figure B.3** Physical system implications of different policies on Egypt. Figures on the left summarise demanded and received water flow over the whole simulation horizon. The line graph shows the mean values corresponding to the month in the x-axis over twenty years. Shaded area covers the range of values in each month. Figures on the right show the monthly time series of the HAD elevation over the simulation horizon.



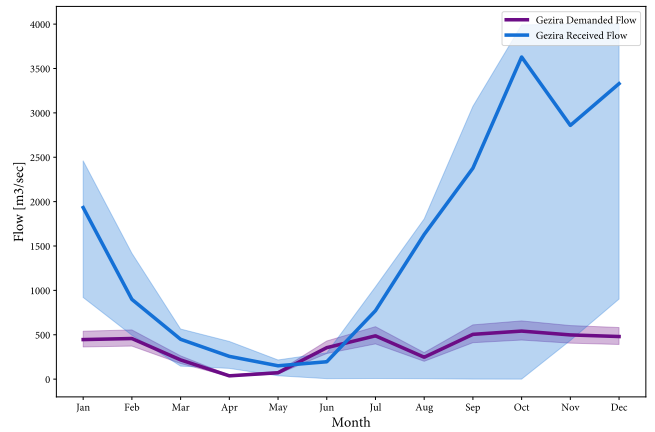
(a) Best Egypt Irr.



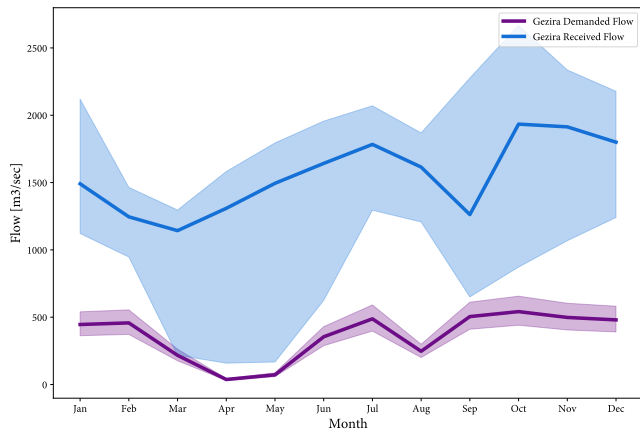
(b) Best Egypt 90th



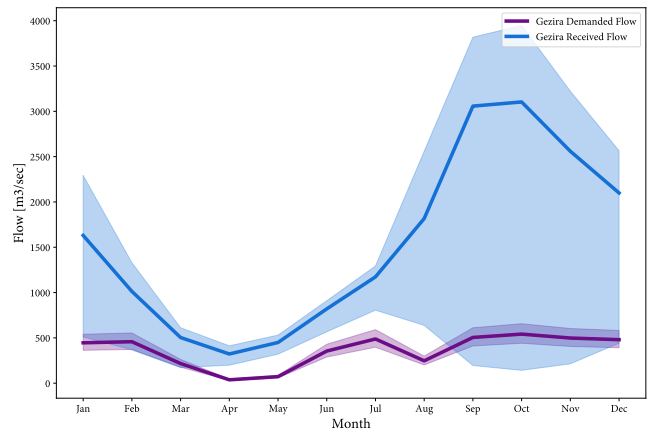
(c) Best Egypt HAD



(d) Best Ethiopia Hydropower



(e) Compromise: Percentile Threshold



(f) Compromise: Absolute Threshold

Figure B.4 Gezira received flow versus demand with all policies.



### B.3 DIMENSIONAL STACKING

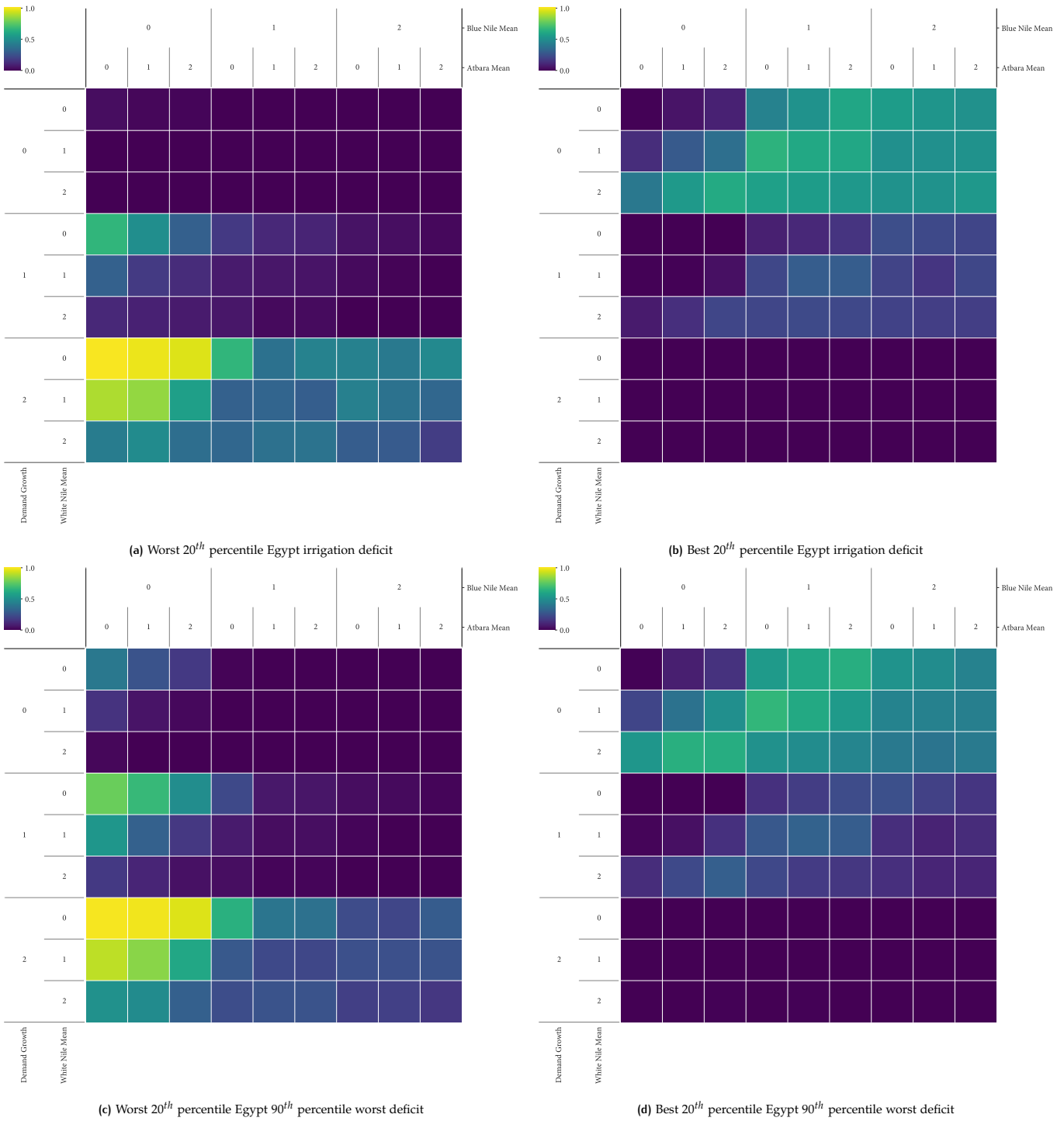
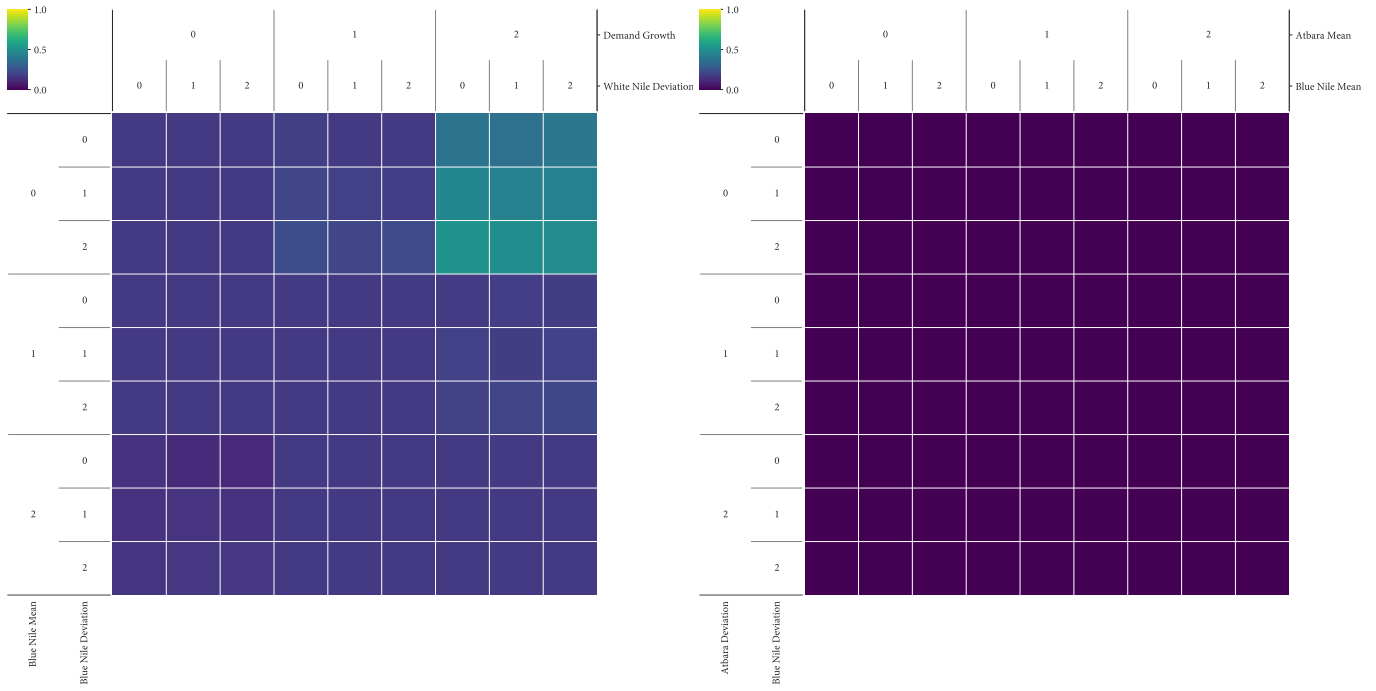
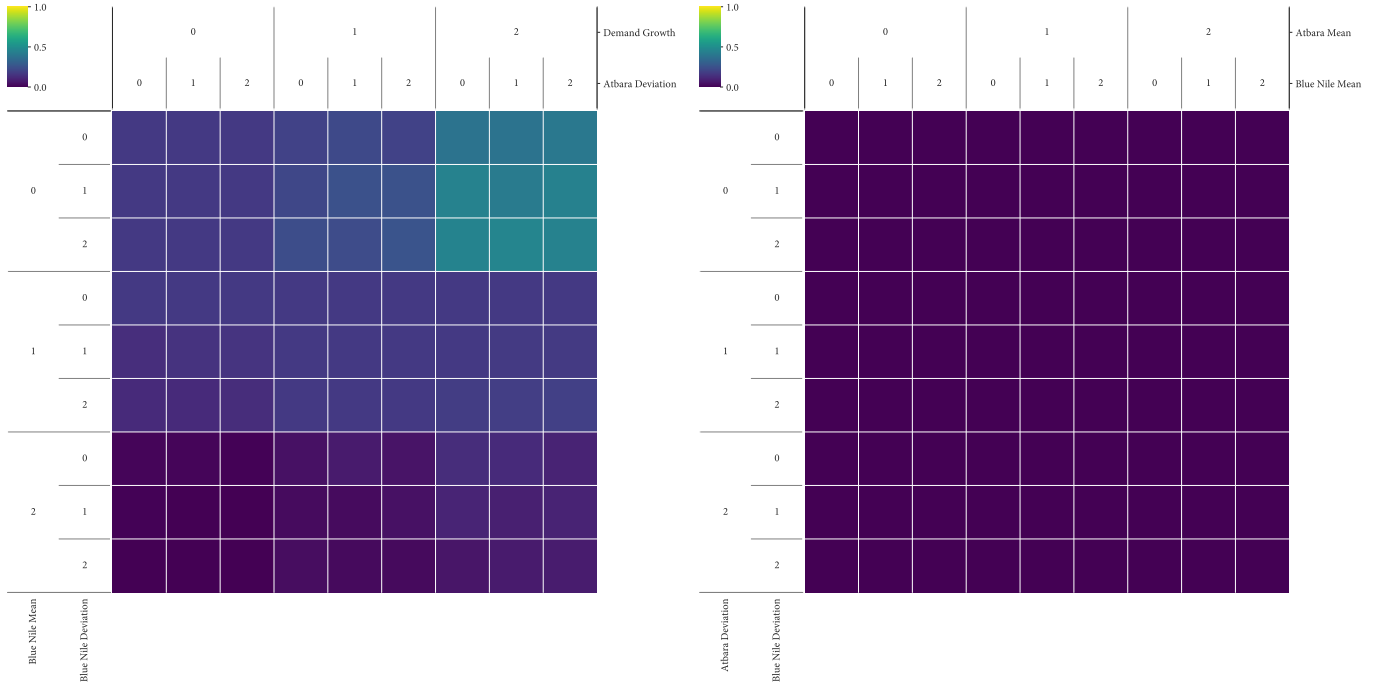


Figure B.5 Dimensional stacking for Egypt's irrigation deficits.



(a) Worst 20<sup>th</sup> percentile Sudan irrigation deficit

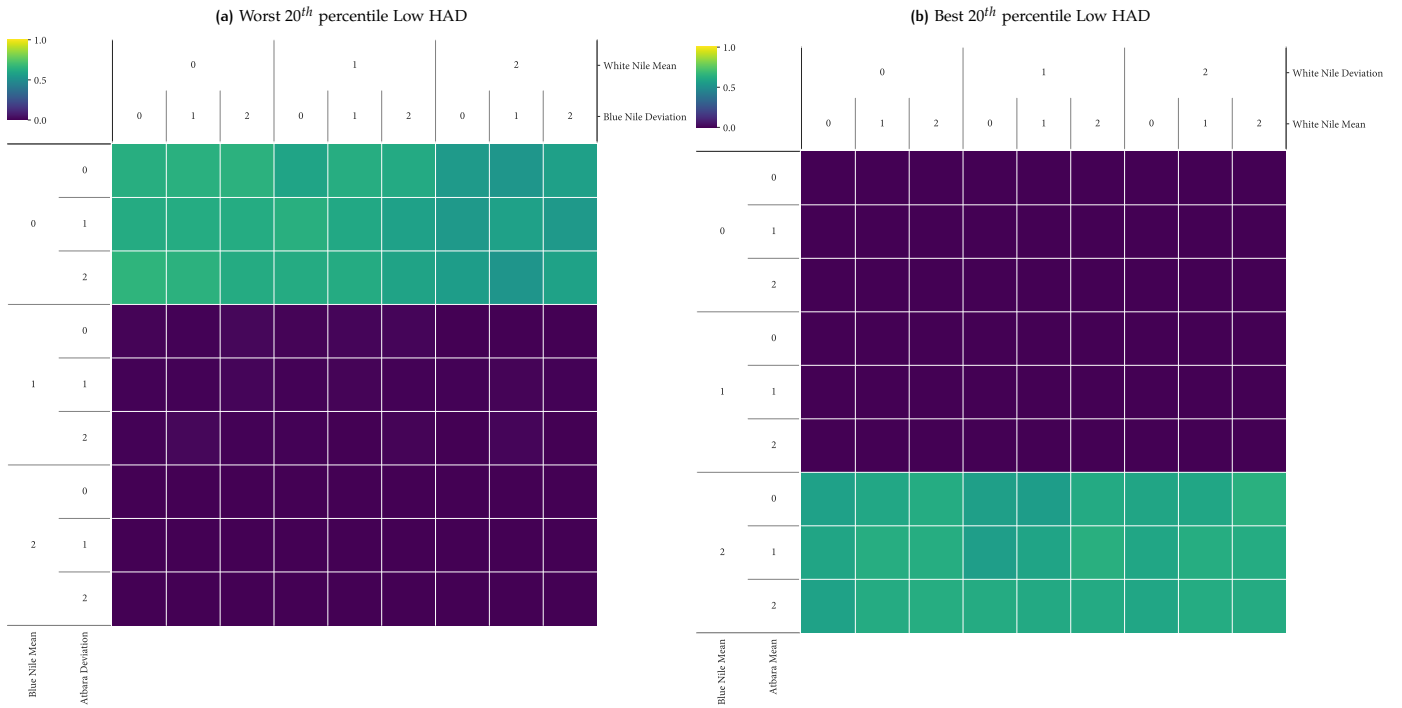
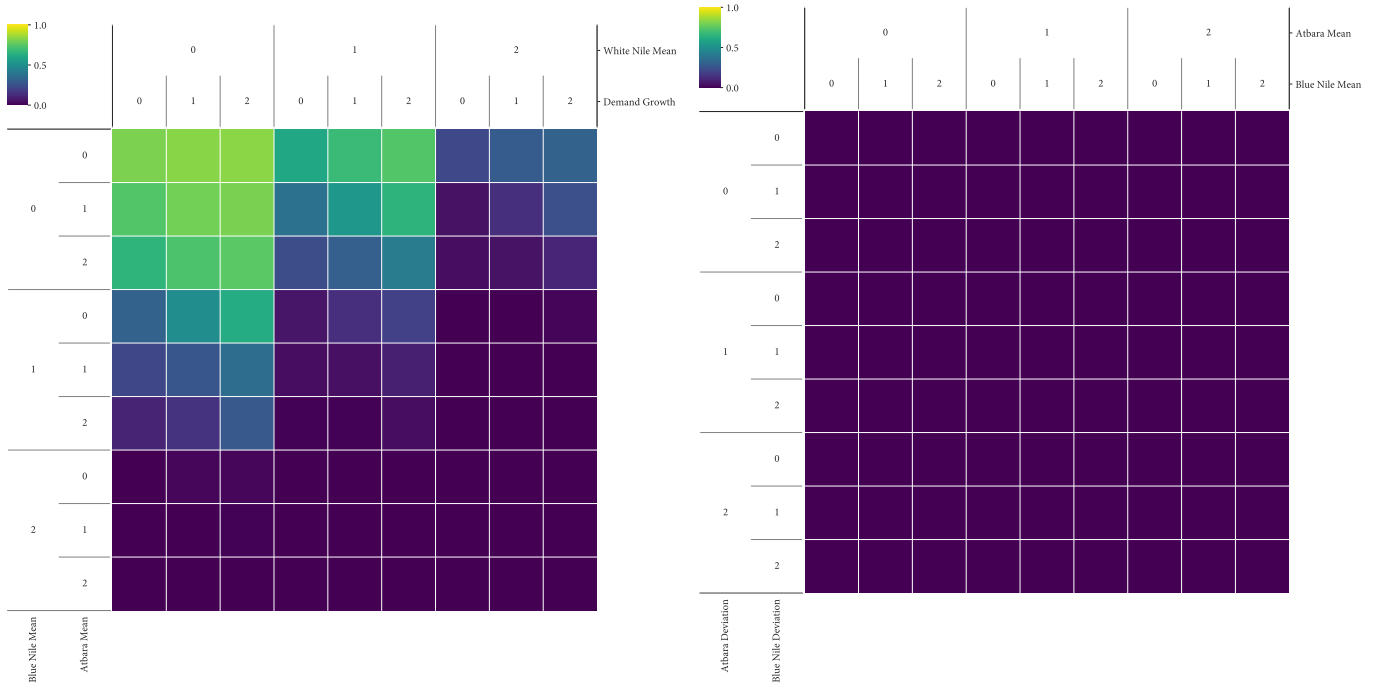
(b) Best 20<sup>th</sup> percentile Sudan irrigation deficit



(c) Worst 20<sup>th</sup> percentile Sudan 90<sup>th</sup> percentile worst deficit

(d) Best 20<sup>th</sup> percentile Sudan 90<sup>th</sup> percentile worst deficit

Figure B.6 Dimensional stacking for Sudan's irrigation deficits.



(c) Worst 20<sup>th</sup> percentile Ethiopia Hydropower

(d) Best 20<sup>th</sup> percentile Ethiopia Hydropower

Figure B.7 Dimensional stacking for reservoir related objectives.

## B.4 SCENARIO DESCRIPTIONS

Scenario	Description
Baseline	<ul style="list-style-type: none"> <li>● Yearly Demand Growth Rate : 0.0212               <ul style="list-style-type: none"> <li>● Blue Nile Mean Coefficient : 1</li> <li>● White Nile Mean Coefficient : 1                   <ul style="list-style-type: none"> <li>● Atbara Mean Coefficient : 1</li> </ul> </li> <li>● Blue Nile Deviation Coefficient : 1</li> </ul> </li> <li>● White Nile Deviation Coefficient : 1               <ul style="list-style-type: none"> <li>● Atbara Deviation Coefficient : 1</li> </ul> </li> </ul>
Extreme Stress	<ul style="list-style-type: none"> <li>● Yearly Demand Growth Rate : 0.03               <ul style="list-style-type: none"> <li>● Blue Nile Mean Coefficient : 0.75</li> <li>● White Nile Mean Coefficient : 0.75                   <ul style="list-style-type: none"> <li>● Atbara Mean Coefficient : 0.75</li> </ul> </li> <li>● Blue Nile Deviation Coefficient : 1</li> </ul> </li> <li>● White Nile Deviation Coefficient : 1               <ul style="list-style-type: none"> <li>● Atbara Deviation Coefficient : 1</li> </ul> </li> </ul>
High Blue Nile	<ul style="list-style-type: none"> <li>● Yearly Demand Growth Rate : 0.0212               <ul style="list-style-type: none"> <li>● Blue Nile Mean Coefficient : 1.25</li> <li>● White Nile Mean Coefficient : 1                   <ul style="list-style-type: none"> <li>● Atbara Mean Coefficient : 1</li> </ul> </li> <li>● Blue Nile Deviation Coefficient : 1</li> </ul> </li> <li>● White Nile Deviation Coefficient : 1               <ul style="list-style-type: none"> <li>● Atbara Deviation Coefficient : 1</li> </ul> </li> </ul>

Table B.1 Description of selected scenarios